Chemical Weathering and Erosion Rates of the Colorado Front Range West of Boulder, CO

by

Matthew C. Jungers

A Thesis submitted in partial fulfillment

of the requirements for the Degree of Bachelor of Arts

with Honors in Geosciences

Williams College,

Williamstown, Massachusetts

2003

ACKNOWLEDGMENTS

I could not have completed this thesis without the support of my advisor, David Dethier. David has been patient with me since my sophomore year, and I owe much of my growth as a scientist and a geologist to him. His care for both my academics at Williams and my life in general always motivated me to succeed when I could. Thank you, David, for always putting me back on an even keel.

I'd like to thank Karl Remsen for his help collecting well logs before I even got to Boulder, and for his help in the field and on the road. Karl's industriousness sets a standard for which many should strive. Thanks also to Pete Birkeland and Nel Caine for sharing their knowledge of the Front Range with me in Colorado. The cosmogenic analyses that are pending for this thesis will owe a great deal to Paul Bierman and the UVM Cosmogenic Nuclide Extraction Laboratory as well as the Lawrence Livermore National Laboratory. Sharron Macklin was indispensable when my questions regarding GIS arose, and she always urged me on when it came time to write. Heather Stoll's comments as my second reader were extremely helpful while revising my thesis. I owe my initial entrance into the world of Williams Geosciences to Bud Wobus who inspired me to pursue the field during Winter Study my freshman year, and the rest of the department was wonderful throughout all four years of my Williams career.

The Geosciences Class of 2003 kept me smiling throughout the year; Eli Lazarus helped a great deal with the digitization of well log data; Will Ouimet will always be a mentor of mine for better or for worse; Jamon Frostenson always made the GIS lab a fun place to work (we don't need windows!). I'd like to thank my family and my friends for their support, and for their encouragement that it would all work out in the end. Annie always knew when to talk to me and when to let me hang up, and I couldn't have made it through the long nights without her help. Finally, I always knew I could count on my Boulder flat, Carissa Carter, Willard Morgan, the Walrus, PBR, and Hayden for a little inspiration when I needed it.

ABSTRACT

The burial and exhumation history of saprolite in the modern Front Range can help us better understand how modern weathering processes and measured short-term erosion rates may apply to long-term landscape evolution. The geomorphology of the Front Range near Nederland, Colorado has evolved since erosion of the Laramide orogen began in early Cenozoic time. West of Nederland, Colorado, the Front Range has been sculpted by glacial and periglacial processes over the last 10^6 years; glaciers disappeared at the end of the Pinedale glaciation at about 12 ka. East of the glaciated area, gently rolling uplands underlain by saprolite and steep, narrow inner canyon areas expose bedrock and thin surficial deposits that reflect the influence of weathering, slope and fluvial processes. I used field mapping of roadcuts and a compilation of well logs for the greater Nederland area to determine the extent and thickness of deeply weathered material in the gently rolling uplands in the area. Geographic Information Systems (GIS) analyses were then used to analyze the distribution and depth of weathered and alluvial material.

Patterns of saprolite thickness are defined primarily by Bull Lake and Pinedale glacial limits. Deep weathered material is widespread in adjacent non-glaciated areas, and can be found preserved on topographic highs above the areas scoured by Pleistocene valley glaciers. Valley glaciers eroded deep saprolite, but an average of 5 m of weathered material remains in glaciated valleys today. Alluvial deposits thicker than 3 m are scarce in my study area; most deep deposits are located within glacial limits to the west and southwest of Nederland.

Saprolite is thought to form slowly in climates as dry (~50 to 120 cm/yr precipitation) as those of the modern Front Range. Where saprolite forms, it requires ≥100,000 years for 1 m of fresh bedrock to become completely grussified. Thick mantles of saprolite preserved near Nederland may have been buried soon after formation, possibly in late Eocene time, and exhumed in late Cenozoic time. Miocene fill material on Winiger Ridge to the southeast of Nederland preserves a paleovalley that incised material stratigraphically higher than the saprolite of my study area. These geologic relations suggest burial of an Eocene surface in this

section of the Front Range. Assuming that 40 m of weathered material lay beneath the Eocene surface, most saprolite has been stripped to leave the present landscape with a mean saprolite cover of 5 to 6 meters. Cosmogenic nuclides suggest that weathered Precambrian bedrock of the Colorado Front Range is eroding at a rate of 18-30 m/m.y. Using a mean saprolite depth of 5 m for the study area, erosion at this rate would remove most of the weathered material from the modern landscape in about 250 k.y. Extrapolating this rate back in time suggests that exposure occurred at ~ 2 to 3 Ma, approximately the same time as the first continental-scale glaciation of North America.

Removal of the weathered material from the Front Range landscape could have both local and global implications. Locally, removal of weathered material is critical for how relief continues to evolve in the Front Range west of Boulder. On a broader spatial scale, widespread exposure of fresh bedrock may enhance chemical weathering, which Molnar and England (1991) believe can lead to atmospheric drawdown of CO_2 and subsequent global cooling.

TABLE OF CONTENTS

LIST OF FIGURES

LIST OF APPENDICES

INTRODUCTION

The sharp, eastern edge of the Colorado Front Range has long been an enigmatic topographic discontinuity. Some theorize that the sharp relief is evidence for Neogene uplift (Scott, 1975), but recent studies have provided evidence that late Cenozoic erosion also may be responsible for starkly contrasting relief of the Front Range and the High Plains near Boulder, CO (Schildgen et al., 2002). In this thesis, I explore how modern processes, and processes during the last two major glaciations of the Rocky Mountains, have interacted with one another to shape the landscape that we see today in the Colorado Front Range. West of Boulder, CO, the Front Range has been sculpted by glacial and periglacial processes over the last 10^6 years; glaciers disappearing at the end of the Pinedale glaciation 12 ka. East of the glaciated area, gently rolling uplands underlain by saprolite, and steep, narrow inner canyon areas expose bedrock and thin surficial deposits that reflect the influence of weathering, slope and fluvial processes (Birkeland et al., 1999). Recent work by Schildgen and Dethier (2000), established rates of incision for Middle Boulder Canyon during the late Pleistocene and Holocene using cosmogenic isotopes and ^{14}C dating. My work focused to the north, west, and south of Nederland, CO, an area about 20 miles west of Boulder (Fig. 1 and 2).

Near and east of Nederland, streams flow through broader valleys rather than steeply incised canyons, and much of the landscape is overlain with deeply weathered saprolite. Saprolite is thought to form slowly in climates as dry (~50 to 120 cm/yr precipitation) as those of the modern Front Range. Where saprolite forms, it requires

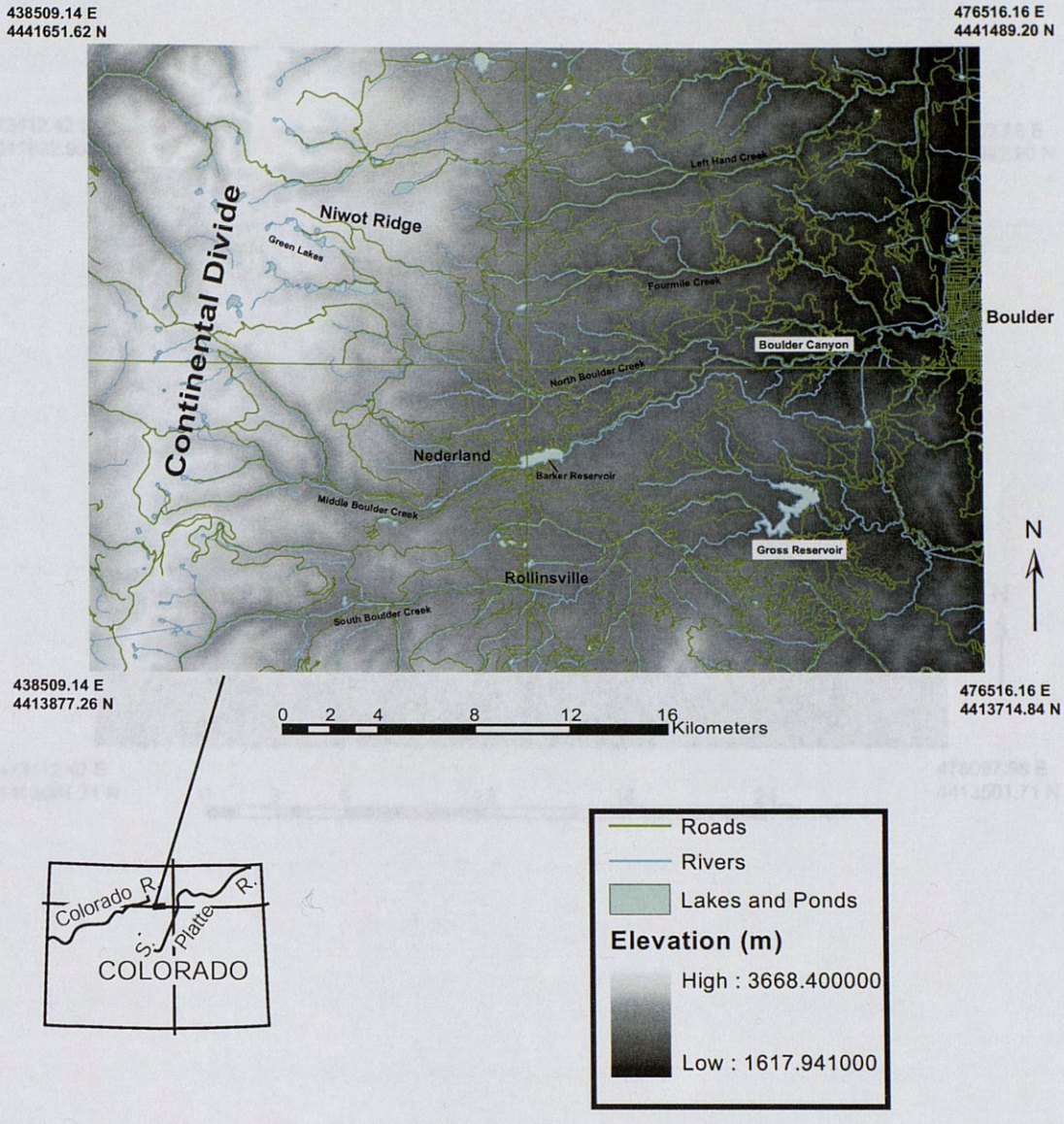

Figure 1. Drainages and place names on a Digital Elevation Model (DEM) mosaic of 1:24,000 Monarch Lake, East Portal, Ward, Nederland, Gold Hill, Tungsten, Eldorado Springs, and Boulder DEMs; coordinates in UTM (NAD 83).

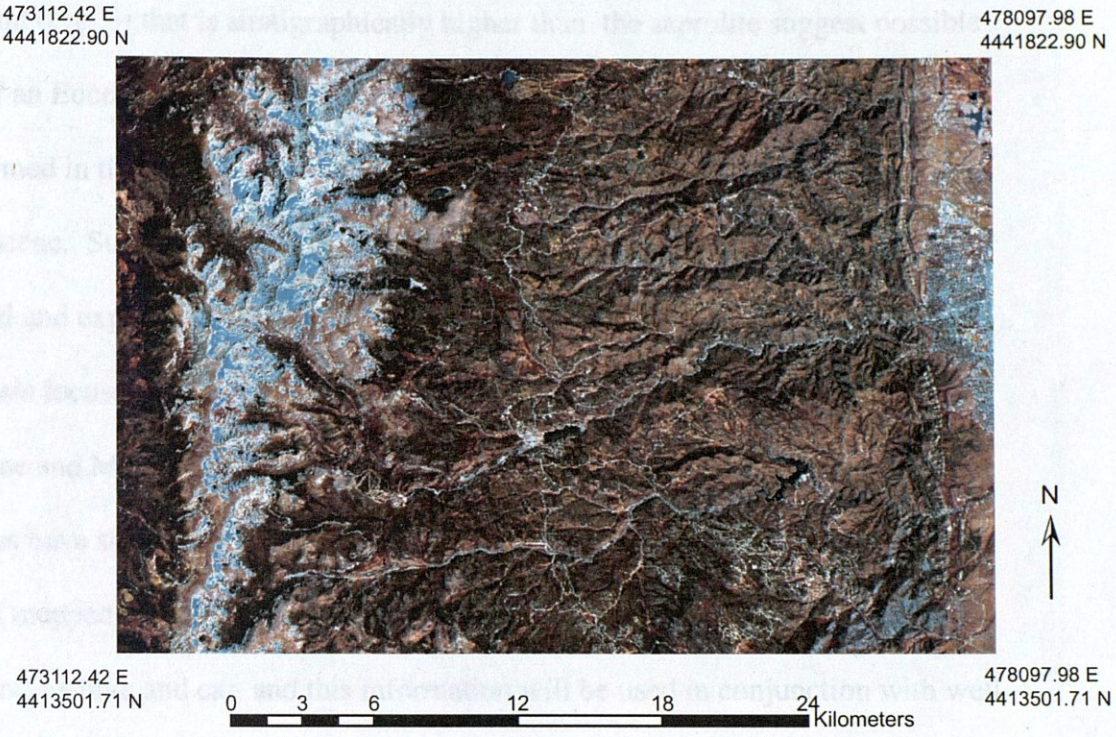

Figure 2. Landsat image (bands 5,3,2) of study area; coordinates in UTM (NAD 83).

≥100,000 years for 1 m of fresh bedrock to become completely grussified (Birkeland, 2002). The presence of Miocene alluvium on Winiger Ridge to the southeast of Nederland (Fig. 3) that is stratigraphically higher than the saprolite suggest possible burial of an Eocene surface in this area of the Front Range. The saprolite then would have formed in the late Eocene and was buried by younger material in the Oligocene and Miocene. Subsequently, the weathered material of the Eocene surface was exhumed and exposed to erosion in the late Tertiary to early Quaternary (Scott, 1975). This thesis focuses on saprolite formation, possible burial of saprolite during the Oligocene and Miocene, exhumation of the saprolite, and how Quaternary erosional processes have shaped the weathered material in the landscape today.

I mapped the location and degree of deep weathering for roadcuts around Nederland by bike and car, and this information will be used in conjunction with well log data for the same area collected by Karl Remsen. The purpose of these two mapping projects was to ascertain the depth to bedrock through weathered material and the distribution of deep chemical weathering with respect to glaciated and non-glaciated areas. I also collected samples for cosmogenic isotope dating of surfaces and for the calculation of erosion rates both in the periglacial environments and in the rolling uplands. I also expanded the scope of my field mapping by utilizing DEMs and Landsat imagery to better visualize my study area. These data will are then integrated using ArcGIS into a GIS environment.

This allows a better understanding of how the geomorphology of the Colorado Front Range is evolving. Answering questions related to the rate that different environments are eroding will not only increase our understanding of the Front

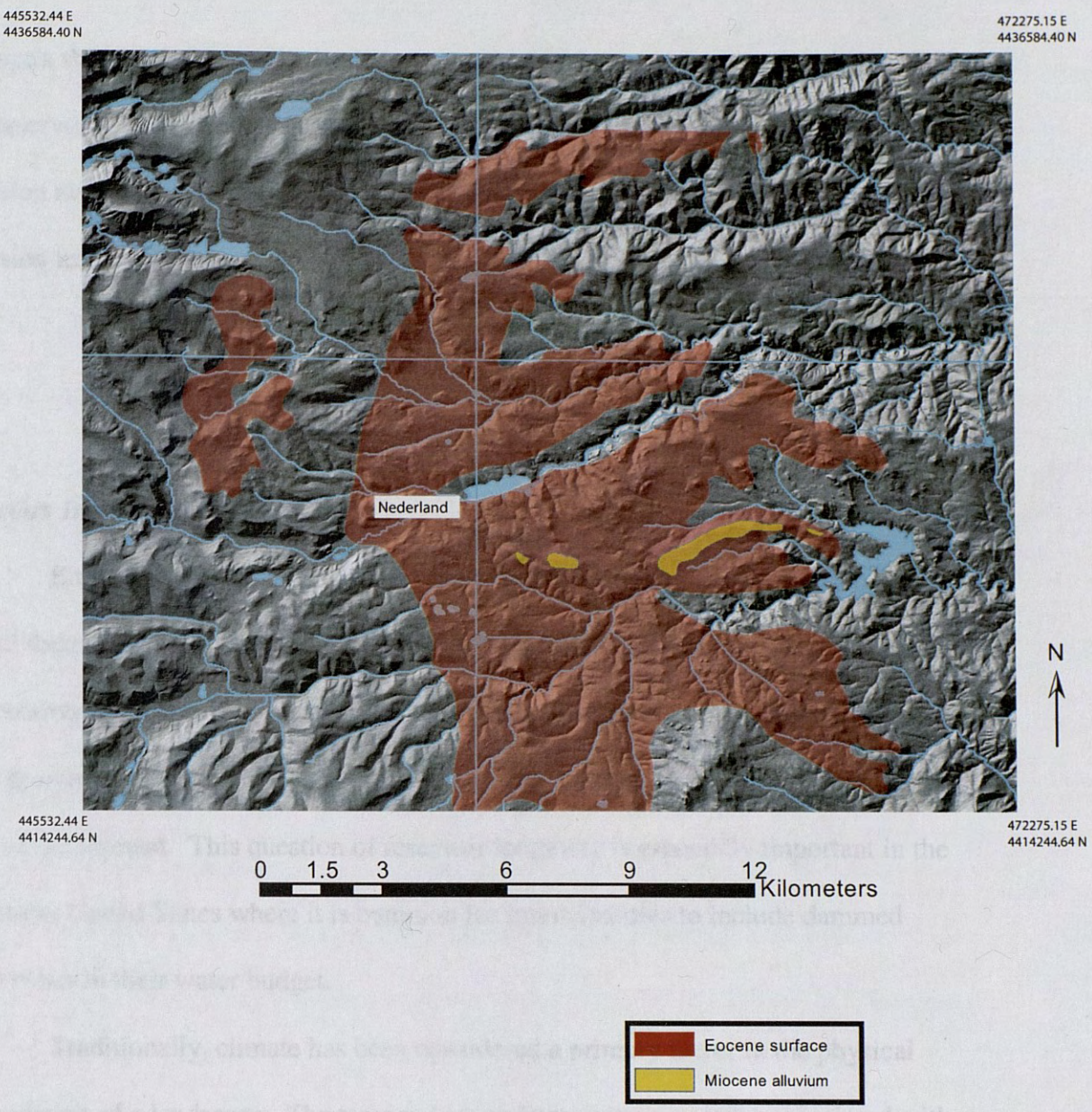

Figure 3. Modern extent of Eocene surface in study area adapted from Scott and Taylor (1986); DEM hillshade base; coordinates in UTM (NAD 83).

Range's sharp relief, but will also help in more practical ways such as the engineering of reservoirs. Examining the history of saprolite formation, burial, exhumation, and erosion also allows a comparison of how measured rates of modern erosion relate to erosion in the long-term.

EROSION RATES

Factors Influencing Erosion

Erosion occurs on a site-to-site, basin, and mountain range scale, but on each level there are common environmental influences that affect erosion rates. The study of erosion on any scale is important for many engineering applications including, but not limited to, the planning of how long a man-made reservoir will take to completely fill with sediment. This question of reservoir longevity is especially important in the Western United States where it is common for municipalities to include dammed reservoirs in their water budget.

Traditionally, climate has been considered a primary factor in the physical denudation of a landscape. The temperature and precipitation ranges associated with climate are important when considering how much and what type of vegetation are on any given hillslope, how big a factor rainsplash and overland flow will be, what the discharge of streams in a basin of interest will be, how snowcover/snowmelt will affect sediment budgets, etc. Climate varies from region to region when considering different mountain ranges, but it also may vary between ecotones within a single mountain range like the Colorado Front Range (Bovis and Thorn, 1981).

The general slope of a basin also affects the erosion rates of the slopes within a drainage. To generalize, basins with a lower average slope will have a lower erosion rate due to slope processes such as soil creep, tree throw, slumping, sliding, etc. Steep slopes often maintain or increase their slope through the continual interaction of slope processes and sediment transport out of the basin by a stream. The continual maintenance of a steep slope can lead to increased relief, incision, and canyon formation in the most extreme cases. Relief is most dramatic in cases where incision is through bedrock which is competent enough to maintain near vertical slopes.

Erosion rates of an area are also closely tied to the region's characteristic rock types. Inevitably, some rocks are more resistant to physical erosion than others, and this can lead to a landscape which is shaped by preferential erosion of weaker rocks. Very closely related to the strength of fresh rock, is how susceptible a particular rock is to chemical weathering. The granites and gneisses that make up the Colorado Front Range can typically weather to grus in about 100,000 years (Birkeland, in press 2003) at which point it is very easily cleared out by physical processes. Deep weathering of rock is also more prone to mass movements and other slope processes that are dependent on the mechanical strength of the rock that makes up the slope. On a less dramatic note, chemical weathering is an important player in soil formation and soil creep. Soil is formed by the chemical breakdown of rock at the boundary between saprolite and fresh rock in a soil profile. Above the saprolite, there is more deeply weathered saprolite which is constantly incorporated into the soil, and mixed with the soil as particles creep downslope.

It is this slow process of soil creep that brings a constant supply of sediment to streams. This sediment is next either flushed out of the drainage, or it remains within the system as upstream sediment storage. It is the interaction of all these processes that I am interested in for this thesis. What are the most important factors from this list? How can we tell? And, perhaps most interestingly, how fast are all these processes working to lower the landscape?

Models of Erosion

Rates of erosion on every scale have always been difficult to measure, and there are often discrepancies between measurements for similar sites. These discrepancies usually find their roots in the differing techniques used to obtain the rates. Erosion rates have traditionally been measured based on sediment yield values measured over the time scale of 10s of years. However, disregarding the time scale, there is reason not to believe that sediment yield for a catchment is equal to, or even proportional to, erosion occurring on the slopes since most modern erosional debris has accumulated as large deposits upstream (Trimble, 1977). Besides problems of sediment storage upstream, sediment yield is often confounded by anthropogenic disturbance (Milliman et al., 1987), tectonics, lithology, and climate (Riebe et al., 2001). Research by Caine and Swanson (1989) shows that it *is* possible for a drainage's sediment yield to be in rough equilibrium with erosion in the short term, but their study site in the Martinelli catchment of the Colorado Front Range seems to be unique in this sense. In contrast to Martinellis', the same authors present evidence from an Oregon Coast Range catchment that is dominated by slope failure and debris

flows which make sediment yield unpredictable on the annual time scale, and perhaps even up to the decadal and century time scale. They propose that for this catchment, equilibrium is achieved over millennia (1989).

As sediment moves down slope, processes related to soil creep mixes grains within the soil column (Heimsath et al., 2002). Soils are produced at the soil-saprolite boundary, and from that point individual grains will visit the surface repeatedly during their movement downslope (Heimsath et al., 2002). This phenomenon is important when determining how the soil-saprolite boundary evolves, how well developed a soil is, and how representative a particular soil sample is of its greater basin. Grain circulation during soil creep also "averages" the soil composition before sediment ever enters a stream. Such mixing is an important factor to consider when calculating denudation rates based on the abundance of cosmogenic nuclides in sediment.

The relatively recent technique of using the accumulation of the cosmogenic radionuclides (CRN) ^{26}Al and ^{10}Be in a catchment's sediment to calculate an erosion rate on the scale of millennia has changed how erosion is studied by many geomorphologists. Cosmogenics takes advantage of streams' natural ability to mix eroded quartz so that nuclide concentration in the quartz reflects the average erosion rate of its contributing area (Riebe et al., 2001; Bierman and Steig, 1996). Because these nuclides accumulate in quartz grains over thousands of years, they are relatively unaffected by recent land use and periodic, shallow slope failure (Riebe et al., 2001; Brown et al., 1998). Erosion rates measured with this technique in the Idaho batholith yielded values that were, on average, 17 times higher than sediment yield

fluxes measured over 10-84 years, but were consistent with 10 m.y. erosion rates measured using apatite fission tracks (Kirchner et al., 2001). These results were interpreted to mean that while incremental erosion is important, it only accounts for a small fraction of total sediment yield, while catastrophic erosion events are rare, but dominate the long-term erosion scheme (Kirchner et al., 2001). Rather than being skewed by these catastrophic events as sediment yield schemes are, cosmogenic erosion rates can average them in on a millennial scale.

Erosion of the Colorado Front Range

The Boulder Creek catchment of the Colorado Front Range incorporates many different climatic environments, and, consequently, many different erosional regimes. There are good values for incision rates east of Nederland, CO in Boulder Canyon itself, and there are values for erosion in the alpine periglacial environment of Niwot Ridge north of Nederland, but erosion has not been measured in the rolling uplands west of Nederland and east of the Continental Divide are somewhat lacking.

Early estimates of fluvial terrace ages within Boulder Canyon were based on stratigraphy, soil development, and clast weathering to make qualitative age estimates (Netoff, 1977; Barber, 1983; Schildgen et al., 2002). These age estimates were very important when modeling river dynamics and erosion over time. Recent work by Schildgen et al. (2002) has used cosmogenic ^{26}Al and ^{10}Be to determine incision rates of Boulder Canyon during the late Pleistocene and Pliocene times. For the late Pleistocene, they determined an erosion rate of ~0.15m ka^{-1} which, if extrapolated to 2500 ka (the initial continental glaciation on North America), would produce 375 m

of net incision in Boulder Canyon. Since this depth exceeds the modern depth of the canyon, they reason that early Pleistocene rates must have been less than late Pleistocene rates of Boulder Canyon, but greater than rates extrapolated from the High Plains near Boulder of 0.04 m ka^{-1} (Schildgen et al., 2002). They concluded that fill terraces formed during periods of high water and sediment availability such as when retreating glaciers exposed unconsolidated sediment to glacial meltwater, and net incision of the canyon probably occurred during interglacial periods when water availability was still high, but surplus sediment had waned (Schildgen et al., 2002).

Periglacial Alpine areas like Niwot Ridge are common above the timberline in the Front Range, and processes there may account for low rates of post-glacial surface lowering at high altitudes (Bovis and Thorn, 1981). Sediment movement in this environment is dominated by solifluction and frost creep, which can achieve maximum annual rates of 4-40 mm yr^{-1} with no movement below 0.5 m depth (Benedict, 1970). Raindrop impact from thunderstorms produces surficial erosion rates four times greater than those in the winter, but at some sites there is a complex interplay between the protection of late-lying snow and erosion by both meltwaters and raindrops (Caine, 1976a; 1976b).

Using lake sediments, Caine measured a lowering rate for these surfaces of 0.004 m ka-1 (1974). Bovis and Thorn calculated a mean surface lowering rate of 0.1 m ka^{-1} for Niwot Ridge using sediment traps on hillslopes. Their measurements took into account different environments on the ridge ranging from nivation hollows to tundra meadows (1981). Their rate exceeds Caine's (1974) rate by two orders of

magnitude for several reasons. High alpine lake sedimentation rates probably underestimate surface lowering across alpine areas because often only the geochemical and aeolian material of the system cross the hillslope-channel boundary and add little volume to lake sedimentation (Caine, 1974). Bovis and Thorn suggests that pocket gophers (*Thomomys talpoides*) may also play a larger role in alpine erosion than previously suggested (1981; Thorn 1978). Their preliminary data suggest that the gophers operate at an order of magnitude higher than in the nivation hollow of Martinelli's snowpatch. There are no cosmogenic erosion rates for Niwot Ridge as of yet.

APPLICATIONS OF COSMOGENIC RADIONUCLIDES

Interactions of secondary cosmic ray particles (neutrons and muons) with surficial materials generates cosmogenic radionuclides (CRN) by neutron spallation (Bierman, 1994). More specifically, neutron spallation results in the formation of ^{10}Be and ^{26}Al from the O and Si in quartz particles as deep as 3 m below the earth's surface (Small et al., 1997). Below 3 m, neutron spallation and the production of cosmogenic isotopes are minimal (Fig. 4), but small amounts of muon-generated CRNs may be found below 3.5 m up to depths of 13 m (Bierman and Caffee, 2002). Since the concentration of cosmogenic isotopes in a volume of material is directly related to material density and residence time near the Earth's surface, CRNs can be used to constrain both surface exposure ages and how fast surfaces are eroding (Bierman, 1994; Heimsath et al., 1999). The relatively short half-lives of cosmogenic

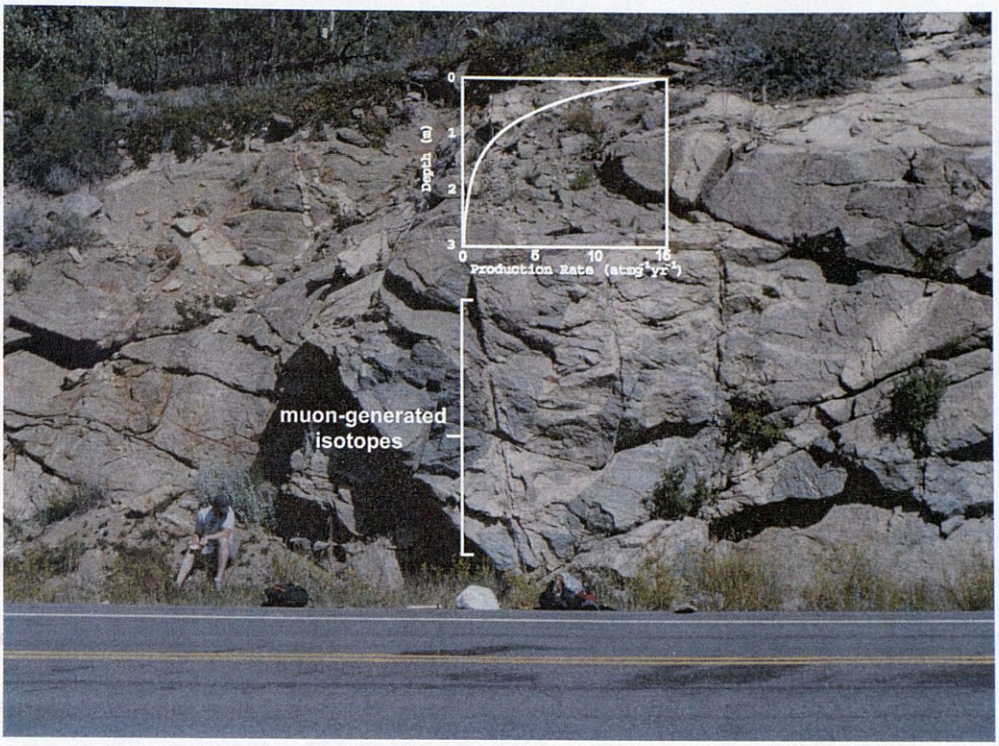

Figure 4. Theoretical profile of cosmogenic radionuclide (CRN) abundance with depth and zone of muon-generation; profile superimposed on MJ-PRFL-1.

isotopes make them especially useful to geomorphologists studying processes on the scale of 10^5 to 10^6 years (Kirchner et al., 2001).

Measuring surface exposure age with CRNs

Measuring the ^{10}Be and ^{26}Al concentration profiles beneath a surface not only allows for a quantitative constraint for the time of surface exposure, but an analysis of the isotope ratio helps to correct for any isotope inheritance or complex burial history that might distort interpretation of the date (Hancock et al., 1999). Cosmogenic analysis has been used to date the formation of fluvial terraces in many areas, including the Wind River Range, Wyoming (Hancock et al., 1999) and the Front Range, Colorado (Schildgen et al., 2002). In both cases, sampled clasts were assumed to be relatively immobile after deposition, and inheritance of isotopes prior to deposition was measured various ways. Schildgen et al. (2002) were able to correlate terrace heights above grade to different periods of flux in stream power presumed to be related to shifts in climate.

Erosion rates for stable bedrock surfaces have also been measured using CRNs. For instance, high concentrations of in situ-produced ^{10}Be and ^{26}Al in granite outcrops in Australia led Bierman and Caffee (2002) to conclude that these bedrock landforms are some of the most stable in the world. Some of the surfaces were measured to have eroded only decimeters over the past million years. These estimates were calculated using both cosmogenic isotopes produced from near surface neutron spalling and muon-generated nuclides for shielded samples as deep as 13 m.

Exhumation rates from the Himalaya measured with CRNs have been shown to agree with previous exhumation rates determined through fission track ages (Vance et al., 2003). Comparing these exhumation rates with erosion rates calculated from CRN abundances in sediment, Vance et al. (2003) conclude that much of the exhumation in the Himalayan mountain chain is now balanced by erosion.

Estimating Rates of Denudation Using Isotope Abundances in Sediment

On the scale of a basin, slope processes should mix sediment enough so that isotope abundances within a sample represent an erosion rate averaged spatially across the basin (Bierman and Steig, 1996). Heimsath et al. (2002) demonstrated that particles within a slope's soil profile do repeatedly visit the surface during soil creep; averaging a basin's isotope abundance based on slope processes this seems like a reasonable assumption.

Sediment storage, in terraces for instance, quartz content, and basin area require careful consideration when measuring rates of denudation based on CRNs. If sediment storage is high for a basin, isotope abundances will not be truly representative of denudation since isotope concentration may be increased by secondary exposures to cosmic radiation. Bierman and Steig (1996) warn against extrapolating rates determined by these methods to large catchments. When collecting sediment for CRN measurements, it is important to make sure that the sample is quartz rich so that there is enough ^{10}Be and ^{26}Al to analyze after preparation for mass spectrometry.

Using CRN abundances to estimate denudation rates in the Idaho batholith, Kirchner et al. (2001) determined values that were, on average, 17 times higher than sediment yield fluxes measured over 10-84 years at stream gauges, but were consistent with 10 m.y. erosion rates measured using apatite fission tracks. These results were interpreted to mean that while incremental erosion is important, it only accounts for a small fraction of total sediment yield, while catastrophic erosion events are rare, but dominate the long-term erosion scheme (Kirchner et al., 2001). Rather than being skewed by catastrophic events as sediment yield schemes commonly are, cosmogenic erosion rates can average them in on a millennial scale. Using CRN abundances in sediment, Dethier et al. (2002) have estimated a modern erosion rate of 18-30 m/m.y. for the saprolite terrain of my study area. This rate is higher than those estimated from soil profiles by 1 to 2 orders of magnitude.

GEOLOGIC HISTORY

Bedrock Geology of the Front Range

The Colorado Front Range is developed on Precambrian igneous and metamorphic rocks; west of Boulder, CO, the Front Range quickly rises to the Continental Divide, mantled on its east flank by the spectacular sedimentary Flatirons. Three groups of intrusive rocks are significant for this study: the Boulder Creek batholith (1,700 Ma), and also including the Silver Plume Quartz Monzonite (1,450 Ma) and the Pikes Peak Granite (1,040 Ma). The Boulder Creek and Silver Plume suites are especially important to our study area, but the Pikes Peak Granite is

important to note since it is the youngest Precambrian intrusive episode of the Front Range; it is peripherally related to my area of focus (Gable, 1980).

The Boulder Creek batholith underlies most of our area, and it is composed of a number of intrusive bodies. The Boulder Creek Granodiorite is a medium- to very coarse grained rock that has both massive and foliated facies. Dominant minerals are plagioclase, potassium feldspar (microcline and microperthite), quartz, and biotite (Gable, 1980). The other main intrusives of the batholith are the gneisses that underlie about two-thirds of the Nederland quadrangle. These metasedimentary rocks were formed by high-grade regional metamorphism, and they display a general parallelism between lithologic layering and metamorphic foliation. This suggests that the foliation of these gneisses was controlled by the primary sedimentary structural features (Gable, 1969). The biotite gneiss is made up of plagioclase, quartz, and biotite, while the microcline gneiss is composed of quartz and plagioclase with varying proportions of potassium feldspar and biotite. In general, the microcline gneiss contains less mica, garnet, and sillimanite than the biotite gneiss. The foliation of the area generally strikes east-west, with dips generally between 30 and 50° north. Faults strike dominantly to the east and northeast (Schildgen, 2000).

The modern Front Range formed during the Laramide Orogeny from 72-70 Ma, when the Precambrian metamorphic rocks were raised over an area 180 miles north-south and 40 miles east-west in central Colorado (Sonnenberg and Bolyard, 1997). This uplift set the stage for later incision and creation of the dramatic relief that is present today in such Front Range locales as Boulder Canyon. The exact mechanisms behind the formation of such relief have long been a point of debate.

Scott suggested that the relief is evidence for Neogene uplift of the mountains (1975), but recent studies by Schildgen et al. (2002) have shown that the topography may be the result of rapid erosion during Pliocene and Pleistocene time. ^{26}Al and ^{10}Be cosmogenic dating implies incision rates of ~0.15 m ka^{-1} and ~0.04 m ka^{-1} respectively for the pre-late Pleistocene and Late Pleistocene in Boulder Canyon. Schildgen et al. (2002) suggest that much of the incision may have occurred during transitions to interglacial periods when sediment supply is low but stream discharges are high. These two examples of differing views are representative of the larger question of how one balances climate versus tectonics as the driving forces behind the sharp relief of the Colorado Front Range.

Quaternary Glacial History

Glaciers in the Colorado Front Range generally originated in cirques, and extended down stream valleys that had been cut during late Miocene and Pliocene time (Dethier, personal communication). Valley deepening during the Pleistocene by fluvial and glacial processes was not more than 100 m (Madole et al., 1998). Most of these valley glaciers were between 12 and 20 km long and 180 and 350 m thick. None of the glaciers reached as far east as the mountain front; most terminated at elevations between 2,700 m and 2,450 m (Dethier, personal communication). There is evidence of the termination of Front Range glaciers on the west shores of Barker Reservoir (Shildgen, 2000), which will be used as the glacial extent for most of this paper's study area (Fig. 5).

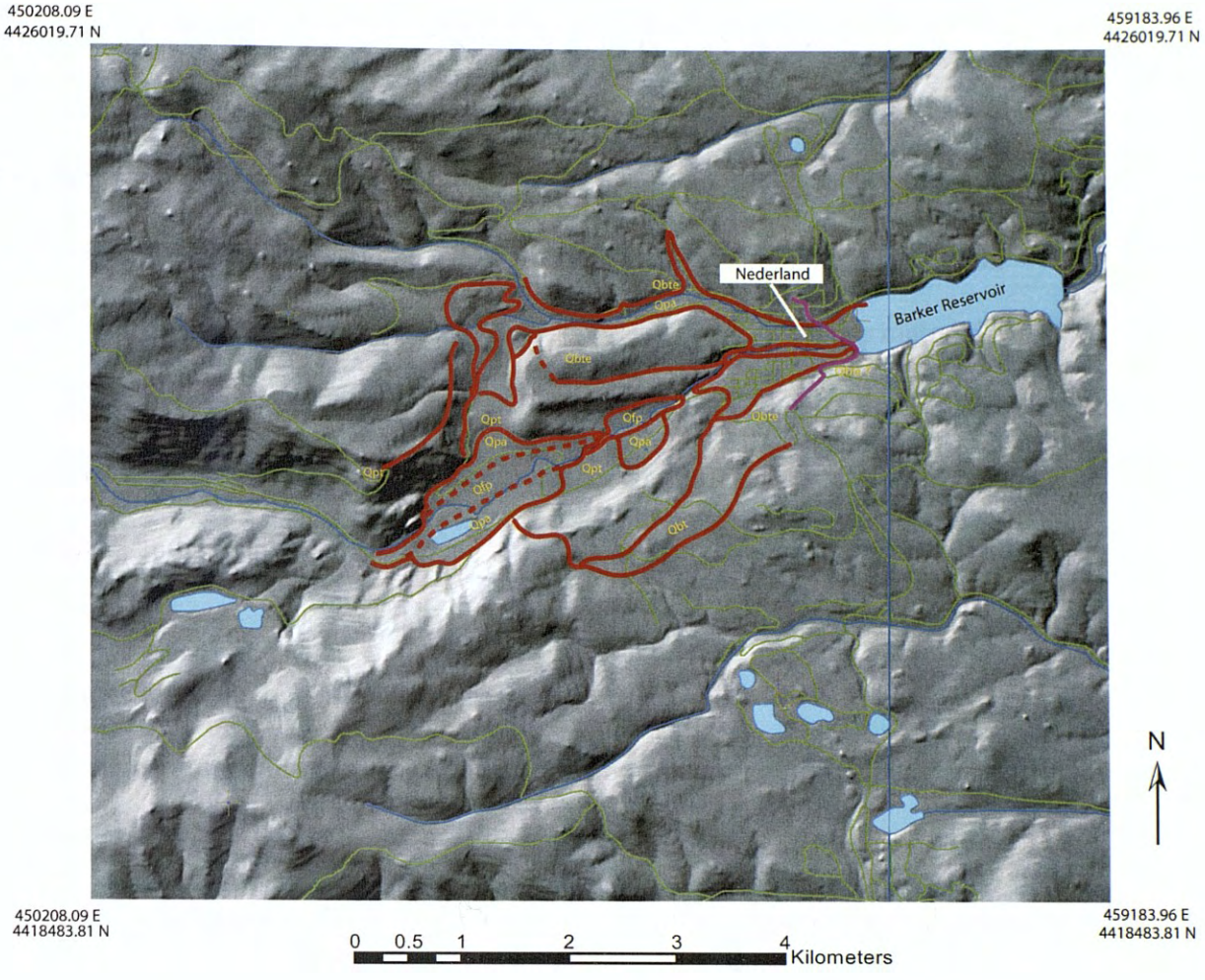

Figure 5. Glacial limits for Pinedale and Bull Lake glaciers(from personal communication with Pete Birkeland, 2002) near Nederland, CO on DEM base.

Glacial deposits are made up primarily of granitic and gneissic rock from the Boulder Creek Batholith, with some fragments from Tertiary intrusives. Glaciofluvial deposits are composed of sand, pebbles, and some boulders. Some valley floors are overlain by as much as 40 m of glaciofluvial deposits. The valley surrounding Eldora, CO, is a good example of such a sediment mantled valley. In general, valleys that were occupied by glaciers were cleared of all loose material which was flushed down valley by glaciofluvial processes. Valleys were then "filled in" by glaciofluvial sediment as glaciers retreated. The Bull Lake glaciation preceded the Pinedale, and a uranium-trend age of 130 ± 40 ka (Shroba and others, 1983) indicates that till mapped as Bull Lake in the valley of North St. Vrain Creek (Madole, 1969; Madole and Shroba, 1979) is, at least in part, equivalent to the Illinoian glaciation of central North America. Recent cosmogenic dating of boulders in the North St. Vrain Creek area (Benson and others, unpublished data) supports this age assignment. An exceptionally large boulder (nearly 3 m tall) provided a ^{36}Cl date of 128 ka; however, a boulder in another nearby deposit mapped as Bull Lake has a ^{36}Cl age of only 88 ka (Dethier, personal communication). Pre-Bull Lake deposits are overlain by both Bull Lake and Pinedale, and are sheet-like in nature with very well developed soil profiles.

CHEMICAL WEATHERING

Formation of Saprolite

In the study of chemical weathering of granitic rocks, the term saprolite is often loosely used to define many degrees of weathering. A strict definition of saprolite says:

> Chemically rotted rock *in situ*. The term is often applied to the lower portion of a weathering profile. The saprolite on granite is locally called 'grus' or 'growan', althought the latter term may include material broken down by mechanical weathering. (Allaby and Allaby, 1999, p. 477)

We are still left with a very loose understanding of what one may classify as saprolite, but further exploration of chemical weathering will allow us to fine tune the term.

The degree to which a particular granitic rock is chemically weathered varies, and certain steps must take place for weathering to gain a foothold. Fracturing or jointing of a rock allows the inflow of water as an important initial step in chemical weathering. The entrance of water sets up a positive feedback loop in which the number of fractures, and thus surface area is increased, which increases the flow of water through a layer of rock, progressively oxidizes zones near fractures (Anderson et al., 2002). Anderson et al. assert that once a layer becomes adequately oxidized, mass loss may occur by chemical degradation and subsequent loss in the mechanical strength of the rock leads to saprolite formation. Even when there is no obvious evidence of chemical weathering in the form of clay minerals or iron oxidation, examination of a rock in thin section can reveal chemical weathering occurring on the

scale of individual grains (Birkeland, 1999). It's been found that as biotite alters, it can increase in volume by up to 40% and in doing so shatter the internal structure of a rock, reducing it to grus (Birkeland, 1999). This process has been attributed to the formation of grus 13 m thick in Australia by Dixon and Young (1981), but even with its supporters, Birkeland (1999) warns that this theory is not unilaterally accepted as the primary mechanism behind grus formation (Gerrard, 1994).

As a rock weathers, the contact between soil/saprolite and fresh rock (Fig. 6) is often maintained as a remarkably distinct junction (Clayton, 1979). Above the fresh rock contact, fragments of weathered rock are degraded by chemical and biological processes within the soil (Velbel, 1985). While it is commonly agreed that soil is an important site for chemical weathering (Riebe et al., 2001; Anderson et al., 2002) there is disagreement about the significance of bedrock as a site of weathering (Riebe, 2001). However, there is good evidence from locales including the Colorado Front Range, the Oregon Coast Range, and the Blue Ridge Highlands of Virginia that deep weathering within the bedrock itself is important for both soil formation and for influencing erosional profiles of landscapes (Birkeland, in press 2003; Anderson et al. 2002; Stolt et al., 1992).

The relationship between chemical weathering and erosion involves a two-way feedback system between the two processes and this system varies with climate and rock type. In the Blue Ridge Highlands, saprolite thickness is directly related to the stability of the landscape. Stable summits have higher rates of saprolite formation, while saprolite formation on slopes is equal to the rate of erosion, and no overburden of weathered rock is seen on steep slopes (Stolt et al., 1992). In the southern Blue

a)

b)

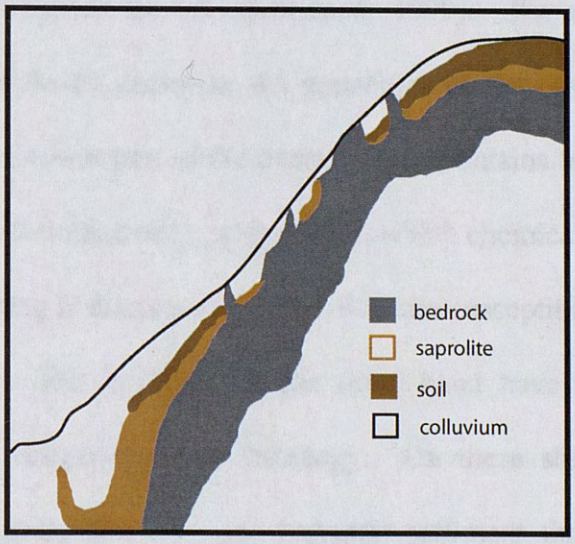

Figure 6. Saprolite Formation; a) MJ-PRFL-3 in the field; b) schematic of soil-saprolite-bedrock contacts (adapted from Graham et al., 1990).

Ridge mountains of North Carolina, weathering data show that modern saprolitization rates (3.8 cm / 1000 yrs) and the long-term average denudation rate of 4 cm/1000 yrs for the Southern Appalachians (Holt, 1989) are comparable. This similarity suggests that modern chemical weathering rates can be similar to long-term average denudation rates and that over time a dynamic equilibrium between chemical weathering and erosion may exist (Velbel, 1985). It is important to note that both of these Appalachian environments are in relatively wet climates with 170 cm to 250 cm of rainfall per year in the southern Blue Ridge mountains. The range of precipitation around the Colorado Front Range is about 46 cm to 102 cm per year and is dependent on elevation (Birkeland, in press 2003). This should serve as a caveat to apply *processes* of saprolitization but not saprolitization *rates* across different climates.

When relating chemical weathering and erosion a landscape can be either weathering limited or transport limited (Birkeland, 1999). For example, in the Amazon River Basin the Andes comprise the upper rim of the basin while lower-relief shields make up the lower part of the basin. The mountains have steep slopes and thin soils, so erosion is limited only by the rate at which chemical weathering can take place. This weathering is directly correlated with the susceptibility of the rocks to chemical weathering. The lowlands on the other hand have thick soils, and weathering takes place independently of lithology. On these shields, erosion is limited only by how quickly the river can transport sediment through the basin. These lowlands are an interesting example of a situation where the conditions are ideal for chemical weathering – i.e., high precipitation and temperature – but very little weathering takes place because the landscape is made up of thick soils and end-

point weathering products, (Birkeland, 1999). If the landscape was stripped of this mantle, weathering might accelerate in the freshly exposed unweathered minerals.

Birkeland uses the Andes to highlight another important consideration related to denudation rates that might be analogous to the Colorado Front Range. Chemical denudation rates are often presented as an average for a whole landscape, but it is important to note that different regions of a basin are often contributing different data to the average rate for the whole basin. In the Andes, the headwaters are in glaciated, U-shpaed, flat-floored valleys, with well-developed A/B/C soil profiles across moraines and other steep slopes. These uplands may be contributing to the dissolved load, but it does not seem that landscape lowering is occurring at any notable rate in these valleys. However, downvalley of the glaciated areas, there are steep, barren, V-shaped valleys that are delivering more of the solid load removal for the basin. Thus, it is probably these lower valleys that are the loci of landscape lowering, but the average for the basin still gets applied to the more stable glaciated valleys (Birkeland, 1999). It is easy to draw comparisons between the uplands and lowlands of the Andes and the glacial and periglacial uplands of the Colorado Front Range and the lower, steep inner canyons of the Front Range. It is not yet clear, though, whether processes are occurring the same way in Colorado as they are in South America.

Whether streams flowing near or over saprolite are first, second, or third order may also play an important role in the relationship between chemical weathering and physical denudation. Costa and Cleaves (1984) found that, in Maryland, first-order streams flowed over saprolite, while second-order and greater streams flowed on

bedrock. They concluded that landscapes associated with second-order or greater streams were eroding at a rate that exceeded the rate of saprolite formations.

Chemical Weathering Reactions

Chemical weathering promotes mineral dissolution; which minerals are most prone to dissolution varies from rock type to rock type. For granitic rock, biotite is often the first mineral to show signs of weathering, and both plagioclase and hornblende are also targets for chemical dissolution (Clayton, 1979).

The weathering of biotite is carried out by the removal of interlayer cations so that the primary phyllosilicate lattice is maintained, and the main weathering product of biotite in saprolite is hydrobiotite, a regularly stratified biotite-vermiculite (Velbel, 1984). The reaction by which this takes place is as follows:

$$K_{0.85}Na_{0.02}(Mg_{1.2}Fe^{II}_{1.3}Al_{0.45})^{VI}(Al_{1.2}Si_{2.8})^{IV}O_{10}(OH)_2 + 0.19O_2 + 0.078H^+ + 0.31H_2O + 0.016Ca^{++} + 0.04Na^+ + 0.35Al(OH)_{2(aq)}{}^+ + 0.3Fe(OH)_{2(aq)}{}^+ \rightarrow \quad (1)$$
$$K_{0.25}Na_{0.06}Ca_{0.016}(Mg_{1.1}Fe^{II}_{0..5}Fe^{III}_{1.1})^{VI}(Al_{1.2}Si_{2.8})^{IV}O_{10}(OH)_2 \bullet 0.133Al_6(OH)_{1.3} + 0.6K^+ + 0.1Mg^{++}$$

This reaction releases some potassium and magnesium from the mineral, and it results in the removal of some calcium and sodium from the surrounding soil or groundwater (Velbel 1985).

The weathering of plagioclase is a two step process that starts with incongruent dissolution of the mineral and finishes with precipitation of clay minerals from the dissolved constituents. This reaction proceeds as follows:

$$Ca_xNa_{(1-x)}Al_{(1-x)}Si_{(3-x)}O_8 + (6-2x)H_2O + (2 + 2x)H^+ \rightarrow \quad (2)$$

$$xCa^{++} + (1-x)Na^+ + (3-x)H_4SiO_{4(aq)} + (1 + x)Al(OH)_{2(aq)}^+$$

(where "x" is a compositional variable that differs betwen rock groups)

and then precipitation of clay mineral products:

$$Al(OH)_{2(aq)}^+ + H_2O \rightarrow Al(OH)_{3(gibbsite)} + H^+ \quad (3)$$

and

$$2Al(OH)_{2(aq)}^+ + 2SiO_{2(aq)} + H_2O \rightarrow Al_2Si_2O_5(OH)_{4(kaolinite)} + 2H^+ \quad (4)$$

The concentration of these cation-depleted clay minerals in a saprolite may be an indicator of either weathering over a long period of time or intense weathering over a short period of time (Velbel, 1985). Again, though, the factor of climate must be considered in any saprolitization scheme.

The rate at which these reactions can fully weather a granitic rock to grus, the end member of any saprolite sequence, is variable between different rock types and climates. However, Birkeland estimates that for the granitic rocks of the Colorado Front Range, it should take a >>100,000 years to form grus (in press 2003).

Degrees of Weathering

During the period that a rock is being weathered, it passes through a number of degrees of weathering along the spectrum from fresh rock to grus. These degrees of weathering can be difficult to resolve from one another, but Clayton et al. (1979) have developed a field classification scheme for granitic rocks that is easy to

understand and apply. The different classifications are based on, among other things, the color of the rock, the rock's mechanical strength, the sound a rock hammer makes when striking the rock, how distinct joints appear, the appearance of biotite, and the appearance of feldspars (Fig. 7).

1. Unweathered rock—with bulk density ~2.7 g/cm^3.
2. Very weakly weathered—some iron stains from biotite weathering, feldspars have some opacity, junctions of joint planes are angular, and bulk density ~2.5.
3. Weakly weathered—hammer blow gives dull ring and results in hand-size fragments, feldspars are opaque, junctions of joint planes are subangular, there is no root penetration, and bulk density ~2.3.
4. Moderately weathered—no ring from hammer blow, biotites have yellow sheen, joint sets are indistinct and junctions are rounded, and bulk density ~2.2.
5. Moderately well weathered—break into small fragments with hands, roots penetrate along fractures, and bulk density ~2.2.
6. Well weathered—fragments disaggregate by hand to sand-size particles (grus), roots penetrate between grains, and bulk density ~2.1.
7. Very well weathered—original rock fabric is preserved but feldspars are weathered to clay, material is plastic when wet, and bulk density ~1.8.

from Clayton et al. (1979)

Figure 7. Clayton's classification scheme for the weathering of granitic rocks

As mentioned before, this field characterization scheme can be used to classify the weathering of most granitic rocks. Birkeland, though, offers the warning that for the Colorado Front Range near Boulder, CO, the first task is to make sure that hydrothermal alteration is not confused with surface weathering (in press 2003). Since much of the rock in our study belt is within the Colorado Mineral Belt, the surface color of a rock is often not a good indicator of its degree of weathering. If these classifications are carefully followed, they can be a useful tool in determining

the stability of a landscape. A setting with large amounts of class 7 rock can be assumed to be very stable with a low erosion rate, for example. Landscapes with lots of class 7 are also more prone to landslides (Birkeland, 1999).

METHODS

Field Methods

Description of Saprolite in Roadcuts

Roadcuts to the west, north, and south of Nederland, CO were characterized in terms of degree of chemical weathering, height of roadcut, and GPS location (Appendix B). The detail with which a roadcut was characterized was directly proportional to the overall height and length of the cut. Different areas were covered either on bike or in a car, with the majority of the most cursory characterizations being done from a car.

The scheme I used for the characterization of the cuts' weathering profile (Fig. 7) was first described by Clayton et al. (1979). Clayton's classification scheme for the weathering of granitic rocks uses a range from fresh rock to rock completely reduced to grus. Various field techniques are used to classify a rock including the sound of the rock when hit with a hammer, the coloration and constitution of biotite crystals, the angularity of joints, and whether or not a rock may be broken or crumbled by hand. Roadcuts' weathering was characterized by what proportion of the cut fit into the different classes that Clayton described. This method of classification has been applied before to the Colorado Front Range by Birkeland et al. (2003). I generally estimated the heights of cuts; low cuts were generally put in a category of <1.0m in height, and for higher cuts I give a reasonable estimate for their highest point. Most roadcuts were short, and for this reason were given only one GPS point. Longer roadcuts were given at least two GPS points, which effectively recorded their length.

Collection of Roadcut Profiles

Detailed saprolite profiles were measured and sampled at three different locations for analyses of geochemistry and/or cosmogenic radionuclides (CRNs). I measured the height of the roadcut in first, and then divided the cut into a profile consisting of at least four and as much as seven layers. The uppermost sample was taken from the topsoil, and included sediment from the surface to the contact with weathered bedrock below. Lower samples were then taken at predetermined intervals (unique for each profile) based on each class of weathering within the roadcut. I prepared these samples later for geochemical and thin section analysis. Densities of the competent rocks were measured in the lab, and we measured the density of topsoil and highly weathered rock in the field by: extracting a sample from the roadcut; filling its hole with a plastic bag; and carefully filling the plastic bag with enough water to equal the volume of the rock that was removed This volume could then be used with the mass of the sample to determine density.

I also measured GPS locations (Fig. 8), described context within our study area, and sketched the roadcut including the number and orientation of the different samples extracted. I also included my level of certainty that the top of the roadcut represented the original surface before the roadcut was blasted. This information is important for constructing a cosmogenic depth profile.

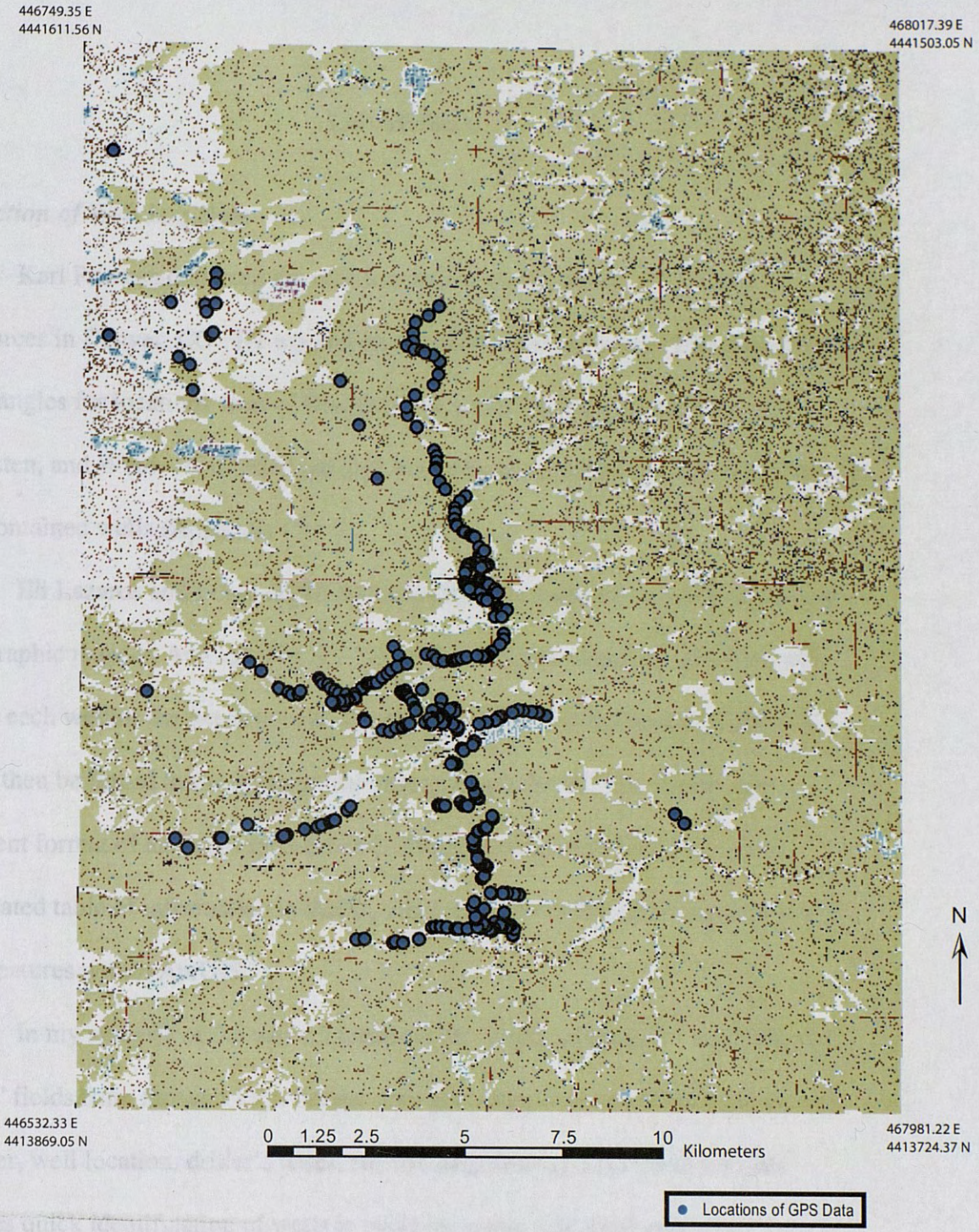

Figure 8. Digital Raster Graphic mosaic of Nederland, Ward, Tungsten, and Gold Hill quadrangles showing locations of roadcut GPS data (225 points); coordinates in UTM (NAD 83).

Lab Methods

Collection of Well Log Data

Karl Remsen collected the well log data at the Department of Water Resources in Denver, CO. He worked on obtaining well locations on various USGS quadrangles for locations west of Boulder, CO, including Nederland, Gold Hill, Tungsten, and Ward. Karl recorded data for wells in each quarter section of the map that contained wells (Appendix C).

Eli Lazarus and I then digitized the location for each of the wells on digital topographic maps in ArcGIS (Fig. 9). Specific information such as alluvial cover above each well or the depth to bedrock through weathered material for each well could then be linked to these digital locations using a dBASE file (essentially a different format of an Excel spreadsheet). This digitization of location and an associated table of information including each well allows for statistical analysis of well features within ArcGIS.

In my analysis of the wells, I focus on the "depth to bedrock" and "alluvial cover" fields from the well logs, but the logs also contain information such as well number, well location, driller's notes, etc. So, digitization of the well log data enables quick identification of wells in addition to any statistical analysis.

Spatial Interpolation of Digital Well Logs

Once point data are entered into a GIS environment, several tools may be used to analyze information associated with each point. One of the most powerful tools

available in ArcGIS is spatial interpolation where specific information from each point is used to predict values in open spaces where there is no data. In effect, this converts point data to surface data, and it produces a surface layer in Arc that can be draped, contoured, etc.

Different methods of interpolation are available, but they all work either globally or locally. Global interpolation gives equal weight to all control points in an analysis when creating a statistical surface, while local interpolations use a specified number of points around a control point for the interpolation. For my data, I explored two different forms of local interpolation, inverse distance weighted (IDW) interpolation and kriging.

IDW assumes that unknown values of points are influenced more by nearby control points than distant ones. The weight of a control point's influence is equal to the inverse of the distance between points raised to a power (Chang, 2002). IDW is a very accurate form of interpolation, but this accuracy can lead to a "bull's eye" effect around outlier points on the statistical surface. Kriging assumes that the spatial variation of an attribute is neither totally random nor deterministic. Instead, spatial variation consists of three possible components: a spatially correlated component, representing the variation of the regionalized variable; a "drift" or structure, representing a trend; and a random error term (Chang, 2002).

Preparation and Analysis of CRNs

The preparation of my cosmogenic samples is underway at the UVM Cosmogenic Nuclide Extraction Laboratory, and further analysis of exhumation and basin-scale erosion will be possible when these data are returned

RESULTS

Compilation of Digital Maps

Visualization of my results in general is aided by three basemaps that I assembled in GIS: a DEM mosaic, a DRG mosaic (essentially a large digital topographic map composed, in this case, of four 7.5' quadrangles), and a georectified mosaic of three scanned geologic maps for my study area.

The DEM (Fig. 10) spans from the Continental Divide on the western fringe to the western city limits of Boulder, CO on the eastern edge. It spans north to south from about Niwot Ridge on the Ward quadrangle to Rollinsville, CO on the Nederland quadrangle. These broad dimensions incorporate all of the area that is immediately relevant to my work.

The DRG (Fig. 9) is made up of the Ward, Nederland, Gold Hill, and Tungsten USGS 1:24,000 topographic quadrangles, and I used it as a reference baselayer for the GPS points that I collected. This more focused look at my study area is equal in area to the middle half of the larger DEM mosaic.

The scanned, georectified geologic maps cover the Nederland, Ward, and Tungsten quadrangles (Fig. 11). A geologic map of equal detail is not available for the Gold Hill quad. These geologic maps are useful for general comparisons between

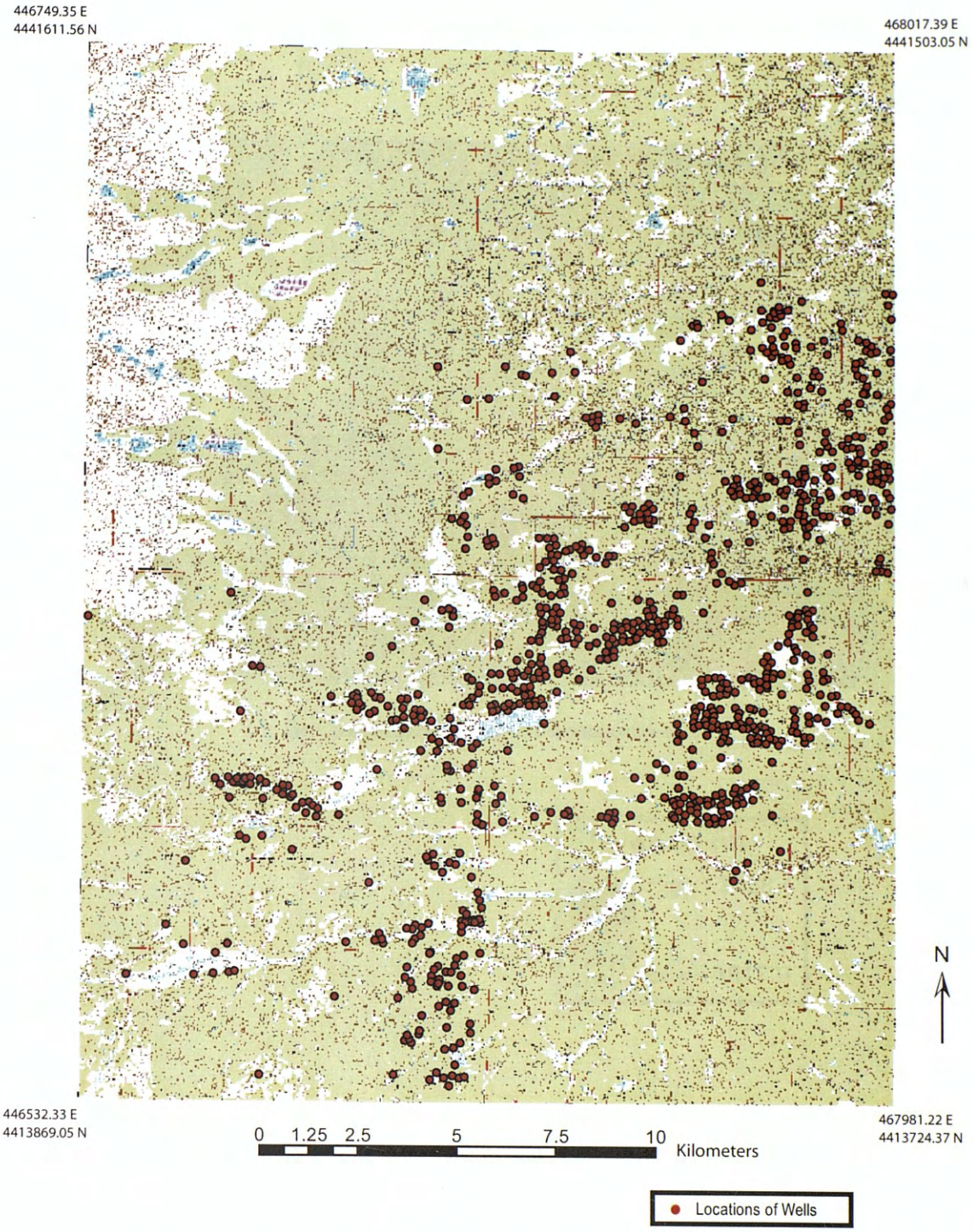

Figure 9. Digital Raster Graphic mosaic of Nederland, Ward, Tungsten, and Gold Hill quadrangles showing locations of well log data (894 wells); coordinates in UTM (NAD 83).

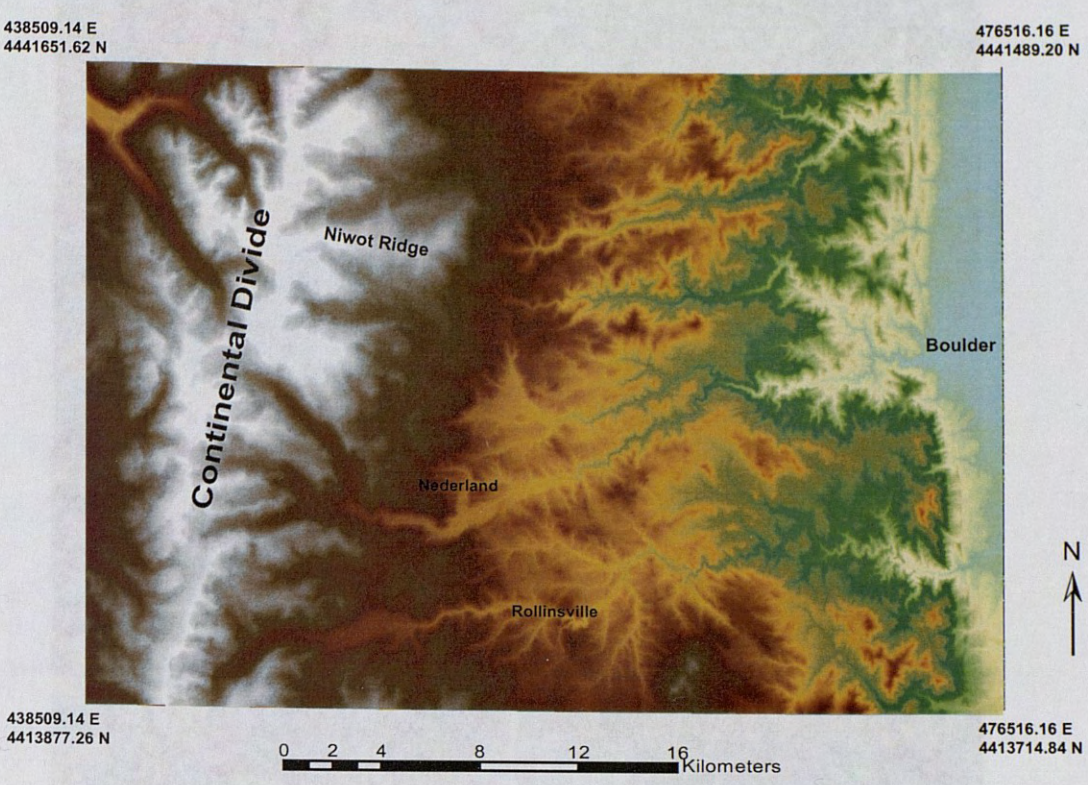

Figure 10. Digital Elevation Model (DEM) mosaic of 1:24,000 Monarch Lake, East Portal, Ward, Nederland, Gold Hill, Tungsten, Eldorado Springs, and Boulder DEMs; coordinates in UTM (NAD 83).

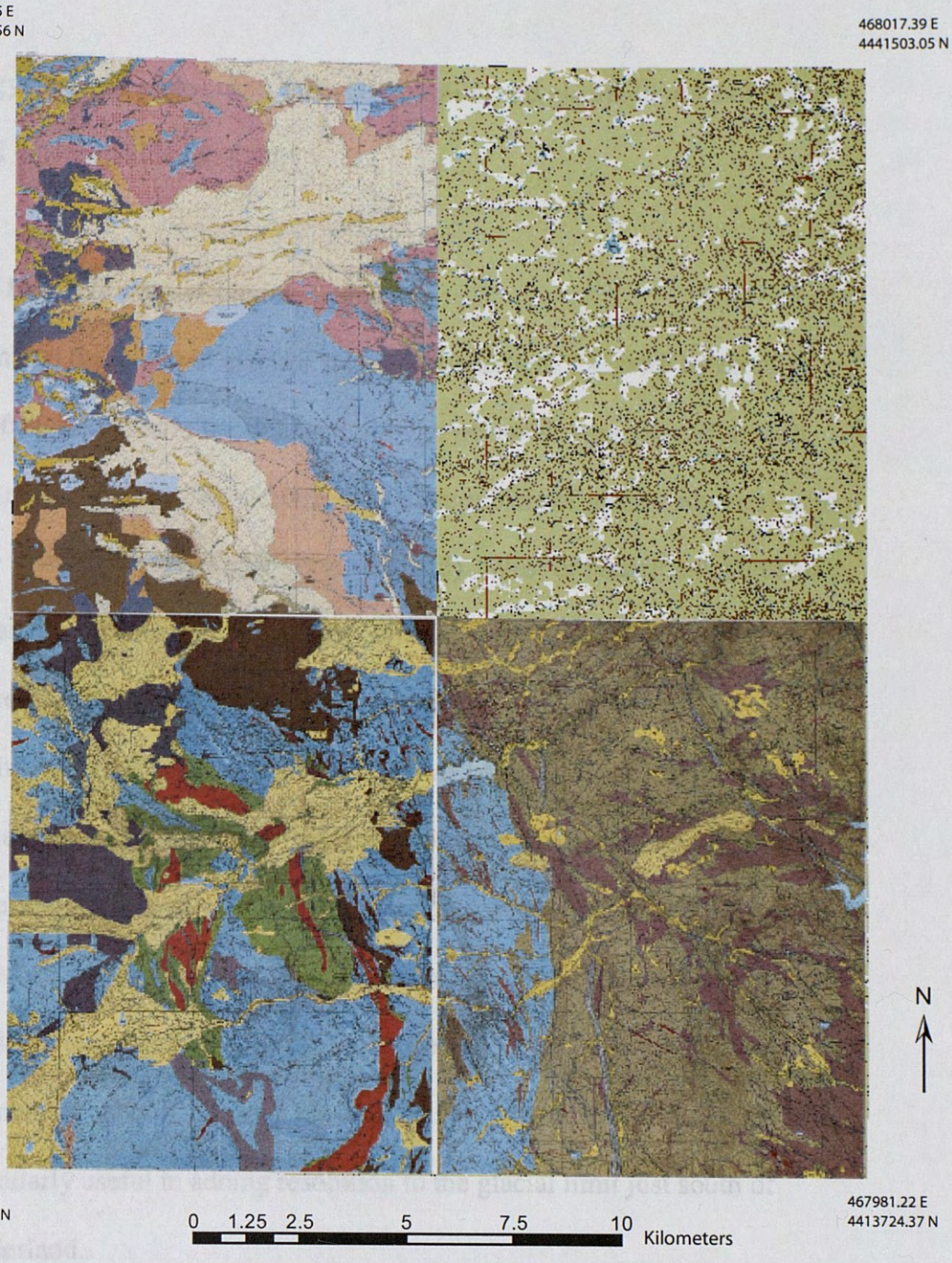

Figure 11. Mosaic of Nederland geologic quadrangle (Gable, 1969), Ward geologic quadrangle (Gable and Madole, 1976), and Tungsten geologic quadrangle (Gable, 1972); coordinates in UTM (NAD 83).

bedrock geology, patterns of deep and surficial saprolite, and glacial limits that Peter Birkeland and I determined in the field.

Bull Lake and Pinedale Glacial Limits

I determined the extent of glaciation around Nederland, CO both by direct observation of fringe erratics in the field and through personal communication with Pete Birkeland during the summer of 2002. The eastern limit of glacial advances is to the present day west bank of Barker Reservoir (Fig. 5). West of Nederland, there are a number of glacial moraines and alluvial deposits that Birkeland mapped by bicycle. Birkeland's careful mapping only goes as far west as the town of Eldora. However, surficial deposits west of Eldora are composed mainly of broad alluvial deposits and erratics. Their extent is important, but they are minimal in volume compared to the weathered material which covers the rest of the landscape.

I mapped the maximum extent of the glaciers as extending from a hairpin turn south of Nederland, down to the banks of Barker Reservoir, and then north to the Nederland elementary school. My own observations fit in well with Birkeland's map, and were particularly useful in adding resolution to the glacial limit just south of downtown Nederland.

Distribution and Thickness of Saprolite

The spatial distribution and thickness of saprolites throughout the study area aids our understanding of deep weathering patterns in the greater Nederland area. My saprolite data was necessarily collected along primary, secondary, and tertiary roads,

and this pattern of collection may produce some artifact patterns in statistical interpolations.

Both Kriging and IDW interpolations of my Clayton (1979) classifications for surface saprolite exposures produced similar patterns (Fig. 12 and 13). The most highly weathered material (classes 5-7) are located in a pocket south of Barker Reservoir and in a pocket near Rollinsville. Intermediately weathered rock (classes 3-4) trend NW-SE in a band 4-6 km wide, and their extent remains statistically significant (within the bounds of the interpolation models) for 20-30 km both north and south of Nederland. Fresh rock (classes 1-2) fringes the intermediately weathered rock, and it is located in two significant pockets in Nederland proper and in the vicinity of Winiger Ridge.

A bar graph for the different classes of weathered rock throughout the study area (Fig. 14) is roughly symmetrical around a mode of class 4, although there is more weight to the left of the mode which corresponds with less weathered rock. In general, the landscape is dominated by rock that is weathered to intermediate values.

Distribution of Depth to Bedrock from Well Logs

Depth to bedrock varies widely both in magnitude and in the spatial distribution of different depths throughout my study area. A histogram for depths to bedrock from the 894 well logs from the Nederland, Ward, Gold Hill, and Tungsten quadrangles, shows a distribution that is highly skewed to the right (Fig. 15a). There is a minimum value of 0 m for well #54404 and a maximum value of 92.5 m for well #183705 with a mode between 0 and 10m. Excluding the thickest 7% of the

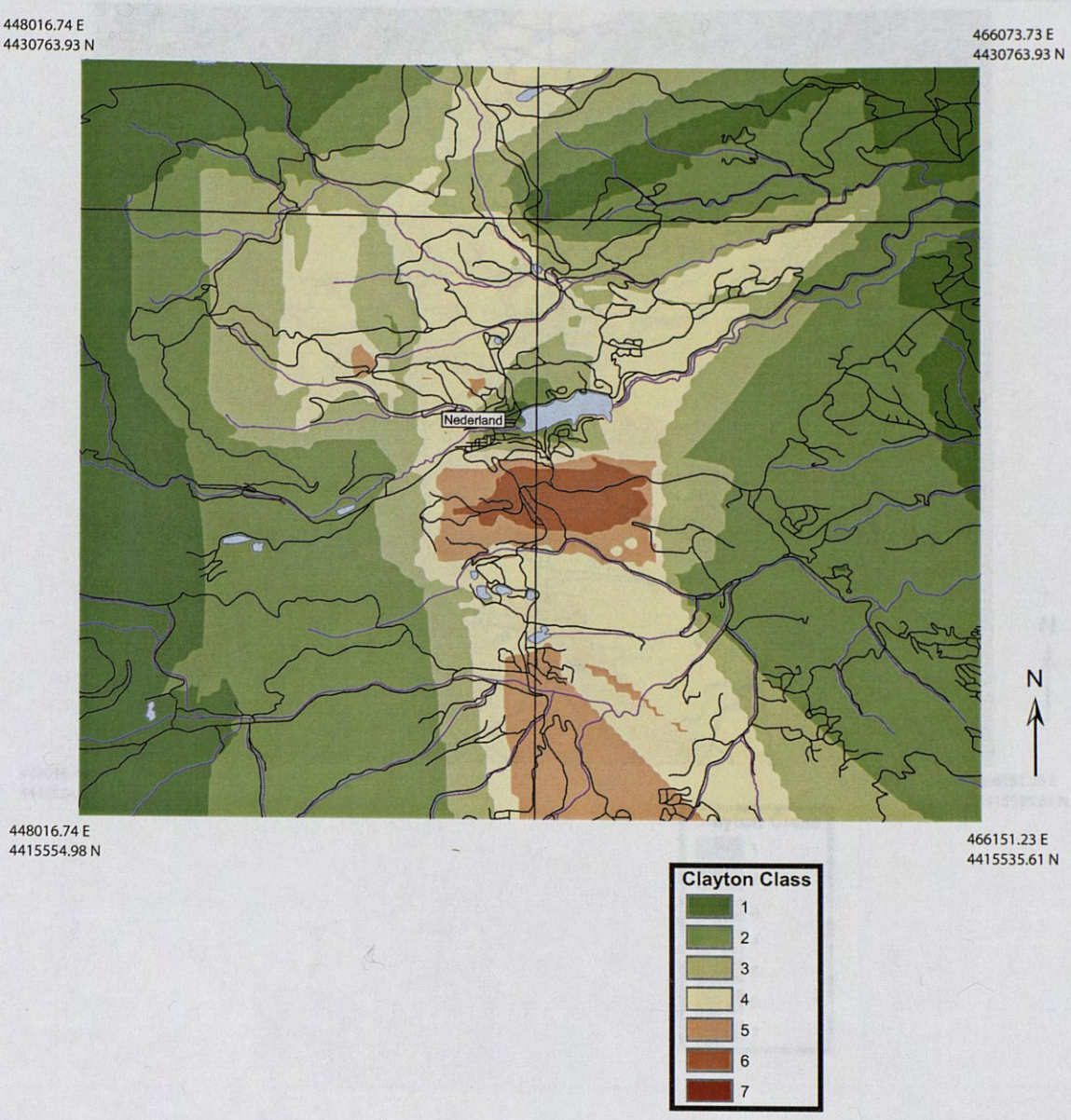

Figure 12. Krige spatial interpolation of saprolite classifications (Clayton, 1979); 1 is least weathered, 7 is most weathered; Based on 225 points; Coordinates in UTM (NAD 83).

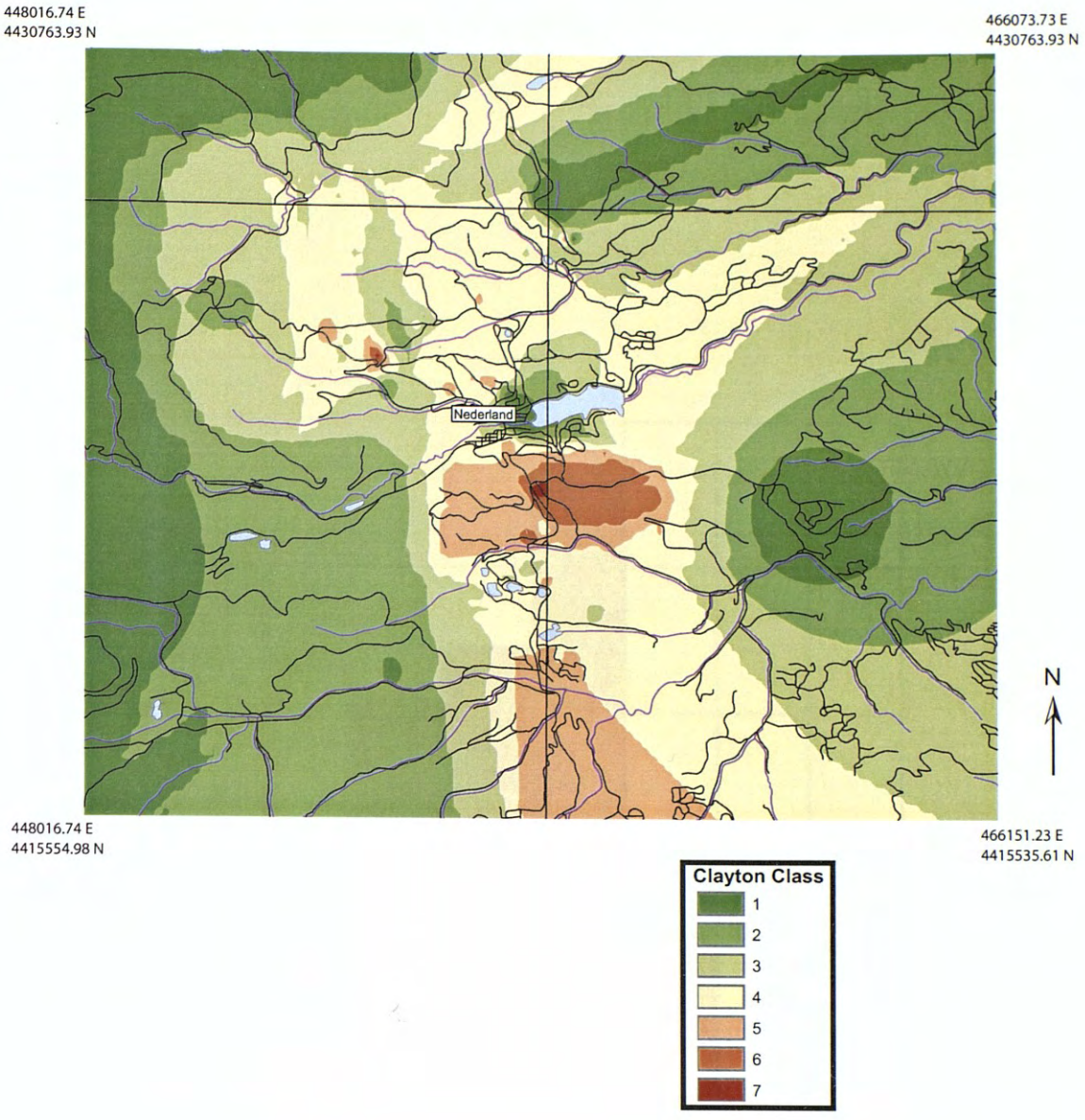

Figure 13. Inverse Distance Weighted (IDW) spatial interpolation of saprolite classifications (Clayton, 1979); 1 is least weathered, 7 is most weathered; Based on 225 points; Coordinates in UTM (NAD 83).

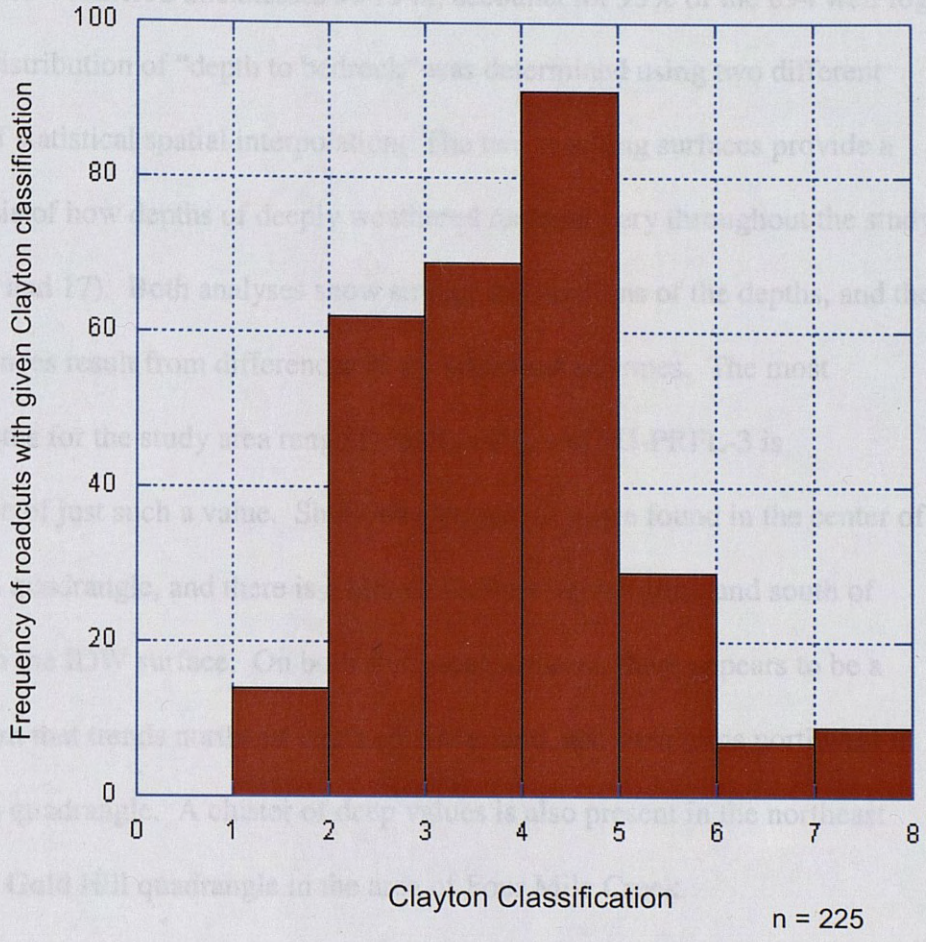

Figure 14. Histogram for Clayton (1979) classifications of roadcuts near Nederland.

data yields a distribution for depths less than 15 m which is still skewed (Fig. 15b), but much more useful for the analysis of this variable. This limited distribution is right skewed with a minimum value of 0 m and a maximum value of 15 m with two modes around 0m and 4m. As mentioned before, this more restricted histogram, which excludes weathered thicknesses >>15 m, accounts for 93% of the 894 well logs. The spatial distribution of "depth to bedrock" was determined using two different techniques of statistical spatial interpolation. The two resulting surfaces provide a visual analysis of how depths of deeply weathered material vary throughout the study area (Fig. 16 and 17). Both analyses show similar distributions of the depths, and the slight differences result from differences in the statistical schemes. The most common depths for the study area range from 3 to 6m, and MJ-PRFL-3 is representative of just such a value. Shallower values <3 m are found in the center of the Tungsten quadrangle, and there is a hint of shallow values north and south of Nederland on the IDW surface. On both statistical surfaces, there appears to be a band of >10 m that trends northeast south of Nederland, and then turns northwest in the Tungsten quadrangle. A cluster of deep values is also present in the northeast corner of the Gold Hill quadrangle in the area of Four Mile Creek.

Distribution of Alluvial Cover from Well Logs

There is very little thick alluvial cover in my study area, and where it is present, it is concentrated in pockets within valleys. The distribution of alluvial cover is extremely skewed to the right with a maximum of 55 m for well #86739 and a minimum of 0 m for well #160369 with a mode of 0m (Fig. 18a). Excluding

a)

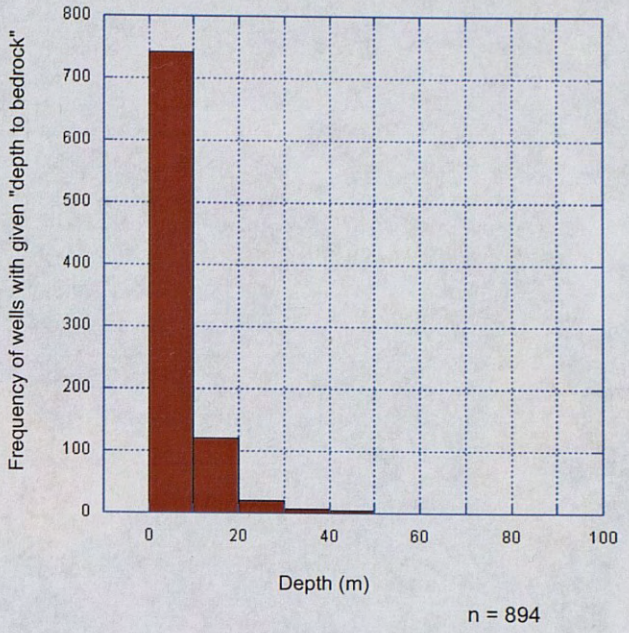

b)

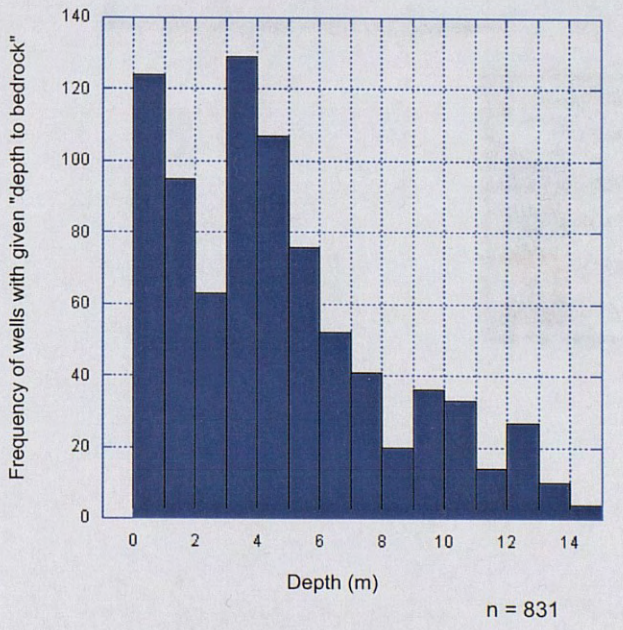

Figure 15. Histograms for "depth to bedrock" including all values (a), and values <15 m (b).

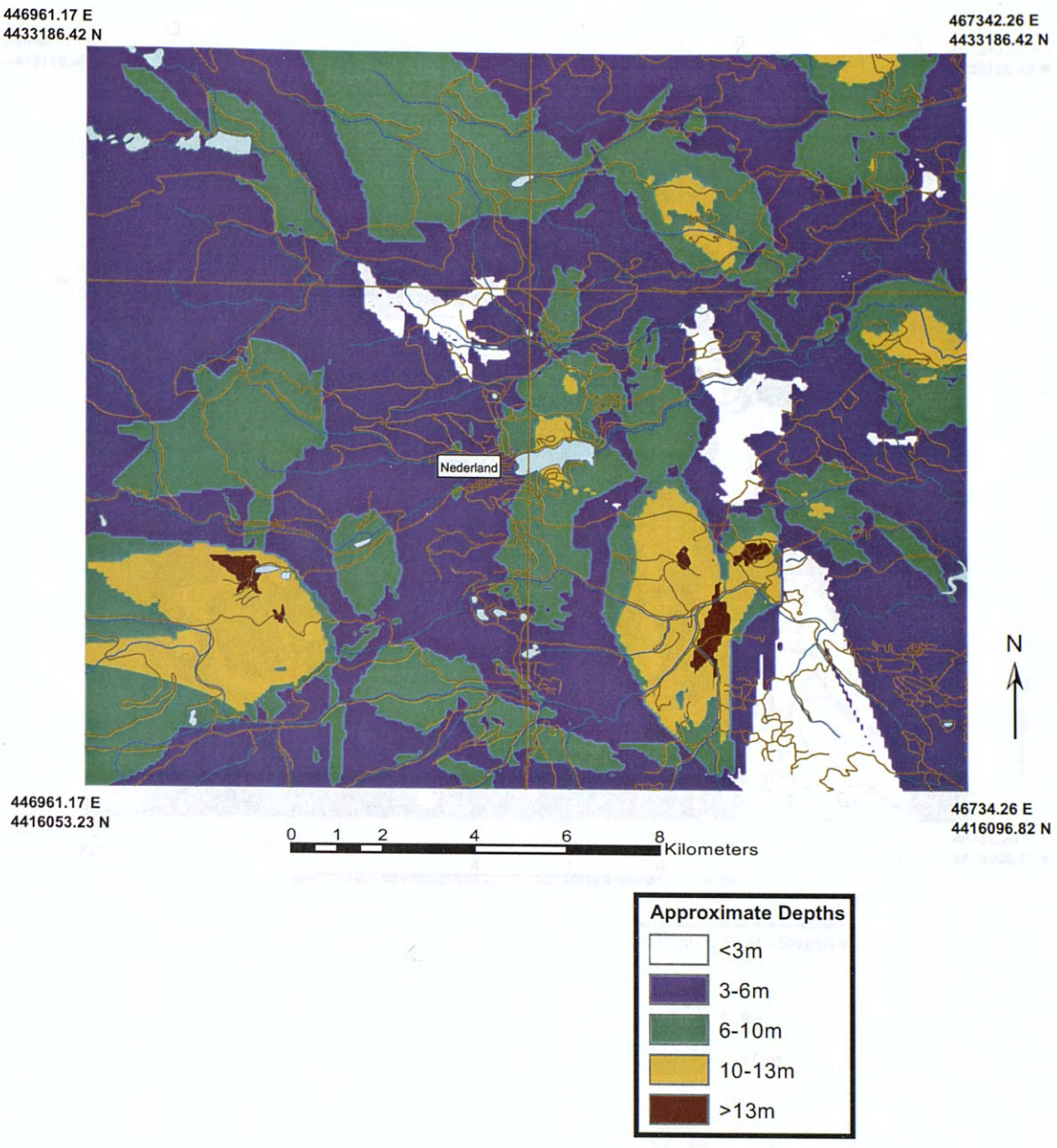

Figure 16. Krige spatial interpolation for "depth to bedrock" from 894 well logs in the Nederland, Ward, Tungsten, and Gold Hill USGS 7.5' Quadrangles; coordinates in UTM (NAD 83).

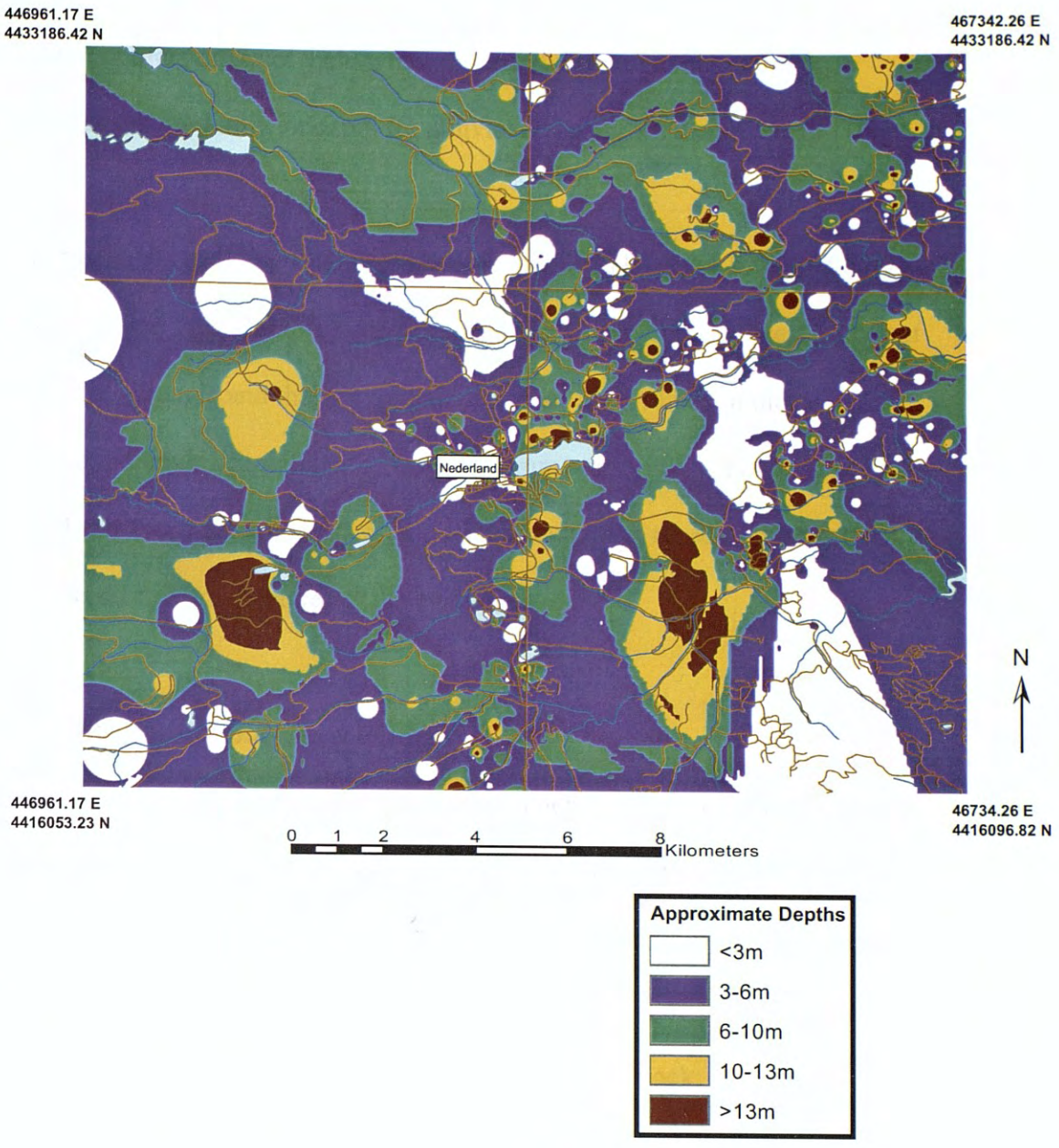

Figure 17. Inverse Distance Weighted (IDW) spatial interpolation for "depth to bedrock" from 894 well logs from the Nederland, Ward, Tungsten, and Gold Hill USGS 7.5 ' Quadrangles; Coordinates in UTM (NAD 83).

extremely high outliers does not yield a more useful distribution, but rather underscores that the predominant depth for alluvial cover across the area is 0m (Fig. 18b).

The spatial distribution of alluvial cover is simple in both the IDW and Krige analyses (Fig. 19 and 20). Depths of >6m are concentrated in the southwest corner of the Nederland quadrangle and there is a small pocket of deep values in the center of the Tungsten quadrangle. Significantly, deep alluvium apparently is not present in the Gold Hill and Ward quadrangles. Shallow alluvium, <3 m (predominantly 0 m), is found across all four quadrangles of the study area.

Saprolite Profile Density and Geochemistry

The density of saprolite should increase with depth to the fresh bedrock contact, where the density should be approximately 2.6 g/cm^3. Profile MJ-PRFL-3 serves as a good example of such a relationship above the lithology shift at 4m (Fig. 21). This change in density (along with a change in color), is a distinguishing feature that drillers use to determine when the have reached fresh bedrock; the density boundary at about 3m in MJ-PRFL-3 is consistent with many of the "depth to bedrock" values reported from the well log data for the area.

The geochemical data returned for saprolite profiles MJ-PRFL-1, MJ-PRFL-2, and MJ-PRFL-3 give a mixed impression of how the rocks have been weathered from the surface down to the fresh bedrock contact. Ideally, oxides such as Fe_2O_3 should become concentrated in highly weathered rock as other oxides such as CaO and Na_2O are removed in solution. Using MJ-PRFL-3 as an example, this pattern is followed in

a)

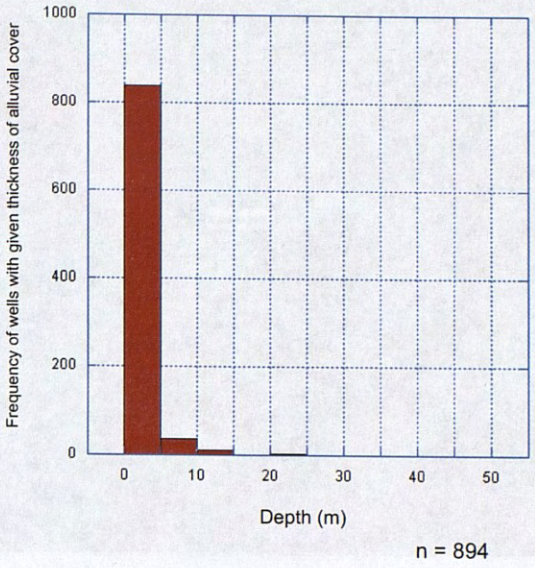

b)

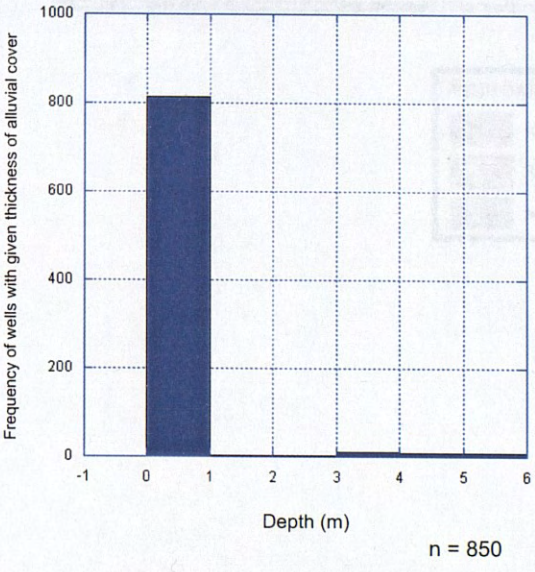

Figure 18. Histograms for alluvial cover including all values (a), and values <6 m.

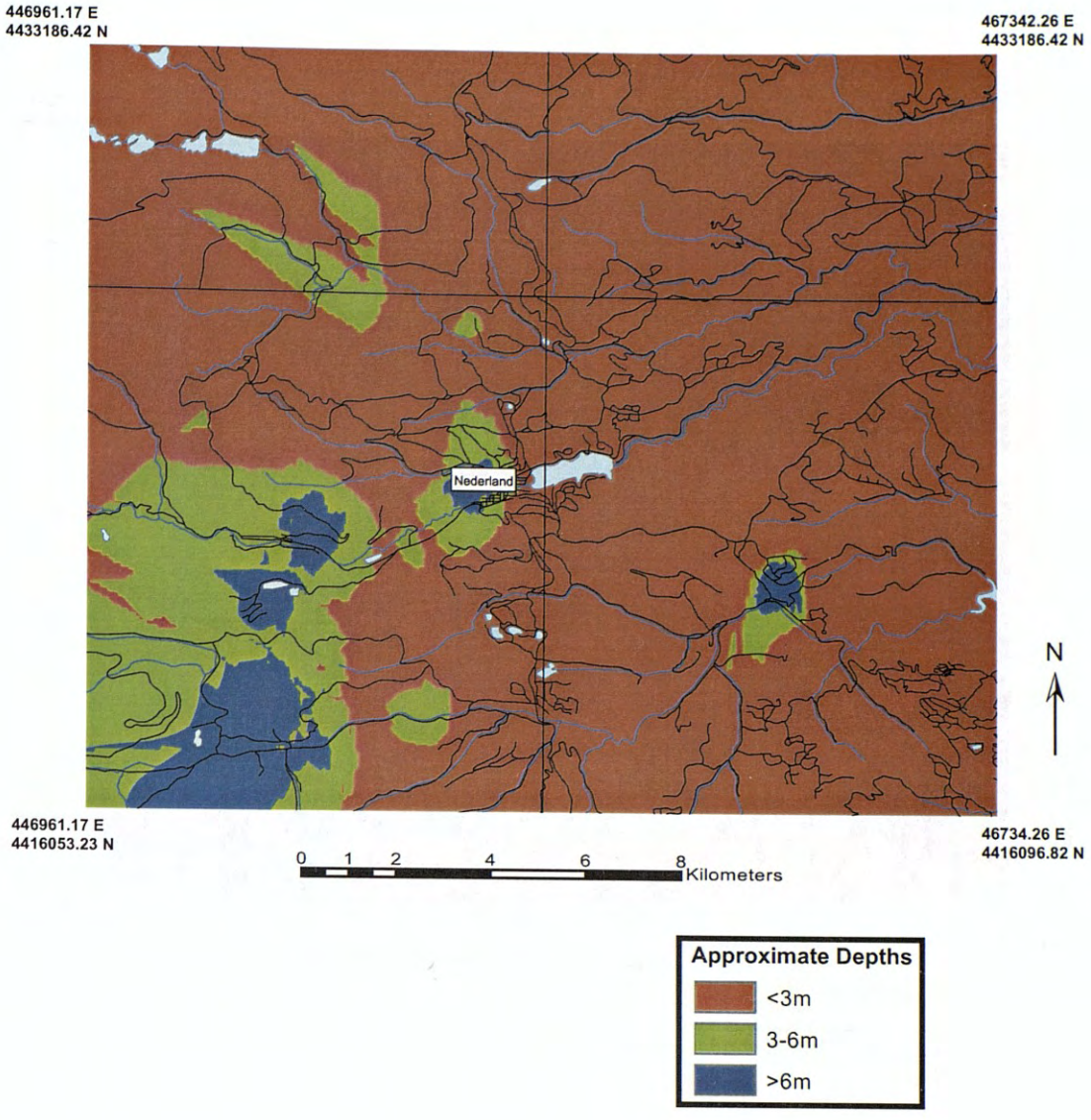

Figure 19. Krige spatial interpolation for thickness of "alluvial cover" from 894 well logs (69 wells with thickness >3 m) from the Nederland, Ward, Tungsten, and Gold Hill USGS 7.5' Quadrangles; coordinates in UTM (NAD 83).

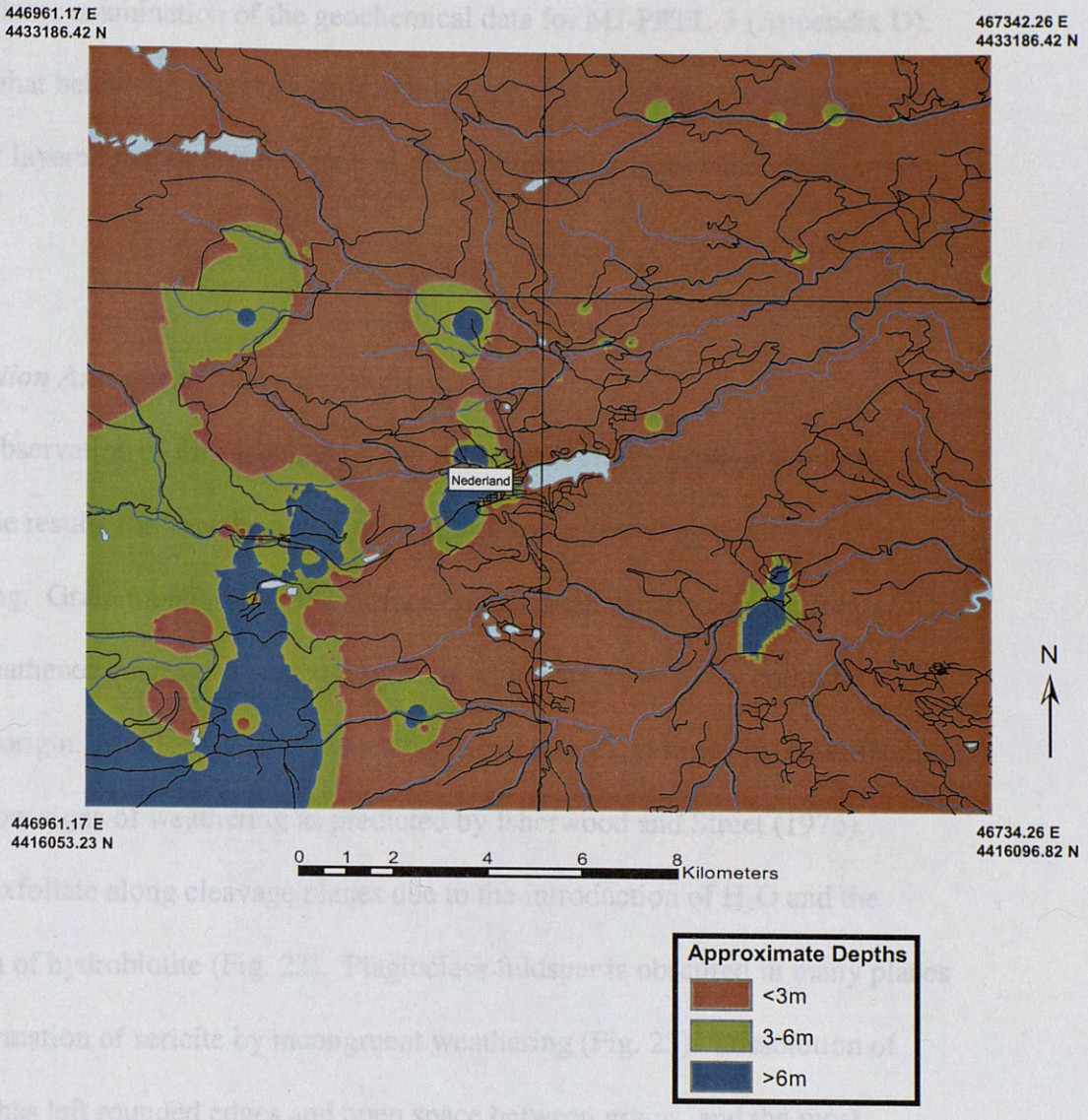

Figure 20. Inverse Distance Weighted (IDW) spatial interpolation for thickness of "alluvial cover" from 894 well logs (69 wells with thickness > 3 m) from the Nederland, Ward, Tungsten, and Gold Hill USGS 7.5' Quadrangles; Coordinates in UTM (NAD 83).

part to a depth of 4m, but after that the relationship becomes noisy (Fig. 22).

Closer examination of the geochemical data for MJ-PRFL-3 (Appendix D), suggests that below 4m there is a shift in lithology. Local changes in lithology are typical of layered metasediments such as the biotite gneiss from which this saprolite formed.

Thin Section Analysis of Saprolite Profiles

Observation of thin sections for my different saprolite profiles produced reasonable results for how the rocks' mineralogy was affected by degree of weathering. Grain mounts from the surface contain both weathered rock fragments and unweathered quartz-dominated fragments which are most likely colluvial or eolian in origin. Shallow samples which correspond to Clayton (1979) classifications of 5-7 show signs of weathering as predicted by Isherwood and Street (1976). Biotites exfoliate along cleavage planes due to the introduction of H_2O and the formation of hydrobiotite (Fig. 23). Plagioclase feldspar is obscured in many places by the formation of sericite by incongruent weathering (Fig. 23). Dissolution of minerals has left rounded edges and open space between grains, and the most weathered samples needed to be impregnated with epoxy before mounting.

Deeper samples corresponding to classes 1-2 mainly are unweathered and their mineral grains are completely intact with sharp coherent boundaries between one another. Plagioclase is unburdened by sericite, and twinning is still crisp and unaltered (Fig. 23). Biotites have crisp edges and strong cohesiveness along cleavage planes. Samples for classes 3-4 are necessarily transitional with some

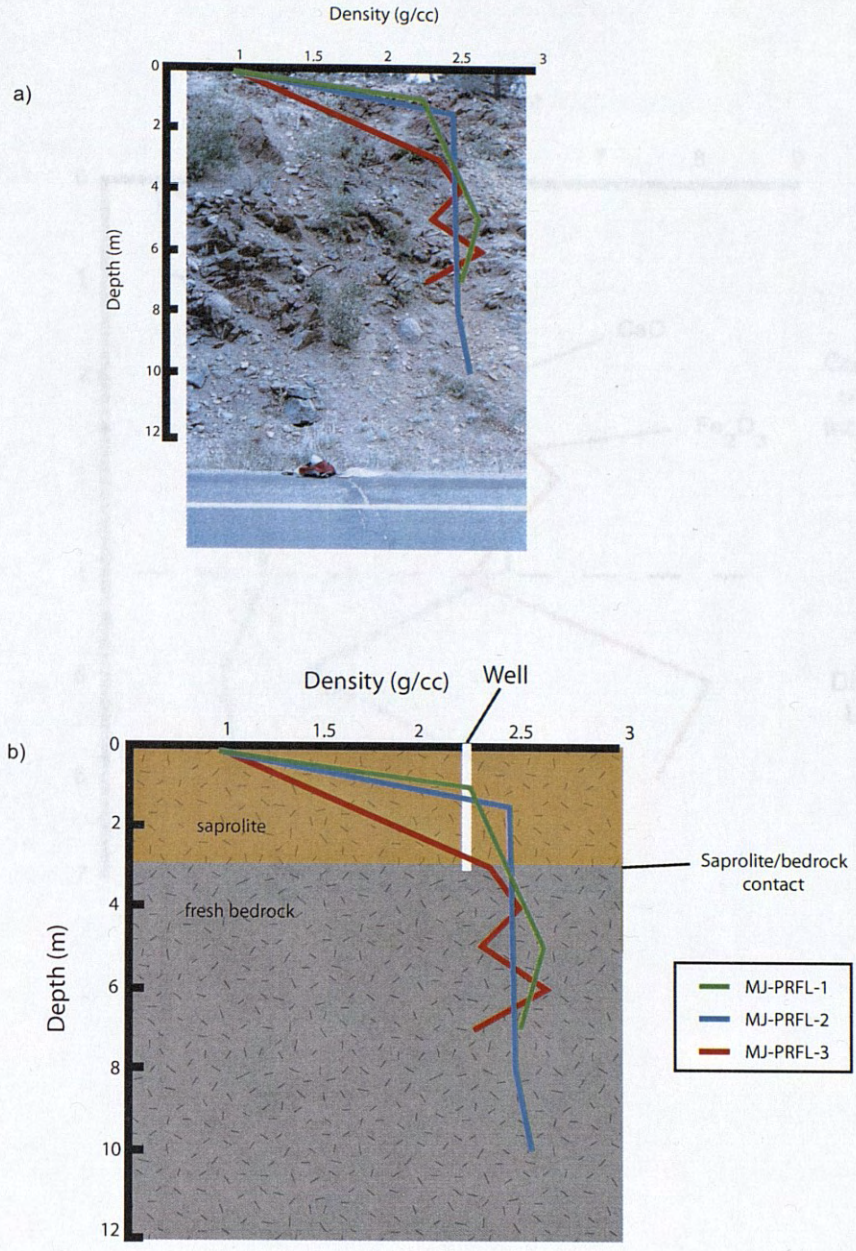

Figure 21. a) Photograph of MJ-PRFL-3 with saprolite density profiles from MJ-PRFL-1, MJ-PRFL-2, and MJ-PRFL-3 superimposed; b) sketch of saprolite density profile using samples from MJ-PRFL-1, MJ-PRFL-2, and MJ-PRFL-3.

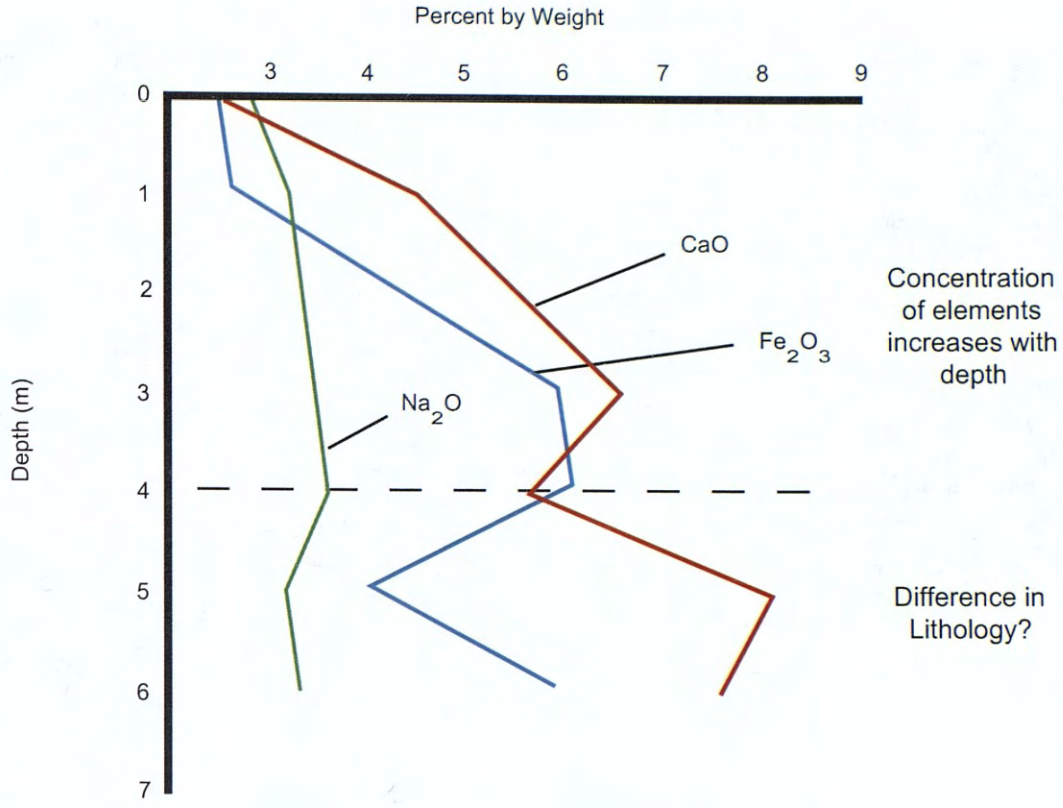

Figure 22. Plot of weight percent by depth for selected oxides from MJ-PRFL-3.

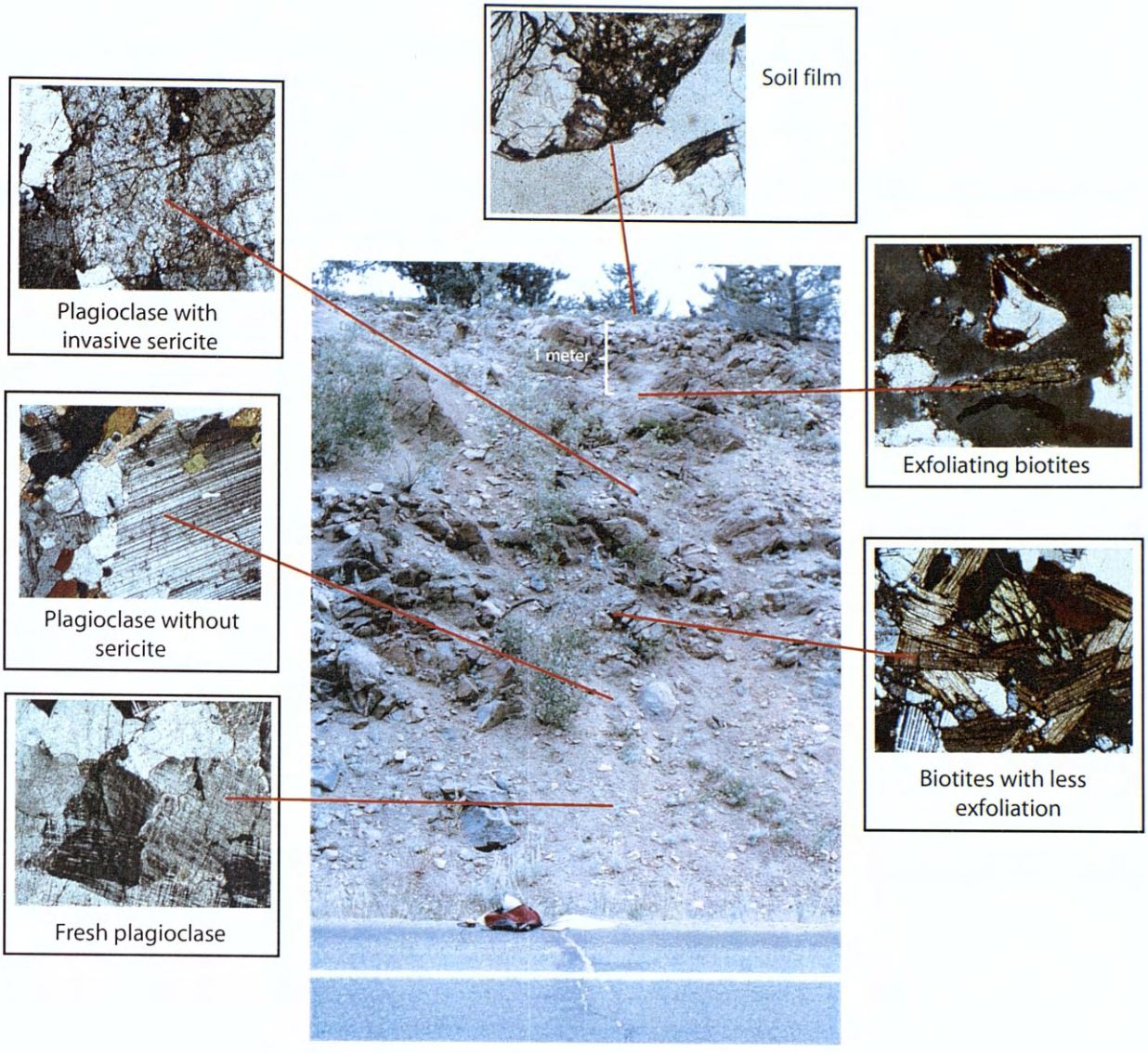

Figure 23. Saprolite profile with photomicrographs of mineral composition by depth for MJ-PRFL-3.

mineral grains beginning to show signs of weather while others remain fresh. The samples at the extremes of the profiles are most illustrative when considering chemical weathering on the scale of mineral grains.

DISCUSSION

Birkeland and his coauthors (2003, in press) estimate that it takes >>100,000 years for deeply weathered saprolite to form in the climate of the Colorado Front Range near Boulder, CO. Thick soils and saprolite must be preserved on stable sites. Dethier and others (2002) estimate, however, that erosion rates in the saprolite area are ~20 m/m.y. for at least the last 30 ka. How can these estimates be reconciled and what controls where weathered material still remains within my study area? When did the weathered material form? An understanding of how the locations of weathered vs. unweathered material are affected by modern erosion rates and recent shifts in climate can help provide us with a clearer picture of how the regional landscape is evolving.

Saprolite and the Glacial Margin

A comparison of the distribution of surficial and deep saprolite deposits with the glacial margin as mapped by Birkeland and myself suggests that glacial scouring must have constrained where weathered material remained after the last glacial advance approximately 15,000 years ago. A pocket of highly weathered (class 7) rock fringes the glacial limit just south of Nederland, and there is another significant area of deep saprolite to the southeast of Barker Reservoir. Another pocket of highly weathered surficial deposits is located several kilometers south of Nederland in the neighborhood of Rollinsville, CO. These sites are also outside of the glacial limit for the region, although its extent may be an artifact of the statistical modeling.

Within the glacial limit near Nederland, rocks are not deeply weathered (Fig. 5, 12, 13, 16, and 17). In fact, the boundary between fresh rock and weathered rock both north and south of Nederland proper could almost be used, along with glacial erratics and moraines, to map the glacial limit. Small pockets of weathered material fringe the margin as it tapers to the northeast, and from the depths to bedrock, a thick deposit of weathered material is located just beyond the easternmost extent of the glacial limit.

Weathered bedrock vs. Alluvial Deposits

Topographical highs and lows are an important defining factor in the relationship between weathered bedrock vs. alluvial material. Alluvial material is scarce in my study area and it is limited primarily to glaciated valleys, whereas deeply weathered material is found outside glaciated areas and on topographic highs between glaciated valleys (Fig. 5, 19, and 20). The largest volume ($2.0 * 10^8$ m^3) of alluvial material is found across an area of about 20 km^2 to the southwest of Nederland near Boulder Park, along South Boulder Creek. Like the other alluvial deposits in the area, these are primarily limited to the valley. There is a similar deposit of alluvium due north from the Boulder Park alluvium in the valley of Middle Boulder Creek which covers about 30 km^2 with a volume of $1.53 * 10^8$ m^3. These two models' patterns are supported by Gable's (1969) maps of Quaternary deposits in the same areas. Gable maps this material more extensively than my spatial interpolations predict, but both my model and her mapping agree that there is extensive alluvial cover along Middle and South Boulder Creeks on the Nederland

quadrangle, and a tongue of deposits extends to the glacial limit on the west bank of Barker Reservoir. A third, more elongate area of deep alluvium is across Winiger Ridge on the Tungsten quadrangle, which is mapped by Scott and Taylor (1986) to be sedimentary fill within a Miocene paleovalley.

In general, deep saprolite deposits have distinct boundaries that separate them from alluvial material. Between Middle and South Boulder Creeks' alluvial deposits, deep saprolite can be found on a ridge, and the roadcut saprolites just south of Nederland are similarly found on a topographical high. This pattern of saprolite along ridges can be seen more generally in one of the 3-D renderings of the depth to bedrock interpolations (Fig. 24, 25, 26, and 27). Deep weathered material in the northeast corner of the Gold Hill quadrangle is perched on a ridge and deeply weathered rock that extends along a ridge north of Fourmile Creek. The broader pattern of intermediately weathered and intermediately deep saprolite (3 to 6 m) crosscuts valleys and ridges, making it harder to assign a topographical control to them.

The presence of intermediate thicknesses of saprolite within glaciated margins is not contradictory to glacial scouring of glacial material. It can be presumed that glaciers removed the most highly weathered material in their paths and greatly reduced the depth of saprolite within glaciated valleys without removing *all* the weathered material.

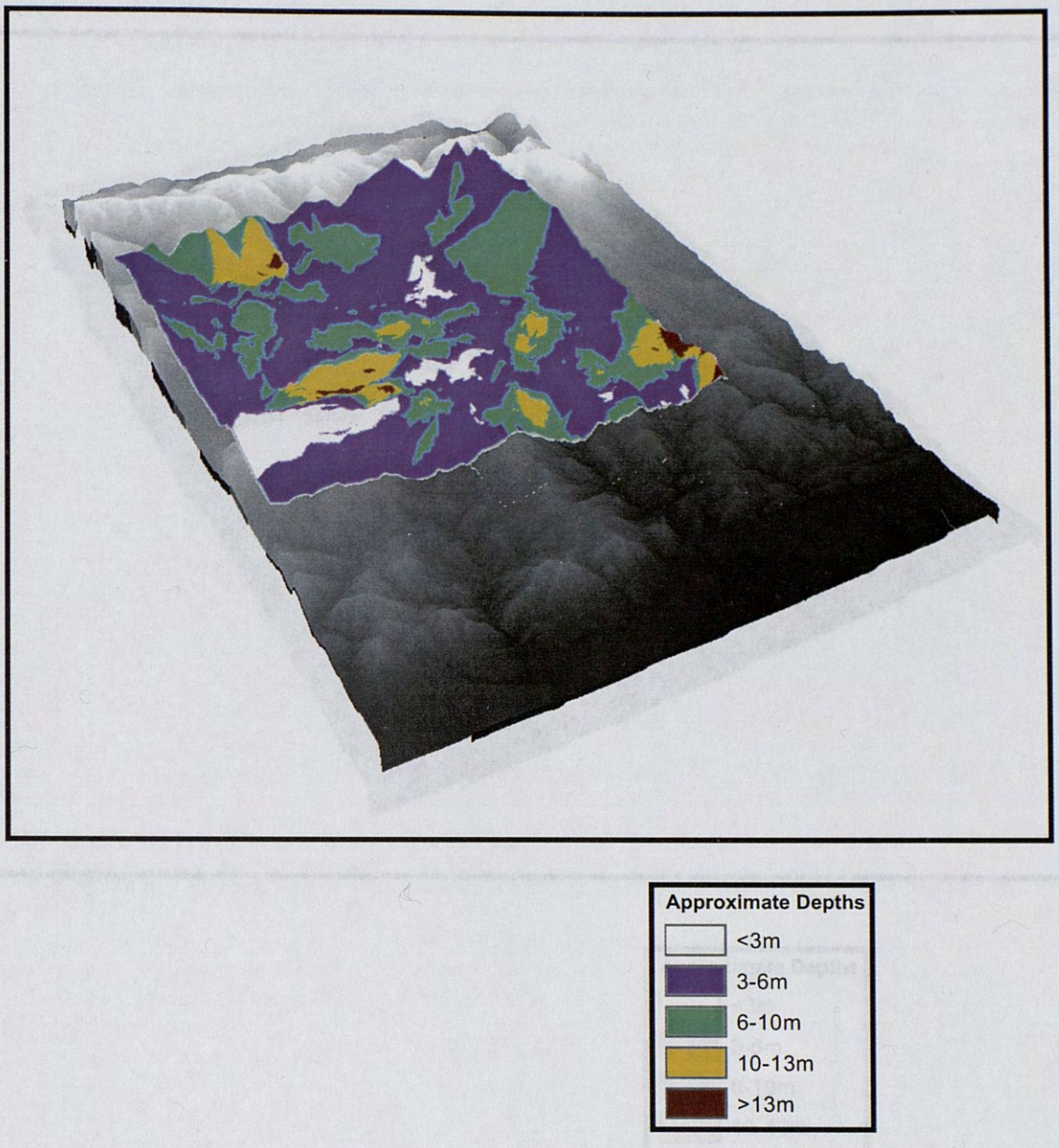

Figure 24. Krige spatial interpolation for "depth to bedrock" from 894 well logs in the Nederland, Ward, Tungsten, and Gold Hill USGS 7.5' Quadrangles draped over DEM (V.E. = 2.5); view from SE.

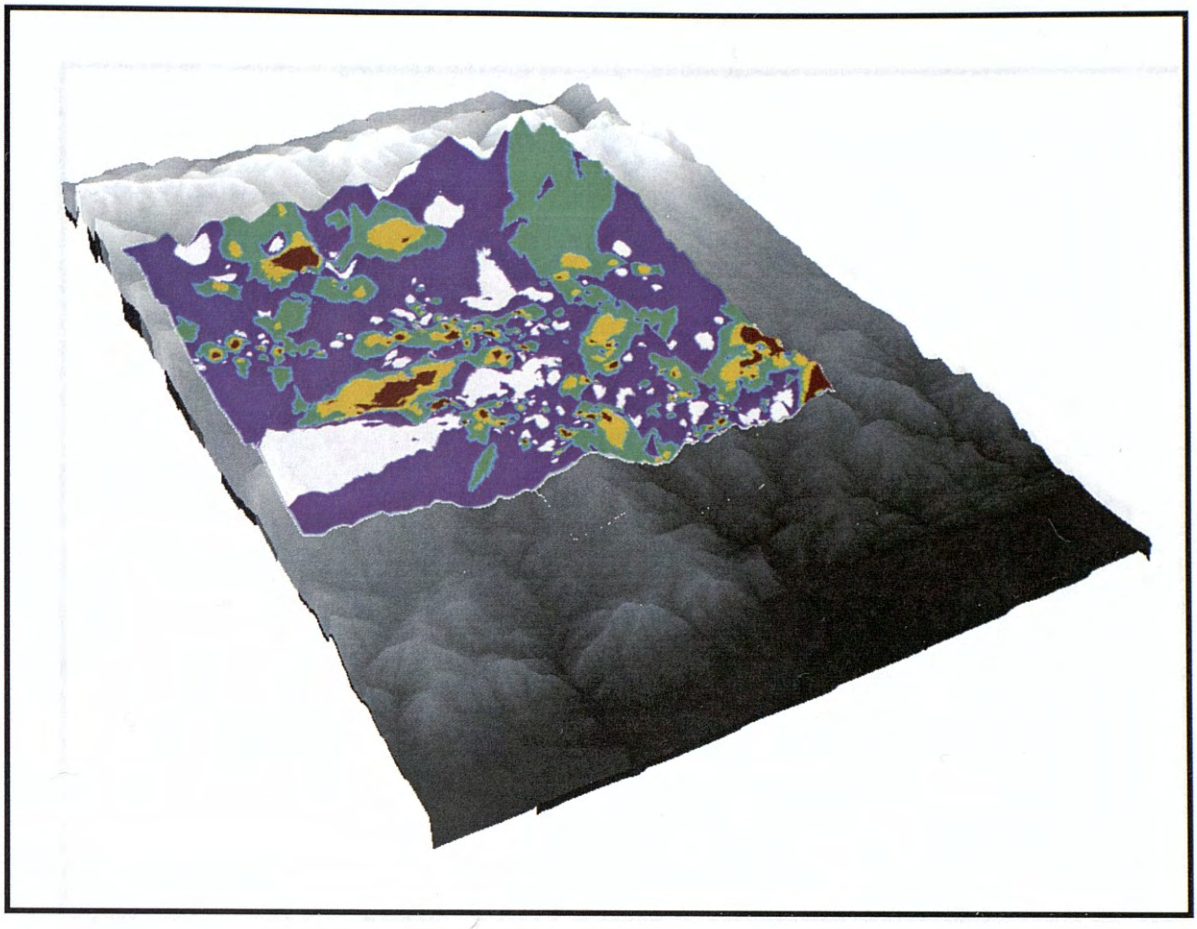

Figure 25. IDW spatial interpolation for "depth to bedrock" from 894 well logs in the Nederland, Ward, Tungsten, and Gold Hill USGS 7.5' Quadrangles draped over DEM (V.E. = 2.5); view from SE.

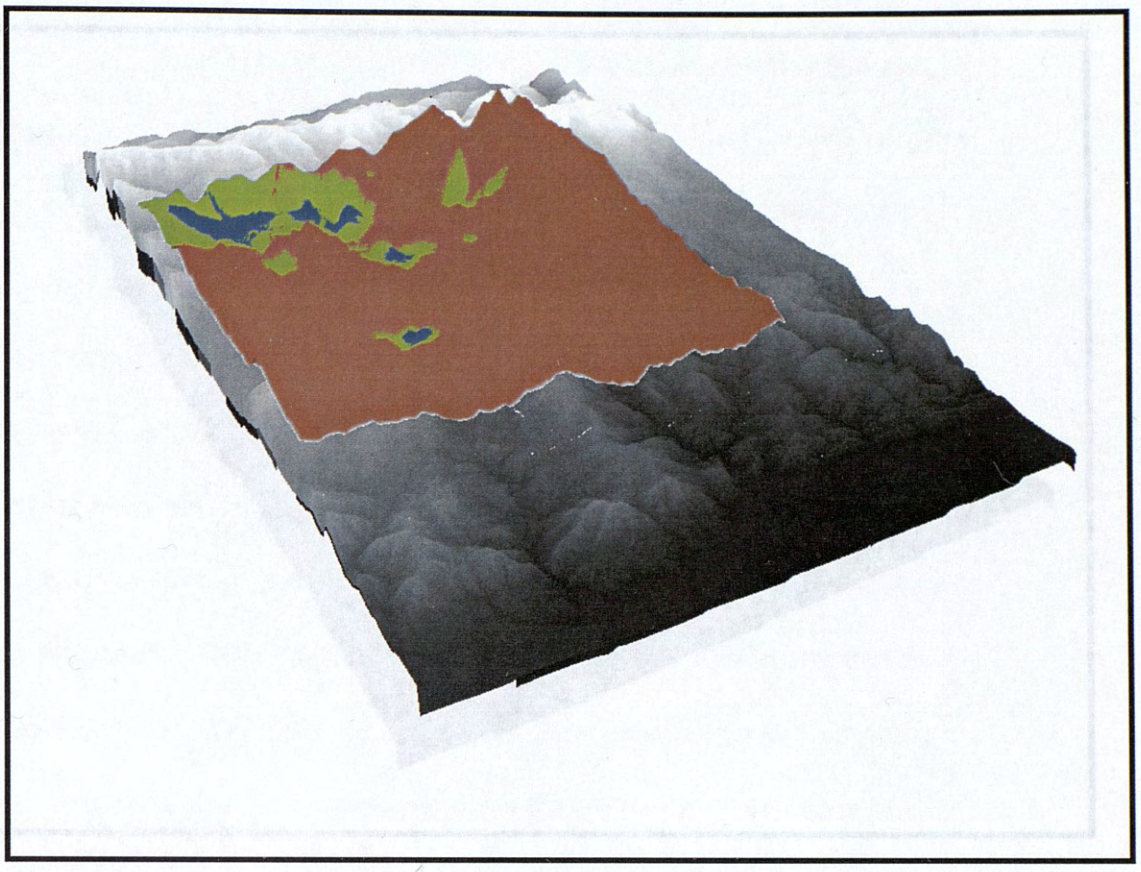

Figure 26. Krige spatial interpolation for thickness of "alluvial cover" from 894 well logs from the Nederland, Ward, Tungsten, and Gold Hill USGS 7.5' Quadrangles; draped over DEM (V.E. = 2.5); view from SE.

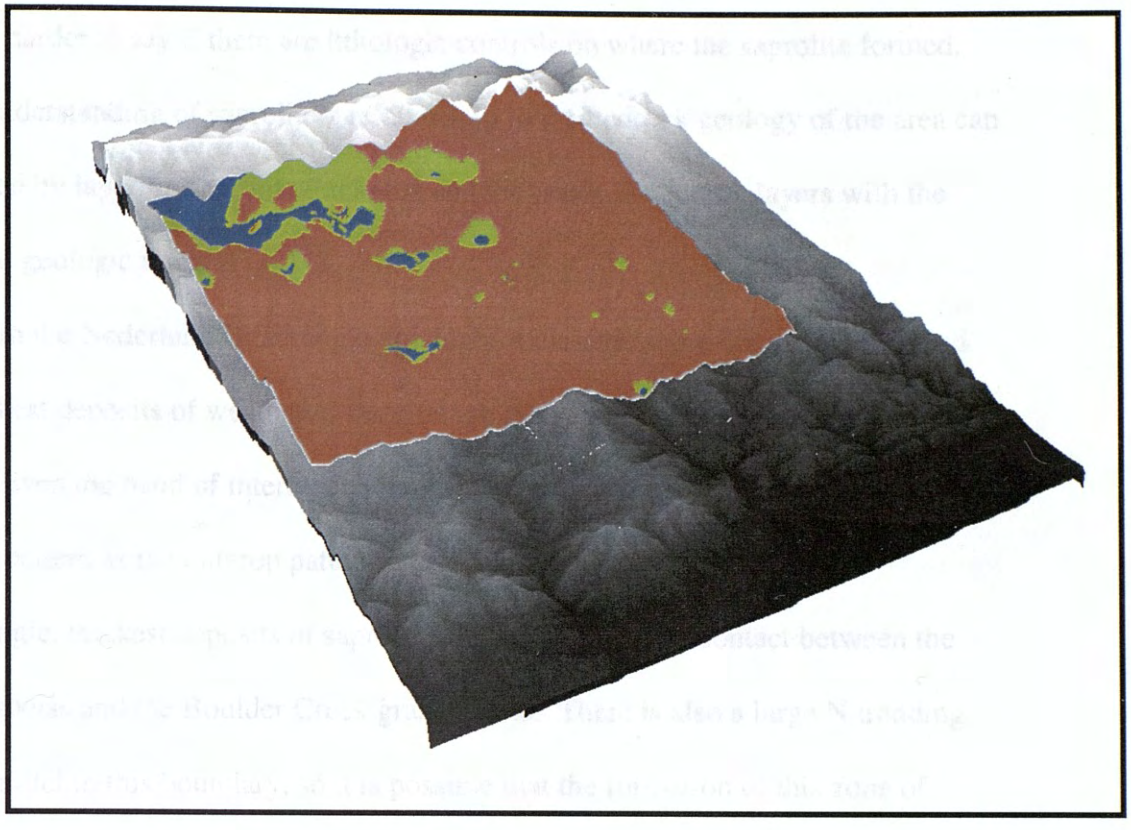

Figure 27. IDW spatial interpolation for thickness of "alluvial cover" from 894 well logs from the Nederland, Ward, Tungsten, and Gold Hill USGS 7.5' Quadrangles; draped over DEM (V.E. = 2.5); view from SE.

Ltihologic Controls on Saprolite Patterns

Topography constrains where weathered material remains in my study area, but it is harder to say if there are lithologic controls on where the saprolite formed. Some understanding of saprolite's relationship to the bedrock geology of the area can be gained by layering saprolite thickness and the depth to bedrock layers with the digitized geologic maps (Fig. 11).

In the Nederland Quadrangle, the highest classifications for weathering and the thickest deposits of weathered material are developed in the biotite gneiss (Gable, 1969). Even the band of intermediately weathered saprolites follows the same general pattern as the outcrop pattern of the biotite gneiss. In the Tungsten Quadrangle, thickest deposits of saprolite are found along the contact between the biotite gneiss and the Boulder Creek granodiorite. There is also a large N trending fault parallel to this boundary, so it is possible that the formation of this zone of saprolite was constrained by structure and lithology. Increased fluid flow along this fault could certainly enhance the dissolution reactions associated with saprolite formation.

The loose association of saprolite formation biotite gneiss (as opposed to the Boulder Creek Granodiorite) supports both my observations and Isherwood and Street's (1976) conclusions about how rocks in this region become grussified. Exfoliation of biotite and the formation of hydrobiotite seems to play the most fundamental role in turning fresh rock to weathered rock, and gneiss rich in biotite might be more susceptible to such processes. This is not to say that saprolite cannot form in other rock types; it is common to see saprolite formation in the granodiorite

as well. However, the mineralogical properties of the gneiss probably do allow for easier initiation of weathering and perhaps faster weathering rates.

A final lithologic control on weathering may be proximity to the Colorado Mineral Belt (Dethier, personal communication 2003). Enhanced weathering within the belt is suggested by the class 7 weathering in the heavily prospected area south of Barker Reservoir. Alteration within the mineral belt may weaken the fabric of rocks and make them more susceptible to weathering.

Explanation of Saprolite Exposure in the Greater Nederland Area

The mantle of weathered rock in my study area could not have formed during the Holocene considering the modern climate and Birkeland's estimates for how long it takes to form 1 m of saprolite. Assuming this is true, there must have been some condition that has allowed for the preservation of this easily eroded material.

According to Scott (1975), by late Eocene time a broad surface of low-relief had been formed in the Front Range due to post-Laramide erosion. Precambrian rocks underlying this surface in the modern landscape may have been weathered to depths of up to 10 to 40 meters (Scott 1975). Scott and Taylor (1985) mapped Late Eocene erosion surfaces across much of my study area east of Eldora and west of Boulder (Fig. 3). They also mapped a Miocene paleovalley which is preserved by fill material across Winiger Ridge to the southeast of Nederland on the Tungsten quadrangle. A paleovalley above the saprolite in my study area lends further evidence to burial of an Eocene surface during the Oligocene and/or Miocene. This

Eocene surface is by no means continuous in the modern landscape, but remnants persist above Boulder Canyon.

I propose that the saprolite in my study area formed as long ago as 30 to 40 Ma when the climate was wetter and warmer and thus more suited to chemical weathering. The Boulder Creek granodiorite and adjacent gneisses may have been weathered as deeply as 40 m, and then subsequently covered by younger deposits during Oligocene time, or the Miocene at the latest. Erosion after the Miocene could then have exhumed this saprolite and exposed it to enhanced erosion during the cyclic glaciations of the Quaternary.

Current Erosion Rates of Saprolite Terrain

Assuming that there was as much as 40 m of weathered material underlying an Eocene erosion surface in my study area, there must be some rate at which this saprolite is being stripped to leave the present landscape with a mean saprolite cover of 5 to 6 meters. Cosmogenic nuclides suggest that weathered Precambrian bedrock of the Colorado Front Range is eroding at a rate of 18-30 m/m.y. (Dethier et al., 2002). Extrapolating this rate back in time suggest that exposure of the saprolite occurred at 2 to 3 Ma, approximately the same time as the first continental-scale glaciation of North America. Such extrapolation is of course made cautiously since it assumes both a constant erosion rate over that time period and that saprolite deposits were distributed evenly and eroded evenly.

Related to this uneven erosion, Birkeland and his coauthors (in press 2003) estimate erosion rates for the Eocene surface on the order of << 1 m/100 k.y. and

perhaps as low as 0.1 m/100 k.y. These estimates are made from observations of very well developed soil profiles that should have taken about 100 k.y. to form with B_t horizons at ~1 m depth. Rates of denudation must have been low over a 100 k.y. period for these soils to have formed. It may be, though, that these well-developed soils are the exceptions rather than the rule across the Eocene surface. The Front Range is not lowering evenly across my study area, and these well-developed soils are likely located in areas whose stability has allowed not only their development, but also their preservation.

An erosion rate of 20 m/m.y. supports the claim that this saprolite must have formed at some time in the past, and that it could not have reached its current depths through modern weathering. If we generalize with a mean saprolite depth of 5m, erosion at Dethier et al.'s rate would strip the modern landscape of most of its weathered material in about 250 k.y. If it does indeed take the saprolite $\geq$100,000 years to form, then it does not seem feasible for today's weathered landscape to have formed under modern erosional conditions.

It is important to note that these inferences are drawn using the erosion rate measured for this terrain by Dethier et al. Many of these conclusions may or may not be modified when my own cosmogenic results are returned. My own erosion rates and surface exposure rates will provide additional insight into how both the saprolite terrain is eroding and how adjacent periglacial environments are evolving.

Implications for the Removal of Weathered Material from the Front Range

Modern patterns of erosion can be inferred both from the relationships observed between weathered material and the glacial limit and weathered material vs. alluvial material. It seems that during the last two glacial periods, a great deal of deeply weathered saprolite was scoured out of valleys, but saprolite still remains on some topographical highs. Modern erosion rates of 20 m/m.y. should remove most of the remaining saprolite in as little time as 250 k.y. From a brief analysis with ArcGIS, there does not seem to be any relationship between the preservation of saprolite and the localized slope. If this is the case, then erosion may remove saprolite relatively evenly across the landscape.

Removal of the weathered material from the Front Range landscape could have both local and global implications. Locally, removal of weathered material could have geomorphic implications for how relief continues to evolve in the Front Range west of Boulder. If the landscape is stripped of all the loose, weathered material, it could accelerate the migration of the steep inner canyon toward the uplands (Kooi and Beaumont, 1994). Such a migration could cause the smaller drainages around Nederland to steepen in reaction to a shift in proximity to the inner canyon. Using Schildgen et al.'s (2002) rate of ~0.15 m/ka for Late Pleistocene incision in Boulder Canyon, a freshly denuded upland canyon could be incised as deeply as 100 m over 600-700 ka. Application of this incision rate requires that the fresh rock remains uncovered by alluvial deposits during the period of bedrock incision.

On a more broad spatial scale, widespread exposure of fresh bedrock would begin a new cycle of chemical weathering which Molnar and England (1991) believe can lead to atmospheric drawdown of CO_2 and subsequent global cooling. For the Front Range's chemical weathering cycle to have global influence, though, such renewal of weathering would be necessary in other mountain belts around the world. Presuming the climate did begin to cool, the next cycle of Quaternary glaciation could be initiated and a new cycle of deposition and incision would begin in the Front Range.

CONCLUSIONS

- The saprolite in the modern Front Range west of Boulder, CO must have taken greater than 100,000 years to form
- This saprolite may have formed as long ago as 30 to 40 Ma, and was subsequently covered by younger deposits during the Eocene or as late as the Miocene
- Erosion exhumed the saprolite at approximately 2 to 3 Ma corresponding with the initial continental glaciation of North America, and it is currently being eroded at a rate of 18-30 m/m.y.
- During Quaternary glacial episodes, saprolite was eroded by valley glaciers, but deeper saprolite was locally preserved on adjacent topographic highs
- Assuming a mean depth of 5 m for the saprolite cover in the modern landscape, at the present erosion rate it will take 250,000 years to remove the weathered material in my study area
- Widespread exposure of fresh rock in the Front Range and other global mountain ranges could lead to drawdown of atmospheric CO_2 and consequently a cooling of the climate
- Exposure ages and erosion rates determined by my own cosmogenic dating will add further insight into the question of how the saprolite terrain and other environments of the Front Range around Nederland have evolved

REFERENCES

Allaby, A. and Allaby, M., 1999, Dictionary of Earth Sciences: New York, Oxford University Press, 619 p.

Anderson, S.P., William E. Dietrich, George H. Brimhall Jr., 2002, Weathering profiles, mass-balance analysis, and rates of solute loss: Linkages between weathering and erosion in a small, steep catchment: Geological Society of America Bulletin, v. 114, p. 1143-1158.

April, R., Newton, R., Coles, L.T., 1986, Chemical weathering in two Adirondack watersheds: Past and present-day rates: Geological Society of America Bulletin, v. 97, p. 1232-1238.

Barber, L.B., 1983, Correlation of river terrace deposits along Boulder Creek east slope, Colorado Front Range, University of Colorado, Boulder.

Benedict, J.B., 1970, Downslope soil movement in a Colorado alpine region: rates, processes and climatic significance: Arctic and Alpine Research, v. 2, p. 165-226.

Bierman, P. and Steig, E.J., 1996, Estimating Rates of Denudation using Cosmogenic Isotope Abundances in Sediment: Earth Surface Processes and Landforms, v. 21, p. 125-139.

Bierman, P., R. and Caffee, Marc, 2002, Cosmogenic exposure and erosion history of Australian bedrock landforms: Geological Society of America Bulletin, v. 114, p. 787-803.

Birkeland, P.W., 1999, Soils and Geomorphology: New York, Oxford University Press, 430 p.

Birkeland, P.W., Miller, D.C., Patterson, P.E., Price, A.B., and Shroba, R.R., 1999, Soil-geomorphic relationships near Rocky Flats, Boulder and Golden, Colorado area, with a stop at the Pre-Fountain Formation paleosol of Wahlstrom (1948): Geological Society of America Field Trip # 18, 13 p.

Birkeland, P.W., Shroba, R.R., Burns, S.F., Price, A.B., Tonkin, P.J., 2003, Integrating soils and geomorphology in mountains -- An example from the Front Range of Colorado: Geomorphology, in press.

Bovis, M.J. and Thorn, C.E., 1981, Soil Loss Variation within a Colorado Alpine

Area: Earth Surface Processes and Landforms, v. 6, p. 151-163.

Brown, E.T., Stallard, R.F., Larsen, M.C., Raisbeck, G.M., Yiou, F., 1995, Denudation rates determined from the accumulation of in situ-produced ^{10}Be in the Luquillo Experimental Forest, Puerto Rico: Earth and Planetary Science Letters, v. 129, p. 193-202.

Brown, E.T., Stallard, Robert F., Larsen, Matthew C., Bourles, D.L., Raisbeck, Grant M., and Yiou, Francois, 1998, Determination of predevelopment denudation rates of an agricultural watershed (Cayaguas River, Puerto Rico) using in situ-produced ^{10}Be in river-borne quartz: Earth and Planetary Science Letters, v. 160, p. 723-728.

Caine, N. and Swanson, F.J., 1989, Geomorphic coupling of hillslope and channel systems in two small mountain basins: Zeitschrift für Geomorphologie, v. 33, p. 189-203.

Caine, T.N., 1974, The geomorphic processes of the alpine environment, *in* Ives, J.D. and Barry, R.G., eds., Arctic and Alpine Environments: London, Methuen.

—, 1976a, Summer rainstorms in an alpine environment and their influence on soil erosion, San Juan mountains, Colorado: Arctic and Alpine Research, v. 8, p. 183-196.

—, 1976b, A uniform measure of sub-aerial erosion: Geological Society of America Bulletin, v. 87, p. 137-140.

Chang, K.-t., 2002, Introduction to Geographic Information Systems: Boston, McGraw Hill, 348 p.

Clayton, J.L., Megahan, W.F., and Hampton, D., 1979, Soli and bedrock properties: weathering and alteration products and processes in the Idaho batholith. U.Sl Department of Agriculture Forest Services Research Paper INT-237, 35 p.

Costa, J.E., and Cleaves, E.T., 1984, The Piedmont landscape of Maryland: a new look at an old problem: Earth Surface Processes and Landforms, v. 9, p. 59-74.

Dethier, D.P., Ouimet, W., Bierman, P., and Finkel, R.C., 2002, Long-term erosion rates determined from ^{10}Be in sediment from small catchments, Northern Front Range and Southern Wyoming [abs]: Geological Society of America 2002 Annual Meeting, Abstracts with Programs, v. 34, p. 181-10.

Dietrich, W.E. and Dunne, Thomas, 1978, Sediment budget for a small catchment in mountainous terrain: Zeitschrift für Geomorphologie, v. 29, p. 191-206.

Dixon, J.C., and Young, R.W., 1981, Character and origin of deep arenaceous weathering mantles on the Bega Batholith, southeastern Australia.: Catena, v. 8, p. 97-109.

Gable, D.J., 1969, Geologic map of the Nederland quadrangle, Boulder and Gilpin Counties, Colorado: U.S. Geological Survey Geologic Quadrangle Map GQ-833, scale 1:24,000.

—, 1972, Geologic map of the Tungsten Quadrangle, Boulder, Gilpin, and Jefferson Counties, Colorado: U.S. Geological Survey Geologic Quadrangle Map GQ-978, scale 1:24,000.

—, 1980, The Boulder Creek Batholith, Front Range, Colorado: U.S. Geological Survey Professional Paper 1101, 88 p.

Gable, D.J.and Madole, R.F., 1976, Geologic map of the Ward Quadrangle, Boulder County, Colorado, U.S. Geological Survey Map GQ-1277, scale 1:24,000.

Gardner, L.R., Kheoruenromne, I., Chen, H.S., 1978, Isovolumetric geochemical investigation of a buried granite saprolite near Columbia, SC, U.S.A.: Geochimica et Cosmochemica Acta, v. 42, p. 417-424.

Gerrard, J., 1994, Weathering of granitic rocks: environment and clay mineral formation, *in* Robinson, D.A., and Williams, R.B.G., ed., Rock weathering and landform evolution: Chichester, England, John Wiley & Sons Ltd., p. 3-20.

Graham, R.C., Daniels, R.B., Buol, S.W., 1990, Soil-Geomorphic Relations on the Blue Ridge Front: I. Regolith Types and Slope Processes: Soil Science Society of America Journal, v. 54, p. 1362-1367.

Greensfelder, L., 2002, Subtleties of Sand Reveal How Mountains Crumble: Science, v. 295, p. 256-258.

Hancock, G.S., Anderson, R.S., Chadwick, O.A., Finkel, R.C., 1999, Dating fluvial terraces with ^{10}Be and ^{26}Al profiles: application to the Wind River, Wyoming: Geomorphology, v. 27, p. 41-60.

Heimsath, A.M., Dietrich, William E., Nishiizumi, Kunihiko, Finkel, Robert C., 1997,

The soil production function and landscape equilibrium: Nature, v. 388, p. 358-361.

Heimsath, A.M., Chappell, J., Spooner, N.A., Questiaux, D.G., 2002, Creeping soil: Geology, v. 30, p. 111-114.

Isherwood, D. and Street, A., 1976, Biotite-induced grussification of the Boulder Creek Granodiorite, Boulder County, Colorado: Geological Society of America Bulletin, v. 87, p. 366-370.

Kirchner, J.W., Finkel, R.C., Riebe, C.S., Granger, D.E., Clayton, J.L., King, J.G., Megahan, W., 2001, Mountain erosion over 10 yr, 10 k.y., and 10 m.y. time scales: Geology, v. 29, p. 591-594.

Kooi, H., and Beaumont, C., 1996, Large-scale geomorphology; classical concepts reconciled and integrated with contemporary ideas via a surface processes model: Journal of Geophysical Research, B, Solid Earth and Planets, v. 101, p. 3361-3386.

Lee, M.R., Hodson, M.E., Parsons, I., 1998, The role of intragranular microtextures and microstructures in chemical and mechanical weathering: Direct comparisons of experimentally and naturally weathered alkali feldspars: Geochimica et Cosmochemica Acta, v. 62, p. 2771-2788.

Madole, R.F., 1969, Pinedale and Bull Lake glaciation in upper St. Vrain drainage basin: Arctic and Alpine Research, v. 1, p. 279-287.

Madole, R.F., and Shroba, R.R., 1979, Till sequence and soil development in the North St. Vrain drainage basin, east slope Front Range, Colorado, *in* F.G. Ethridge, ed., Field Guide, northern Front Range and northwest Denver Basin, Colorado: Fort Collins, Colorado State University Department of Earth Resources, p. 123-178.

Madole, R.F., 1980, Time of Pinedale deglaciation in north-central Colorado: Further considerations: Geology, v. 8, p. 118-122.

Madole, R.F., VanSistine, D.P., Michael J.A., 1998, Pleistocene glaciation in the upper Platte River drainage basin, Colorado, U.S. Geological Survey Geologic Investigations Series I-2644.

Milliman, J.D., Qin, T.-S., Ren, M.-E., and Saito, T., 1987, Man's influence on the

erosion and transport of sediment by Asian rivers: Journal of Geology, v. 95, p. 751-762.

Molnar, P. and England, P.C., 1990, Late Cenozoic uplift of mountain ranges and global climate change; chicken or egg?: Nature, v. 346, 6279, p. 29-34

Moore, F.J., 1984, A Dynamic Model of Basin Sediment Yield: Water Resources Research, v. 20, p. 89-103.

Moulton, K.L. and Berner, R.A., 1998, Quantification of the effect of plants on weathering: Studies in Iceland: Geology, v. 26, p. 895-898.

Netoff, D.I., 1977, Soil clay mineralogy of Quaternary deposits in two Front Range-Piedmont transects, Colorado [Ph. D. thesis thesis], University of Colorado, Boulder, Col.

Nugent, M.A., Brantley, S.L., Pantano, C.G., and Maurice, P.A., 1998, The influence of natural mineral coatings on feldspar weathering: Nature, v. 395, p. 588-591.

Riebe, C.S., Kirchner, J.W., Granger, D.E., and Finkel, R.C., 2001, Strong tectonic and weak climatic control of long-term weathering rates: Geology, v. 29, p. 511-514.

—, 2001, Minimal climatic control on erosion rates in the Sierra Nevada, California: Geology, v. 29, p. 447-450.

Schildgen, T., Dethier, D.P., Bierman, P., Caffee, M., 2002, ^{26}Al and ^{10}Be Dating of Late Pleistocene and Holocene Fill Terraces: A Record of Fluvial Deposition and Incision, Colorado Front Range: Earth Surface Processes and Landforms, v. 27, p. 773-787.

Schildgen, T.F. and Dethier, D.P., 2000, Fire and ice: using isotopic dating techniques to interpret the geomorphic history of middle Boulder Creek Colorado: Geological Society of America Abstracts with Programs, v. 32, p. p. A. 18.

Schildgen, T.F., 2000, Fire and Ice: the Geomorphic History of Middle Boulder Creek as Determined by Isotopic Dating Techniques, Colorado Front Range (undergraduate thesis): Williams College, Williamstown, MA., 103 p.

Scott, G.R., 1975, Cenozoic Surfaces and Deposits in the Southern Rocky Mountains: Geological Society of America Bulletin, v. 144, p. 227-248.

Scott, G.R. and Taylor, R.B., 1986, Map Showing Late Eocene Erosion Surface,

Oligocene-Miocene Paleovalleys, and Tertiary Deposits in the Pueblo, Denver, and Greeley 1° x 2° Quadrangles, Colorado, U.S. Geological Survey Miscellaneous Investigations Series Map I-1626, scale 1:250,000.

Shroba, R.R., Rosholt, J.N., and Madole, R.F., 1983, Uranium-trend dating and soil B horizon properties of till of Bull Lake age, North St. Vrain drainage basin, Front Range, Colorado: Geological Society of America Abstracts with Programs, v. 15, p. 431.

Small, E.E., Anderson, R.S., Repka, J.L., Finkel, R., 1997, Erosion rates of alpine bedrock summit surfaces deduced from in situ ^{10}Be and ^{26}Al: Earth and Planetary Science Letters, v. 150, p. 413-425.

Sonnenberg, S.A., and Bolyard, D.W., 1997, Tectonic history of the Front Range in Colorado, *in* Bolyard, D.W., and Sonnenberg, S.A., eds., Geologic History of the Colorado Front Range: RMS-AAPG Field Trip #7, p. 1-7.

Stolt, M.H., Baker, J.C., Simpson, T.W., 1991, Micromorphology of the Soil-Saprolite Transition Zone in Hapludults of Virginia: Soil Science Society American Journal, v. 55, p. 1067-1075.

—, 1992, Characterization and Genesis of Saprolite Derived from Gneissic Rocks of Virginia: Soil Science Society of America Journal, v. 56, p. 531-539.

Thorn, C.E., 1978, A preliminary assessment of the geomorphic role of pocket gophers in the alpine zone of the Colorado Front Range: Geografiska Annaler, v. Series A, 60, p. 181-187.

Trimble, S.W., 1977, The Fallacy of Stream Equilibrium in Contemporary Denudation Studies: American Journal of Science, v. 277, p. 876-887.

Velbel, M., A., 1985, Geochemical Mass Balances and Weathering Rates in Forested Watersheds of the Southern Blue Ridge: American Journal of Science, v. 285, p. 904-930.

Velbel, M.A., 1984, Weathering processes of rock-forming minerals, *in* Fleet, M.E., ed., Environmental Geochemistry, Volume 10, Mineralogical Association of Canada, p. 67-111.

White, A.F. and Blum, Alex E., 1995, Effects of climate on chemical weathering in watersheds: Geochimica et Cosmochemica Acta, v. 59, p. 1729-1747.

White, A.F., Blum, A.E., Schulz, M.S., Vivit, D.V., Stonestrom, D.A., Larsen, M., Murphy, S.F., Eberl, D., 1998, Chemical weathering in a tropical watershed, Luquillo Mountains, Puerto Rico: I. Long-term versus short-term weathering fluxes: Geochimica et Cosmochemica Acta, v. 62, p. 209-226.

APPENDICES

Appendix A. GIS Techniques

(assumes some familiarity with ArcGIS, ENVI, and Windows XP)

Mosaicking DEMs and Exporting them to ArcGIS

In ENVI:

-In ENVI, select *File/Open External File/Digital Elevation/USGS SDTS DEM,* and open the CATD format of your downloaded DEM

-In the Input Parameters window, input the additional files that you need to mosaic

-Select "Mosaic Files"

-Enter an output filename and click OK

-In the Available Bands List, load your DEM Image in Gray Scale

-In your viewing window, select *Enhance/Interactive Stretching*, and then record the minimum and maximum values displayed in the Stretch boxes

-Under the main menu, select *File/Save File As/GeoTIFF*, select your mosaicked file and click OK. Enter an appropriate Output Filename, and click OK

In ArcMap:

-Load your newly created GeoTIFF into ArcMap

-Under the Properties for your GeoTIFF, select the Symbology tab

-Under "Stretch Type", select "Minimum-Maximum"

-Select "Edit High/Low Values, and enter the maximum and minimum values that you recorded from within ENVI

-Select "Display Background Value": 0 as "No Color", and click Apply

-You may need to reapply these last steps when you subsequently open your mosaicked DEM GeoTIFF

Digitizing Geologic Maps

-Open interface for rolling scanner

-Enter proper output name and destination for your scan

-Measure your maps dimensions in scanning units off of scanner

-Feed map into scanner being careful to keep edges straight

-Click *Scan*

-Crop image in Adobe Photoshop if necessary

Georectifying Scanned Maps in ArcGIS

In ArcMap:

-Load your unregistered scanned map

-Load the corresponding DRG USGS topographic map

-Open the Georectifying toolbar

-Select your scanned image as the target

-Rectify image using the corners of the DRG

-Under Georectifying toolbar, click *Update Gereferencing* and *Rectify*

Digitizing Well Log Point Data

This section is appropriate for point data that exists both physically on a paper topographic map and in table format within an Excel file. It is imperative that you digitize your points in the order that they appear in the Excel file so that any subsequent Joining is effective.

In ArcCatalog:

-Create a new point shapefile which will be edited to contain the digitized points

-Within your Personal Geodatabase, select *Import/Shapefile to Geodatabase Wizard*, choose to import the point shapefile that you just created, and click Next

-Click Next again, accept default parameters, and click Next

-Click Finish

In ArcMap:

-Load your point shapefile from your Personal Geodatabase

-Load a base map to work from (in my case a digital topographic map in DRG format)

-Open the Editor toolbar, and select *Start Editing*

-Check that the Target is your shapefile and the Task is Create New Feature

-Begin entering digital points, and remember to Save Edits along the way

-When you are finished, select Stop Editing

Joining Shapefile Attribute Tables with Excel Files

In order to make your newly digitized point data useful, it is necessary to join an Excel file with specific information about each point to the attribute table of the shapefile. Further GIS analysis of your shapefile is not possible without this joining step. The first step is saving your Excel table as a .dbf file that Arc can recognize.

In Microsoft Excel:

-Add a column to your table labeled "Join", and, for each well, enter the Object ID number for each point you created from the shapefile's attribute table.

In Microsoft Access:

-Open your Excel file, and click through the spreadsheet wizard, creating an appropriate filename for your spreadsheet before you click Finish

-Right click your newly opened Excel file in Access, and select *Export*

-Save as Type: .dbf, select an appropriate Output Filename and click Export

In ArcMap:

-Load your edited shapefile and its corresponding .dbf file that you just created

-Right-click your shapefile, and select *Joins and Relates/Join*

-Select Join attributes from a table, select Object ID as the join field from your shapefile's attribute table, select the correct .dbf file as the table you want to join the attribute table to, and select the Join field from your .dbf file.

-Click OK

Merging Digitized Well Logs

In ArcMap:

-Load all of your edited shapefiles and their joined tables

-Select *Tools/GeoProcessing Wizard*

-Select Merge layers together, and select your shapefiles as the files you want to merge

-Click OK

In ArcMap:

-Load merged point shapefiles

-Load the Spatial Analyst extension

-In Spatial Analyst, select *Interpolate to Raster/Inverse Distance Weighted (or Kriging)*

-Select the shapefile which contains the points you want to interpolate

-Select the field that you want to interpolate from your shapefile

-Choose an appropriate output filename (if you want a permanent raster)

-Click OK

You may modify the number of points interpolated by selecting a certain profile of your data previous to interpolation:

In ArcMap:

-Load merged point shapefiles

-Open attribute table of shapefile you plan to interpolate

-Click *Options/Select by Attribute*

-Using the Boolean operators, select a subsection from your data's field of interest

-Maintain this selection while interpolating

Converting Raster Graphics to Features

I converted raster graphics to feature graphics when I needed the option of visualizing feature classes with patterns rather than colors. Once the feature has been created, you may load patterns by clicking on the feature classes' colors in the ArcMap table of contents and selecting *More Symbols/Geology 24k.*

To convert a raster:

In ArcMap:

-Load your permanent raster layer that needs to be converted

-Under Spatial Analyst, click *Reclassify*

-Save as a permanent ERDAS IMAGINE file with an appropriate output filename

-Under Spatial Analyst, click *Convert/Raster to Features*

-Select your newly created image file as the input raster

-Select "Polygon" as output geometry type

-Create an appropriate output filename

-Click OK

-Within the properties of this newly created polygon feature, click on the Symbology tab

-Select Categories, and click "Add all values"

The different classes of your feature should now be displayed in different colors, and you are ready to replace those colors with patterns as described above.

Appendix B. GPS locations and Clayton (1979) classifications for roadcuts near Nederland, CO

Datum	WGS 84	site			Clayton classification
WP	UTM	SAP1	456049	4434981	4
WP	UTM	SAP2	455772	4434731	4
WP	UTM	SAP3	455421	4434554	5
WP	UTM	SAP4	455354	4434268	3
WP	UTM	SAP5	455361	4434062	4
WP	UTM	SAP6	455202	4433934	4
WP	UTM	SAP7	455397	4433836	4
WP	UTM	SAP8	455595	4433805	6
WP	UTM	SAP9	455895	4433700	5
WP	UTM	SAP10	456066	4433540	3
WP	UTM	SAP11	456027	4433201	3
WP	UTM	SAP12	455903	4432922	3
WP	UTM	SAP13	455410	4432648	3
WP	UTM	SAP14	455179	4432329	4
WP	UTM	SAP15	457223	4428597	4
WP	UTM	SAP16A	457327	4428221	2
WP	UTM	SAP16B	457244	4428184	2
WP	UTM	SAP17A	457087	4427840	5
WP	UTM	SAP17B	457134	4427811	4
WP	UTM	SAP17C	457159	4427788	4
WP	UTM	SAP18A	457246	4427749	4
WP	UTM	SAP18B	457288	4427734	5
WP	UTM	SAP18C	457340	4427705	3
WP	UTM	SAP19A	457502	4427583	2
WP	UTM	SAP19B	457814	4427051	4
WP	UTM	S20A	458689	4424332	4
WP	UTM	S20B	458837	4424276	4
WP	UTM	S21	458630	4424363	4
WP	UTM	S21B	458599	4424366	4
WP	UTM	S21C	458452	4424382	4
WP	UTM	S22A	458239	4424412	2
WP	UTM	S22B	458108	4424422	2
WP	UTM	S23A	457961	4424364	2
WP	UTM	S23B	457666	4424243	2
WP	UTM	S24A	457584	4424226	2
WP	UTM	S24B	457504	4424153	2
WP	UTM	S24C	457284	4424107	2
WP	UTM	S25A	457269	4424106	2
WP	UTM	S25B	457081	4424057	2
WP	UTM	S26A	453267	4424549	3
WP	UTM	S26B	453440	4424552	3
WP	UTM	S27	453538	4424524	3
WP	UTM	S28	454060	4424166	2
WP	UTM	S29A	454091	4424101	2
WP	UTM	S30A	454552	4423871	3
WP	UTM	S30B	454739	4423843	3
WP	UTM	S31A	454907	4423939	2
WP	UTM	S31B	455069	4423948	2
WP	UTM	S32A	455078	4423977	4
WP	UTM	S32B	455179	4424021	4
WP	UTM	S33	455271	4424052	5
WP	UTM	S34	455666	4424081	4
WP	UTM	S35	455837	4424029	3
WP	UTM	S36A	457028	4418764	4
WP	UTM	S36B	457003	4418956	4
WP	UTM	S37A	456982	4419018	3
WP	UTM	S37B	456908	4419299	3
WP	UTM	S37C	456948	4419409	3
WP	UTM	S38A	457146	4420030	2
WP	UTM	S38B	457169	4420049	5
WP	UTM	S38C	457203	4420094	5

WP	UTM	S39A	457270	4420343	6
WP	UTM	S39B	457203	4420379	6
WP	UTM	S40A	457117	4420397	3
WP	UTM	S40B	457056	4420462	3
WP	UTM	S41A	457042	4420527	3
WP	UTM	S41B	457030	4420642	3
WP	UTM	S42A	456931	4420834	3
WP	UTM	S42B	456954	4420904	3
WP	UTM	S43A	456959	4421021	7
WP	UTM	S43B	456923	4421054	7
WP	UTM	S44A	457042	4421252	5
WP	UTM	S44B	457085	4421267	5
WP	UTM	S45A	457217	4421333	1
WP	UTM	S45B	457280	4421361	5
WP	UTM	S46A	457443	4421580	6
WP	UTM	S46B	457413	4421654	6
WP	UTM	S47A	457059	4422100	7
WP	UTM	S47B	457042	4422122	7
WP	UTM	S48A	456991	4422216	7
WP	UTM	S48B	456973	4422265	7
WP	UTM	S49A	456898	4422465	4
WP	UTM	S49B	456869	4422534	4
WP	UTM	S50A	456484	4422990	6
WP	UTM	S51A	456393	4423022	5
WP	UTM	S51B	456358	4422993	5
WP	UTM	S52A	450264	4421033	1
WP	UTM	S52B	450323	4421028	1
WP	UTM	S53A	451006	4421391	1
WP	UTM	S54A	451921	4421083	2
WP	UTM	S54B	451939	4421082	2
WP	UTM	S55A	451961	4421088	2
WP	UTM	S55B	452037	4421125	2
WP	UTM	S56A	452508	4421279	2
WP	UTM	S57A	452847	4421341	2
WP	UTM	S57B	452957	4421386	2
WP	UTM	S58A	453174	4421472	1
WP	UTM	S58B	453248	4421503	1
WP	UTM	S59A	453306	4421524	2
WP	UTM	S60A	453623	4421788	1
WP	UTM	S60B	453704	4421872	1
WP	UTM	S61A	451042	4425617	1
WP	UTM	S62A	451350	4425391	2
WP	UTM	S63A	451807	4424962	2
WP	UTM	S63B	451834	4424938	2
WP	UTM	S64A	452068	4424851	2
WP	UTM	S64B	452174	4424779	2
WP	UTM	S65A	452346	4424802	4
WP	UTM	S66A	452401	4424874	4
WP	UTM	S66B	452397	4424873	4
WP	UTM	S67A	452878	4425218	4
WP	UTM	S68A	452931	4425156	5
WP	UTM	S68B	452996	4425074	5
WP	UTM	S69A	453117	4425048	4
WP	UTM	S70A	453195	4424964	3
WP	UTM	S70B	453295	4424904	3
WP	UTM	S71A	453302	4424898	4
WP	UTM	S72A	453399	4424832	3
WP	UTM	S72B	453594	4424800	3
WP	UTM	S73A	453820	4424805	7
WP	UTM	S74A	453830	4424704	7
WP	UTM	S74B	453820	4424711	7
WP	UTM	S75A	453681	4424663	4
WP	UTM	S75B	453656	4424653	4
WP	UTM	S76A	453649	4424656	4
WP	UTM	S77A	453537	4424627	4

WP	UTM	S78A	453431	4424612	3
WP	UTM	S79A	453281	4424587	3
WP	UTM	S79B	453226	4424601	3
WP	UTM	S80A	456738	4430021	3
WP	UTM	S81A	456598	4429893	4
WP	UTM	S81B	456591	4429882	4
WP	UTM	S82A	456472	4429713	4
WP	UTM	S83A	456467	4429599	4
WP	UTM	S84A	456444	4429424	4
WP	UTM	S85A	456479	4429264	4
WP	UTM	S86A	456509	4429233	2
WP	UTM	S87A	456675	4429088	2
WP	UTM	S88A	456722	4429078	4
WP	UTM	S89A	456872	4429000	2
WP	UTM	S89B	456907	4428984	2
WP	UTM	S90A	456981	4428947	2
WP	UTM	S91A	457101	4428684	2
WP	UTM	S92A	457089	4428484	2
WP	UTM	S92B	457116	4428395	2
WP	UTM	S93A	457108	4428379	2
WP	UTM	S94A	457029	4428268	2
WP	UTM	S94B	456880	4428242	2
WP	UTM	S95A	456827	4428225	2
WP	UTM	S95B	456794	4428216	2
WP	UTM	S96A	456749	4428130	2
WP	UTM	S96B	456761	4428101	2
WP	UTM	S97A	456724	4427999	4
WP	UTM	S97B	456706	4427765	4
WP	UTM	S98A	456728	4427706	4
WP	UTM	S98B	456780	4427638	4
WP	UTM	S99A	456843	4427583	4
WP	UTM	S100A	456877	4427539	2
WP	UTM	S100B	456909	4427520	2
WP	UTM	S101A	456947	4427479	4
WP	UTM	S101B	456961	4427482	4
WP	UTM	S102A	457122	4427504	3
WP	UTM	S102B	457172	4427331	3
WP	UTM	S103A	457291	4427294	4
WP	UTM	S104A	457585	4427098	2
WP	UTM	S104B	457597	4427110	2
WP	UTM	S105A	457633	4427086	6
WP	UTM	S106A	457699	4427046	4
WP	UTM	S107A	454845	4426062	4
WP	UTM	S108A	454968	4425832	4
WP	UTM	S109A	455130	4425631	4
WP	UTM	S110A	454024	4424951	3
WP	UTM	S111A	454018	4424961	3
WP	UTM	S112A	454013	4424968	3
WP	UTM	S113A	454143	4425091	2
WP	UTM	S114A	454190	4425090	2
WP	UTM	S115A	454251	4425108	2
WP	UTM	S116A	454301	4425104	2
WP	UTM	S116B	454408	4425122	2
WP	UTM	S117A	454550	4425248	3
WP	UTM	S118A	454679	4425346	4
WP	UTM	S119A	454785	4425447	3
WP	UTM	S120A	454943	4425544	3
WP	UTM	S121A	455191	4425620	3
WP	UTM	S122A	455698	4425872	3
WP	UTM	S123A	455883	4425832	5
WP	UTM	S124A	455978	4425732	3
WP	UTM	S125A	456160	4425682	3
WP	UTM	S126A	456381	4425700	4
WP	UTM	S126B	456446	4425721	4
WP	UTM	S127A	456528	4425743	4

WP	UTM	S128A	456618	4425773	4
WP	UTM	S129A	456754	4425798	3
WP	UTM	S130A	456192	4424172	4
WP	UTM	S131A	453877	4418418	2
WP	UTM	S132A	454087	4418437	1
WP	UTM	S133A	454832	4418349	1
WP	UTM	S133B	454897	4418380	1
WP	UTM	S134A	455087	4418339	3
WP	UTM	S135A	455500	4418433	2
WP	UTM	S136A	455846	4418744	3
WP	UTM	S137A	455854	4418744	3
WP	UTM	S138A	455943	4418762	3
WP	UTM	S139A	456079	4418760	2
WP	UTM	S139B	456089	4418757	2
WP	UTM	S140A	456236	4418741	4
WP	UTM	S141A	456471	4418723	4
WP	UTM	S142A	456549	4418719	4
WP	UTM	S143A	456769	4418712	4
WP	UTM	S144	455587	4424937	3
WP	UTM	S145	455150	4424906	2
WP	UTM	S146	455033	4424883	3
WP	UTM	S147	455084	4424836	5
WP	UTM	S148	455155	4424797	3
WP	UTM	S149	455212	4424761	6
WP	UTM	S150A	455214	4424760	4
WP	UTM	S150B	455219	4424755	4
WP	UTM	S151	455284	4424698	3
WP	UTM	S152	455340	4424593	3
WP	UTM	S153	455388	4424450	3
WP	UTM	S154	455422	4424389	4
WP	UTM	S155	456089	4424686	3
WP	UTM	S156	456042	4424441	3
WP	UTM	S157	455991	4424327	4
WP	UTM	S158A	455882	4424391	4
WP	UTM	S158B	455864	4424387	4
WP	UTM	S159	456213	4424301	4
WP	UTM	S160	456264	4424284	4
WP	UTM	S161	456428	4424463	3
WP	UTM	S162	456454	4424381	4
WP	UTM	S163	456315	4424420	3
WP	UTM	S164	456116	4424259	5
WP	UTM	S165A	456156	4424199	5
WP	UTM	S165B	456189	4424176	5
WP	UTM	S166	456187	4424097	5
WP	UTM	S167	456131	4424059	3
WP	UTM	S168	455997	4424201	3
WP	UTM	S169	455863	4424196	5
WP	UTM	S170	455803	4424181	4
WP	UTM	S171	455785	4424185	4
WP	UTM	S172	455858	4424088	3
WP	UTM	S173	445811	4427366	
WP	UTM	S174	456011	4421918	4
WP	UTM	S175	456092	4421902	5
WP	UTM	S176	456183	4421906	5
WP	UTM	S177	456588	4422004	4
WP	UTM	S178	456661	4421930	4
WP	UTM	S179	456700	4421922	4
WP	UTM	S180	456786	4421908	4
WP	UTM	S181	456990	4422208	4
WP	UTM	S182	457088	4419060	4
WP	UTM	S183A	457089	4419056	4
WP	UTM	S183B	457079	4419024	4
WP	UTM	S184	457093	4418792	5
WP	UTM	S185	457110	4418724	5
WP	UTM	S186	457203	4419239	4

WP	UTM	S187	457721	4419141	4
WP	UTM	S188	457482	4418902	4
WP	UTM	S189	457955	4418552	4
WP	UTM	S190	457962	4418567	4
WP	UTM	S190B	457983	4418708	4
WP	UTM	S191	457884	4418818	2
WP	UTM	S192	457839	4418828	3
WP	UTM	S193A	457786	4418783	5
WP	UTM	S193B	457796	4418741	5
WP	UTM	S194A	457779	4418741	5
WP	UTM	S194B	457679	4418777	5
WP	UTM	S195	457653	4418785	4
WP	UTM	S196	457614	4418813	3
WP	UTM	S197	457465	4418727	3
WP	UTM	S198	457399	4418660	5
WP	UTM	S199	457335	4418688	5
WP	UTM	S200	457334	4418694	4
WP	UTM	S201	457256	4418791	4
WP	UTM	S202	457179	4418840	4
WP	UTM	S203	457174	4418840	4
WP	UTM	S204	457170	4418844	5
WP	UTM	S205	458116	4419615	2
WP	UTM	S206	458106	4419615	3
WP	UTM	S207	457980	4419616	4
WP	UTM	S208	457811	4419654	4
WP	UTM	S209	457694	4419655	4
WP	UTM	S210	457693	4419649	3
WP	UTM	S211	457688	4419648	3
WP	UTM	S212	457404	4419633	3
WP	UTM	S213	457367	4419651	3
WP	UTM	S214A	455220	4432125	1
WP	UTM	S214B	455458	4431796	1
WP	UTM	S215A	455908	4431208	4
WP	UTM	S215B	455972	4431048	4
WP	UTM	S216A	455984	4430912	2
WP	UTM	S216B	455957	4430751	2
WP	UTM	S217A	455956	4430731	2
WP	UTM	S217B	455952	4430697	2
WP	UTM	S218A	456063	4430391	3
WP	UTM	S218B	456197	4430190	3
WP	UTM	S219A	457684	4426873	5
WP	UTM	S220A	457634	4426884	3
WP	UTM	S220B	457496	4426878	3
WP	UTM	S221A	457733	4426406	3
WP	UTM	S221B	457723	4426423	3
WP	UTM	S222A	457732	4426265	3
WP	UTM	S222B	457629	4426140	3
WP	UTM	S223A	457425	4425952	4
WP	UTM	S223B	457322	4425858	4
WP	UTM	S224	457235	4425811	3
WP	UTM	S225A	457179	4425824	4
WP	UTM	S225B	457040	4425835	4

Appendix C. Well Log Data for Nederland, Ward, Tungsten, Gold Hill, Monarch Lake, and East Portal quadrangles

Well number	Quadrangle	Township	Range	Section	Quarter Section	Quarter Section	Overburden Thickness ft	Alluvial Thickness ft	Highly Weathered Thickness ft	Total Weathered Thickness ft	Depth to Bedrock ft	Minimum Well Depth ft	Notes
185953	Gold Hill	1N	72W	11	NW	NE	0	0	0	27	27	70	gray granite
125685	Gold Hill	1N	72W	11	NE	SE	3	0	0	37	40	80	gray granite and schist
140316	Gold Hill	1N	72W	11	NE	SE	0	0	10	40	40	55	gray granite
7014	Gold Hill	1N	72W	11	NE	SE	4	0	13	13	17	78	granite
24859	Gold Hill	1N	72W	11	NE	SE	1	0	7	8	9	48	gray granite
91952	Gold Hill	1N	72W	11	NE	SE	0	0	4	40	40	145	gray granite and quartz
170854	Gold Hill	1N	72W	11	SE	SE	0	0	12	12	12	261	gray granite and quartz
216659	Gold Hill	1N	72W	11	SE	SE	0	0	0	0	0	240	pink and grey gneiss (medium)
121089	Gold Hill	1N	72W	11	SW	SE	15	0	0	60	70	360	gray granite
13118	Gold Hill	1N	72W	11	NW	SW	16	0	38	54	54	60	fractured gray granite
124306	Gold Hill	1N	72W	11	NW	SW	0	0	5	5	45	60	brown granite/quartz under schist, mica
31662M	Gold Hill	1N	72W	12	SE	NW	0	0	7	7	7	60	gray granite
170430	Gold Hill	1N	72W	12	NW	SW	0	0	27	27	27	78	gray granite, talc
183705	Gold Hill	1N	72W	12	NW	SW	0	0	8	8	300	300	brown, gray, gray-green granite
121425	Gold Hill	1N	72W	12	NW	SW	0	0	0	15	15	100	gray granite and quartz
133510	Gold Hill	1N	72W	12	NW	SW	0	0	0	10	10	465	gray granite
21206	Gold Hill	1N	72W	12	SW	SW	1	0	0	13	14	25	hard brown granite
205568	Gold Hill	1N	72W	12	NW	SW	4	0	0	56	60	400	gray gneiss
142567	Gold Hill	1N	72W	13	NE	NE	0	0	10	10	10	160	gray granite
148962	Gold Hill	1N	72W	13	SE	NE	0	0	0	30	30	60	gray granite
46898	Gold Hill	1N	72W	13	NE	NW	7	0	17	24	24	54	gray granite (medium)
49502	Gold Hill	1N	72W	13	NE	NW	0	0	13	13	13	79	gray granite (medium)
114944	Gold Hill	1N	72W	13	NW	NE	0	0	0	20	20	40	gray granite
130715	Gold Hill	1N	72W	13	NW	NW	2	0	0	60	60	300	gray granite amd schist
69879	Gold Hill	1N	72W	13	NW	NW	0	0	20	65	65	85	granite (hard)
89437	Gold Hill	1N	72W	13	SW	NW	15	0	0	15	15	320	gray granite
142826	Gold Hill	1N	72W	13	SW	NW	0	0	0	0+	40	40	brown granite
81229	Gold Hill	1N	72W	13	SW	NW	0	0	0	67+	67	67	brown granite, quartz (medium)
239670	Gold Hill	1N	72W	13	SW	NW	0	0	0	15	15	185	brown and gray granite
32603	Gold Hill	1N	72W	13	NW	SE	3	0	0	0	24	54	black mica, quartz
39332	Gold Hill	1N	72W	13	NW	SE	0	0	29	60+	60	60	brown broken granite (soft)
67950	Gold Hill	1N	72W	13	NW	SE	0	0	0	0	12	28	gray granite
222074	Gold Hill	1N	72W	13	SW	SE	0	0	15	15	15	70	pink granite
69813	Gold Hill	1N	72W	13	NE	SW	0	3	0	12	40	55	granite
missing	Gold Hill	1N	72W	13	SE	SW	6	0	0	33	39	270	gray granite
97193	Gold Hill	1N	72W	13	SW	SW	12	0	0	30	42	100	gray granite
173374	Gold Hill	1N	71W	7	SE	NE	0	0	0	77	77	95	gray granite and talc
183353	Gold Hill	1N	71W	7	SE	NE	0	0	7	112	112	112	brown and gray granite
173327	Gold Hill	1N	71W	7	NE	SE	15	0	0	0	15	130	gray granite
173328	Gold Hill	1N	71W	7	SE	SE	0	0	9	101	101	101	brown and gray granite
73606	Gold Hill	1N	71W	7	SW	SW	0	0	0	7	7	15	white granite, brown schist, gneiss
223851	Gold Hill	1N	71W	7	SW	SW	0	0	0	30	30	370	gray gneiss (hard)
120164	Gold Hill	1N	71W	18	NW	NE	5	0	0	0	5	140	gray granite
149519	Gold Hill	1N	71W	18	NW	NE	0	0	10	10	10	400	gray granite and quartz
98788	Gold Hill	1N	71W	18	NW	NE	0	0	10	10	10	35	gray granite

160068	Gold Hill	1N	71W	18	SE	NE	0	0	5	5	5	40	gray granite
83258	Gold Hill	1N	71W	18	SE	NE	0	0	0	17	17	225	gray granite
179333	Gold Hill	1N	71W	18	SW	NE	3	0	9	9	12	180	gray granite
78846	Gold Hill	1N	71W	18	SW	NE	3	0	9	9	12	180	gray granite
214378	Gold Hill	1N	71W	18	NE	NW	0	0	4	5	5	155	gray granite and rock
171230	Gold Hill	1N	71W	18	SE	NW	2	0	0	0	2	30	gray schist
132325	Gold Hill	1N	71W	18	SE	NW	0	0	0	12	12	118	gray granite
75161	Gold Hill	1N	71W	18	SW	NW	3	0	0	13	13	55	gray granite
185672	Gold Hill	1N	71W	18	NW	SE	0	0	0	0	0	108	brown and gray granite
136674	Gold Hill	1N	71W	18	SW	SE	0	10	0	0	0	10	alluvium and gravel
163303	Gold Hill	1N	71W	18	SW	SE	0	0	11	11	11	68	brown and gray granite
195301	Gold Hill	1N	71W	18	SW	SE	0	0	0	7	7	154	gray granite
147548	Gold Hill	1N	71W	18	NE	SW	0	0	0	40	40	420	gray granite
188339	Gold Hill	1N	71W	18	NE	SW	3	0	0	0	3	275	layered brown and gray gneiss
142186	Gold Hill	1N	71W	18	SE	SW	0	0	7	7	7	91	gray granite
142187	Gold Hill	1N	71W	18	SE	SW	0	0	14	40	40	170	gray granite
67043	Gold Hill	1N	72W	32	SE	NE	0	0	0	15	24	94	gray schist (soft)
28373	Gold Hill	1N	72W	32	SE	NW	0	0	2	10	10	20	gray granite
31404	Gold Hill	1N	72W	32	SE	NW	8	0	0	0	8	65	gray granite
31468	Gold Hill	1N	72W	32	SW	NW	0	0	32	32	32	37	gray granite (soft)
154669	Gold Hill	1N	72W	32	NE	SE	0	0	14	14	14	187	gray granite and quartz
36931	Gold Hill	1N	72W	32	NE	SE	2	0	0	12	12	56	gray granite
71306	Gold Hill	1N	72W	32	NE	SE	2	0	13	13	15	30	brown granite (medium)
35299	Gold Hill	1N	72W	32	NW	SE	1	0	0	0	1	55	gray granite (hard)
46356	Gold Hill	1N	72W	32	NW	SE	0	0	10	10	10	22	gray granite
69199	Gold Hill	1N	72W	32	NW	SE	1	0	3	3	4	60	gray granite (hard)
132321	Gold Hill	1N	72W	32	SW	SE	1	0	0	29	30	40	gray granite
163234	Gold Hill	1N	72W	32	NE	SW	0	0	7	7	7	227	brown and gray granite
31469	Gold Hill	1N	72W	32	NE	SW	1	0	2	2	3	15	gray granite (hard)
31991	Gold Hill	1N	72W	32	NE	SW	1	0	18	18	19	29	gray granite (hard)
228215	Gold Hill	1N	72W	32	NE	SW	2	0	0	14	16	24	gray granite
111954	Gold Hill	1N	72W	32	SE	SW	3	0	0	3	6	23	gray granite
41479	Gold Hill	1N	72W	32	SE	SW	0	0	0	10	10	100	gray granite
59192	Gold Hill	1N	72W	32	SE	SW	0	0	0	20	20	130	gray granite
32869	Gold Hill	1N	72W	32	SW	SW	8	0	0	22	30	200	gray granite (medium)
47330	Gold Hill	1N	72W	32	SW	SW	4	0	14	14	16	41	gray granite (soft)
91365	Gold Hill	1N	72W	33	NE	NE	0	0	0	4	4	55	brown granite
161743	Gold Hill	1N	72W	33	NE	NE	17	0	0	23	43	76	gray granite
86460	Gold Hill	1N	72W	33	NE	NE	0	0	0	18	18	165	schist with quartz
57876	Gold Hill	1N	72W	33	NW	NE	0	0	0	17	17	120	gray granite
59795	Gold Hill	1N	72W	33	NW	NE	0	0	10	48	48	64	gray granite (medium, soft)
missing	Gold Hill	1N	72W	33	NW	NE	15	0	0	10	25	105	gray granite
48882	Gold Hill	1N	72W	33	NE	SW	0	0	10	10	10	185	gray broken granite (medium)
45704	Gold Hill	1N	72W	33	NE	SW	0	0	10	10	10	185	gray broken granite
168904	Gold Hill	1N	72W	33	NW	SW	0	0	0	12	12	236	gray granite (medium) and quartz
144377	Gold Hill	1N	72W	33	NW	SW	2	0	23	23	25	70	gray granite
100617	Gold Hill	1N	72W	28	SE	SE	0	0	0	1	1	15	gray granite
120897	Gold Hill	1N	72W	28	SE	SE	0	0	0	35	35	80	gray granite
130061	Gold Hill	1N	72W	28	SE	SE	0	0	0	53	53	79	gray granite and talc
45502	Gold Hill	1N	72W	28	SE	SE	2	0	0	33	35	59	brown and gray granite (hard)
179175	Gold Hill	1N	72W	28	SW	SE	0	0	16	16	16	440	brown, gray, gray-green granite

100619	Gold Hill	1N	72W	28	SW	SE	0	0	3	55	55	205	gray granite
66821	Gold Hill	1N	72W	28	SW	SE	12	0	0	35	35	170	gray granite and quartz
69298	Gold Hill	1N	72W	28	SW	SE	0	0	2	40	40	201	gray granite, schist (soft)
53602	Gold Hill	1N	72W	34	NE	NE	2	0	3	15	15	169	gray granite (hard)
165586	Gold Hill	1N	72W	34	NW	NE	0	0	5	12	12	446	gray granite, talc, quartz
83586	Gold Hill	1N	72W	34	NW	NE	5	0	0	70	75	305	gray granite
91743	Gold Hill	1N	72W	34	SE	NE	0	21	0	0	21	85	gray granite
158465	Gold Hill	1N	72W	34	NE	SE	0	0	0	12	12	167	gray granite with quartz (medium)
231845	Gold Hill	1N	72W	34	NE	SE	0	0	0	15	15	380	gray and pink granite (hard)
231828	Gold Hill	1N	72W	34	NE	SE	0	0	0	0	0	140	gray granite (medium)
155370	Gold Hill	1N	72W	36	NW	NE	1	0	19	34	34	185	pink and gray granite
225355	Gold Hill	1N	72W	36	NW	NE	6	0	0	4	10	300	granite
145254	Gold Hill	1N	72W	36	SW	NE	0	0	0	25	25	30	brown, gray granite
164830	Gold Hill	1N	72W	36	SW	NE	0	0	24	24	24	245	gray granite with quartz (medium)
170602	Gold Hill	1N	72W	36	NE	NW	0	0	10	10	10	77	brown and gray granite
14077A	Gold Hill	1N	72W	36	NE	NW	0	0	0	15	15	115	gray granite
87714	Gold Hill	1N	72W	36	NE	NW	0	0	0	20	20	50	gray granite
187216	Gold Hill	1N	72W	36	NW	NW	8	0	10	10	18	332	brown, pink, and gray granite
97501	Gold Hill	1N	72W	36	NW	NW	0	0	0	18	18	285	gray granite
163817	Gold Hill	1N	72W	36	NW	NW	0	0	0	16	16	125	red granite
31768	Gold Hill	1N	72W	36	NW	NW	4	0	0	6	10	41	gray granite
196002	Gold Hill	1N	71W	31	NE	NE	5	0	0	0	5	25	gray granite
146030	Gold Hill	1N	71W	31	NW	NW	0	0	0	18	18	75	gray granite
14674	Gold Hill	1N	71W	31	NW	SE	10	0	8	8	18	100+	gray granite
91956	Gold Hill	1N	71W	31	SW	SE	0	0	0	40	40	50	gray granite
167619	Gold Hill	1N	71W	31	SW	SE	4	0	0	0	4	166	pink and gray granite
130721	Gold Hill	1N	71W	30	NE	NE	0	0	0	15	15	310	gray granite
45040	Gold Hill	1N	71W	30	NE	NE	1	0	21	22	22	54	brown granite (hard) and quartz
46349	Gold Hill	1N	71W	30	NE	NE	1	0	0	4	5	15	hard gray granite
129966	Gold Hill	1N	71W	30	NW	NE	0	0	0	75	75	135	gray granite
45712	Gold Hill	1N	71W	30	NW	NE	3	0	14	14	17	40	gray granite (medium)
56085	Gold Hill	1N	71W	30	NW	NE	3	0	3	40	43	102	gray broken granite (medium)
60847	Gold Hill	1N	71W	30	NW	NE	4	0	0	10	14	52	gray granite
39326	Gold Hill	1N	71W	30	SE	NE	0	0	0	6	6	100	gray granite
40505	Gold Hill	1N	71W	30	SE	NE	0	0	0	30	30	150	gray granite
41228	Gold Hill	1N	71W	30	SE	NE	0	0	0	15	15	140	gray granite
43807	Gold Hill	1N	71W	30	SW	NE	1	0	0	4	5	11	brown granite (hard)
48815	Gold Hill	1N	71W	30	SW	NE	1	0	5	5	6	14	granite (hard)
54534	Gold Hill	1N	71W	30	SW	NE	3	0	57	82	85	95	gray granite (medium)
57875	Gold Hill	1N	71W	30	NE	SW	5	0	0	5	10	77	gray granite
157390	Gold Hill	1N	71W	30	NE	NW	5	0	12	35	35	235	gray granite
45710	Gold Hill	1N	71W	30	NE	NW	14	0	0	0	14	48	gray broken granite (medium)
58471	Gold Hill	1N	71W	30	NE	NW	0	0	0	8	8	65	gray granite
41480	Gold Hill	1N	71W	30	NW	NW	0	0	0	10	10	115	gray granite
52258	Gold Hill	1N	71W	30	NW	NW	1	0	0	8	9	15	brown and gray granite (hard)
83120	Gold Hill	1N	71W	30	SE	NW	1	0	9	9	10	21	granite (hard, medium)
97507	Gold Hill	1N	71W	30	NE	SE	0	0	0	15	15	110	gray granite
98776	Gold Hill	1N	71W	30	NE	SE	0	0	0	15	15	50	gray granite
154053	Gold Hill	1N	71W	30	NW	SE	2	0	0	14	16	205	brown, pink, and gray granite
63568	Gold Hill	1N	71W	30	NW	SE	5	0	0	30	35	80	red granite
138433	Gold Hill	1N	71W	30	SE	SE	4	0	13	13	17	65	gray granite

118777	Gold Hill	1N	71W	30	SW	SE	3	0	0	2	5	15	gray granite
78151	Gold Hill	1N	71W	30	SW	SE	3	0	0	15	18	63	gray granite
36858	Gold Hill	1N	71W	30	NE	SW	0	0	12	25	25	29	pink granite (medium)
59564	Gold Hill	1N	71W	30	NE	SW	5	0	0	0	5	50	gray granite
46027	Gold Hill	1N	71W	30	NW	SW	3	0	0	8	11	44	gray granite (hard)
91384	Gold Hill	1N	71W	30	SW	SW	0	0	0	8	8	46	gray granite
103762	Gold Hill	1N	71W	30	SW	SW	2	0	0	4	6	19	tan granite (hard)
108101	Gold Hill	1N	71W	19	NE	NE	0	0	7	7	7	20	white quartz
102170	Gold Hill	1N	71W	19	NE	NE	3	0	5	5	8	15	gray granite
174474	Gold Hill	1N	71W	19	SE	NE	4	0	0	0	4	500	brown, pink, and gray granite
118776	Gold Hill	1N	71W	19	SE	NE	0	0	19	19	19	35	gray and pink granite
135854	Gold Hill	1N	71W	19	NE	NW	8	0	0	0	8	185	gray granite with talc
30958	Gold Hill	1N	71W	19	NW	NW	1	0	0	8	9	14	gray granite (hard)
48680	Gold Hill	1N	71W	19	NW	NW	1	0	0	17	17	30	solid granite
91955	Gold Hill	1N	71W	19	SW	NW	0	0	0	10	10	250	gray granite
174475	Gold Hill	1N	71W	19	NW	SE	6	0	0	0	6	328	brown and gray granite
175116	Gold Hill	1N	71W	19	SE	SE	0	0	12	12	12	401	brown, pink, and gray granite
65390	Gold Hill	1N	71W	19	SW	SE	0	0	0	10	10	30	gray granite
88916	Gold Hill	1N	71W	19	SW	SE	0	0	0	6	6	180	gray granite
121235	Gold Hill	1N	71W	19	NE	SW	0	0	0	40	40	315	gray granite
57211	Gold Hill	1N	71W	19	NE	SW	0	0	0	3	3	25	gray granite
140314	Gold Hill	1N	71W	19	NW	SW	0	0	0	12	12	20	gray granite
14950	Gold Hill	1N	71W	19	SE	SW	12	0	0	0	12	154	gray granite
82926	Gold Hill	1N	71W	19	SE	SW	3	0	5	5	8	75	red granite
18030	Gold Hill	1N	71W	19	SW	SW	3	0	0	0	3	31	gray granite (hard)
37244	Gold Hill	1N	71W	19	SW	SW	0	0	0	20	20	405	gray granite
44041	Gold Hill	1N	71W	19	SW	SW	1	0	3	3	4	9	gray granite (hard)
106491	Gold Hill	1N	72W	24	NE	NW	0	0	0	45	45	67	gray granite
59302	Gold Hill	1N	72W	24	NE	NW	0	0	28	28	28	40	gray granite with streaks of schist
195978	Gold Hill	1N	72W	24	NE	NW	0	0	16	16	16	300	brown, pink, and gray granite
17872	Gold Hill	1N	72W	24	SW	NW	14	0	10	10+	24	30	brown granite
99766	Gold Hill	1N	72W	24	SW	NW	0	13	0	0	13	105	schist
201960	Gold Hill	1N	72W	24	NE	SE	0	0	0	45	45	63	tan granite
1388541	Gold Hill	1N	72W	24	SE	SE	0	0	0	35	35	118	gray granite
143138	Gold Hill	1N	72W	24	SE	SE	0	0	7	7	7	72	gray granite and talc
50399	Gold Hill	1N	72W	24	SE	SE	0	0	0	15	15	40	gray granite
45737	Gold Hill	1N	72W	24	SW	SE	0	0	0	12	12	187	gray granite (hard)
130641	Gold Hill	1N	72W	24	NE	SW	0	0	0	10	10	50	gray granite amd schist
87745	Gold Hill	1N	72W	24	SE	SW	8	0	0	12	12	270	gray granite
179597	Gold Hill	1N	72W	26	SE	NE	0	0	1	23	23	25	pink granite and epidote
26696	Gold Hill	1N	72W	26	SE	NE	0	0	0	15	15	80	gray granite
69811	Gold Hill	1N	72W	26	SE	NE	0	0	0	0	60	90	granite and quartz
104713	Gold Hill	1N	72W	26	SW	NE	4	0	0	51	55	160	gray granite
140313	Gold Hill	1N	72W	26	SW	NE	5	0	13	20	25	50	gray granite
46815	Gold Hill	1N	72W	26	SW	NE	1	0	2	8	9	16	gray granite (hard)
132719	Gold Hill	1N	72W	26	SE	NW	3	0	0	11	14	110	gray granite
151906	Gold Hill	1N	72W	26	SE	NW	3	0	0	13	16	205	gray, white, and pink granite
166507	Gold Hill	1N	72W	26	SE	NW	0	0	10	21	21	61	gray granite
95475	Gold Hill	1N	72W	26	SE	NW	0	0	0	30	30	55	schist
79531	Gold Hill	1N	72W	26	SW	NW	0	0	17	28	28	55	gray granite and talc (soft)
146217	Gold Hill	1N	72W	26	NE	SE	3	0	0	0+	20	30	brown granite

87744	Gold Hill	1N	72W	26	NE	SE	7	0	0	14	14	138	gray granite
133088	Gold Hill	1N	72W	26	NW	SE	3	0	0	6	9	220	gray granite and quartz
137492	Gold Hill	1N	72W	26	NW	SE	0	0	5	15	15	85	gray granite
160045	Gold Hill	1N	72W	26	NW	SE	0	0	8	8	8	200	brown, gray-green, and pink granite and quartz
80333	Gold Hill	1N	72W	26	SE	SE	0	0	5	5	5	223	gray granite
21931	Gold Hill	1N	72W	26	SW	SE	19	0	0	15	34	48	gray granite (fractured and hard)
89177	Gold Hill	1N	72W	26	NE	SW	0	0	0	17	17	44	gray granite
134783	Gold Hill	1N	72W	26	NE	SW	0	0	0	5	5	15	gray granite
154649	Gold Hill	1N	72W	26	NE	SW	0	0	9	9	9	70	brown and gray granite
46656	Gold Hill	1N	72W	26	NE	SW	1	0	0	0	12	15	gray-green granite (hard)
63083	Gold Hill	1N	72W	25	NE	NE	1	0	0	4	5	14	gray granite (hard)
65020	Gold Hill	1N	72W	25	NE	NE	1	0	0	0	6	59	gray granite (hard)
49501	Gold Hill	1N	72W	25	SE	NE	1	0	0	0+	1	63	schist with quartz (broken, soft)
65021	Gold Hill	1N	72W	25	SE	NE	1	0	4	4	5	18	gray granite (hard)
839	Gold Hill	1N	72W	25	SW	NE	2	0	0	0	2	57	gray granite
135678	Gold Hill	1N	72W	25	NE	NW	5	0	0	0	5	25	gray granite
99026	Gold Hill	1N	72W	25	NE	NW	0	0	0	10+	10	65	brown granite
99772	Gold Hill	1N	72W	25	NE	NW	0	0	0	105	105	490	gray granite
19472	Gold Hill	1N	72W	25	NW	NW	0	0	0	30	30	60	gray Idaho Springs quartzite
130060	Gold Hill	1N	72W	25	SE	NW	0	0	0	40	40	55	gray granite
132737	Gold Hill	1N	72W	25	SE	NW	0	0	0	38	38	45	gray granite
152990	Gold Hill	1N	72W	25	SE	NW	10	0	0	8.5	18.5	200	brown, red, gray granite
153689	Gold Hill	1N	72W	25	SW	NW	5	0	0	14	14	145	gray granite and quartz
94917	Gold Hill	1N	72W	25	NE	SE	0	0	0	15+	15	335	alternate thin layers of gray, brown granite
103781	Gold Hill	1N	72W	25	NE	SE	4	0	0	8	12	93	gray granite
28481	Gold Hill	1N	72W	25	NW	SE	0	0	0	23	23	70	gray granite
136115	Gold Hill	1N	72W	25	NW	SE	0	0	0	15	15	145	gray granite
88553	Gold Hill	1N	72W	25	SE	SE	0	0	12	35	35	210	gray granite
107742	Gold Hill	1N	72W	25	SE	SE	0	0	0	3	3	85	gray granite
106927	Gold Hill	1N	72W	25	SW	SE	1	0	0	3	4	15	schist
48445	Gold Hill	1N	72W	25	SW	SE	3	0	0	0	3	48	gray granite
182799	Gold Hill	1N	72W	25	NE	SW	0	0	39	39	39	400	brown, gray granite and quartz
88140	Gold Hill	1N	72W	25	NE	SW	0	0	0	60	60	85	gray granite
97502	Gold Hill	1N	72W	25	NE	SW	1	0	0	0	1	85	thin layers of brown and gray granite
198912	Gold Hill	1N	72W	25	NE	SW	0	0	0	0	0	225	red gneiss
145115	Gold Hill	1N	72W	25	NW	SW	4	0	0	0	4	100	granite
38021	Gold Hill	1N	72W	25	NW	SW	0	0	15	15+	15	30	brown granite (soft) and quartz
59159	Gold Hill	1N	72W	25	NW	SW	2	0	2	2	4	22	gray granite (medium)
106119	Gold Hill	1N	72W	25	SE	SW	4	0	0	0+	4	70	brown granite
137491	Gold Hill	1N	72W	25	SE	SW	0	0	15	15+	15	130	brown granite
24813	Gold Hill	1N	72W	25	SE	SW	0	0	0	8	8	12	gray granite
26694	Gold Hill	1N	72W	25	SW	SW	0	0	0	15	15	125	gray granite
2121	Gold Hill	1N	72W	10	SW	SE	0	0	14	14	14	35	granite schist
9554	Gold Hill	1N	72W	10	SW	SE	3	0	0	27	29	60	gray granite
23542	Gold Hill	1N	72W	10	SW	SE	1	0	20	20	21	40	solid granite
126028	Gold Hill	1N	72W	18	NE	SE	2	0	0	0	2	30	gray granite
3772	Gold Hill	1N	72W	18	NE	SE	1	0	0	21	22	25	hard granite
181980	Gold Hill	1N	72W	18	NE	SW	0	0	18	41	41	54	gray granite, schist and talc
77301	Gold Hill	1N	72W	17	SW	NE	0	0	18	18	18	28	gray granite
173785	Gold Hill	1N	72W	17	NW	SE	0	0	0	15	15	394	gray granite (hard)
208306	Gold Hill	1N	72W	17	NW	SW	0	0	6	45+	6	45	red and brown gneiss (soft)

67756	Gold Hill	1N	72W	15	NE	NW	2	0	0	3	5	21	gray granite (hard)
55939	Gold Hill	1N	72W	15	NE	SE	0	6	0	0	6+	6	aluvium, black/gray fractured granite
93080	Gold Hill	1N	72W	14	NE	SE	1	0	15	108+	16	108	brown granite
117570	Gold Hill	1N	72W	14	NE	NE	0	0	0	65	65	350	gray granite
156990	Gold Hill	1N	72W	14	SW	NE	0	0	2	25	27	98	gray granite
95067	Gold Hill	1N	72W	14	SE	NE	5	0	0	10	15	130	gray granite
74519	Gold Hill	1N	72W	14	SE	NE	3	0	27	27	30	40	gray granite (medium)
94266	Gold Hill	1N	72W	14	SE	NE	0	0	28	31+	31	140	gray granite (broken, soft)
160421	Gold Hill	1N	72W	14	NW	NE	0	0	12	12	12	231	gray granite with quartz (medium)
73939	Gold Hill	1N	72W	14	NE	NE	4	0	8	18+	12	18	brown granite (soft)
36516	Gold Hill	1N	72W	19	NW	NW	3	0	0	0	3	9	granite
144293	Gold Hill	1N	72W	20	NE	NW	20	0	0	20	20	140	gray granite with white quartz
83718	Gold Hill	1N	72W	20	SE	NE	0	18	0	0	18	285	schist and talc
76649	Gold Hill	1N	72W	20	SE	NE	1	20	0	0	21	74	gray granite and quartz
142768-A	Gold Hill	1N	72W	20	SE	NE	0	0	0	24	24	400	gray granite and quartz
88061	Gold Hill	1N	72W	21	SE	NW	10	0	0	6	18	52	gray granite
174820	Gold Hill	1N	72W	21	SE	NE	10	0	0	24	34	150	gray and purple granite
176710	Gold Hill	1N	72W	21	SE	NW	0	0	16	25+	16	25	red gneiss (medium)
91951	Gold Hill	1N	72W	21	SW	NW	0	15	0	20	35	120	gray granite and talc
119835A	Gold Hill	1N	72W	21	SW	NW	13	0	0	0	13	405	gray granite and talc
51898	Gold Hill	1N	72W	22	NE	NW	0	0	0	16	16	208	gray granite, schist and talc
179943	Gold Hill	1N	72W	22	SE	NW	0	18	0	0	18	120	gray gneiss
83732	Gold Hill	1N	72W	22	SW	NW	4	0	0	0	4	71	gray granite
95767	Gold Hill	1N	72W	22	NW	SE	0	0	0	22	22	205	gray granite
28086	Gold Hill	1N	72W	22	SW	SE	0	0	16	16	16	65	gray granite
139701	Gold Hill	1N	72W	23	SW	SW	0	3	0	0	22	43	gray granite and talc
191117	Gold Hill	1N	72W	23	SE	NW	0	14	0	0	14	200	gray gneiss
69859	Gold Hill	1N	72W	30	SW	NE	20	0	0	0	20	180	granite
195327	Gold Hill	1N	72W	30	SW	NE	0	0	18	18	18	600	granites
28407	Gold Hill	1N	72W	30	SE	NW	4	0	0	46+	4	50	brown granite
102650	Gold Hill	1N	72W	30	SW	NE	15	0	14	14	24	73	gray granite
126084	Gold Hill	1N	72W	30	SW	NW	0	0	0	44+	6	50	brown granite and quartz
161742	Gold Hill	1N	72W	30	NE	SE	0	0	15	15	15	38	gray schist
230773	Gold Hill	1N	72W	30	NW	SE	0	0	0	40	40	220	black schist (medium)
153888	Gold Hill	1N	72W	30	NW	SW	0	0	0	28	28	30	schist
161325	Gold Hill	1N	72W	30	NW	SW	2	0	24	24+	26	82	brown and gray granite
17327	Gold Hill	1N	72W	27	SW	NW	0	0	0	7	7	42	gray granite
32088	Gold Hill	1N	72W	27	SW	SE	4	0	0	11+	4	15	brown and gray granite (mixed)
208896	Gold Hill	1N	72W	27	SW	SE	0	0	6	6	6	72	gray granite
61645	Gold Hill	1N	72W	35	SW	SW	23	0	0	13+	23	36	granite (bronze), quartz (red)
226805	Gold Hill	1N	72W	35	SW	NW	0	0	20	20	20	400	granites and quartz
63008	Gold Hill	1N	72W	35	SW	NE	3	0	0	0	3	60	gray granite (hard)
missing	Gold Hill	1N	72W	35	NW	NE	4	0	0	4	8	100	white quartz and schist
114801	Gold Hill	1N	72W	31	NW	SW	1	0	0	4	5	45	gray granite
148668	Gold Hill	1N	72W	31	NW	SW	0	0	3	3	3	300	gray granite schist with quartz
157294	Gold Hill	1N	72W	31	NW	SW	0	0	12	12	12	85	gray granite
63547	Gold Hill	1N	72W	31	NW	SW	0	0	4	12	12	53	gray granite (medium, hard)
115141	Gold Hill	1N	72W	31	NW	SW	0	0	0	3	3	100	gray granite
102497	Gold Hill	1N	72W	36	NW	SE	0	0	3	70+	3	70	brown granite
44674	Gold Hill	1N	71W	31	NW	SE	0	10	8	8	18	105	gray granite
20796	Gold Hill	1N	71W	31	NW	SE	2	40	0	0	42	46	granite

160369	Nederland	1S	74W	1	NW	SW	3	0	0	0	3	240	quartz and granite
54404	Nederland	1S	73W	5	NE	SE	11	21	0	0	32+	32	sand and gravel
27601	Nederland	1S	73W	2	SE	NE	0	40	0	0	40+	40	sand
102710	Nederland	1S	73W	2	NE	SE	0	18	0	0	18	305	granites
17496	Nederland	1S	73W	1	NE	SW	1	0	0	0	1	50	schist with quartz
17527	Nederland	1S	73W	1	NE	SW	5	0	0	121	5	126	weathered granite
90503	Nederland	1S	73W	1	NE	SW	0	0	3	55	3	55	brown granite
17510	Nederland	1S	73W	1	SW	SW	4.5	0	0	125.5+	4.5	130	weathered granite and schist
17543	Nederland	1S	73W	1	NW	SW	5	11	0	96+	16	112	weathered granite
111951	Nederland	1S	73W	9	SW	NW	42	0	0	33+	42	75	brown granite
111953	Nederland	1S	73W	9	SW	NW	39	0	0	0	39	75	schist
103473	Nederland	1S	73W	10	SE	SW	0	0	10	50+	10	50	brown granite
167384	Nederland	1S	73W	10	SE	SE	15	0	13	28+	28	28	brown and gray granite
160284	Nederland	1S	73W	10	SE	SE	0	0	0	10+	0	10	brown granite
69757	Nederland	1S	73W	10	SE	SE	0	0	0	16+	0	16	brown granite (soft)
179665	Nederland	1S	73W	11	NE	NW	0	0	16	17+	17	17	brown and gray granite
59297	Nederland	1S	73W	11	NW	SE	12	0	35	35+	12	47	broken brown granite (soft)
123976	Nederland	1S	73W	11	SW	SE	2	0	0	0	2	140	gray granite
69300	Nederland	1S	73W	11	SW	SE	0	0	15	31+	15	31	brown granite (soft)
208897	Nederland	1S	73W	11	SW	SE	3	0	25	25+	28	400	brown, gray, and pink granite
164010	Nederland	1S	73W	11	SW	SW	0	0	6	6	6	283	gray granite (medium)
165054	Nederland	1S	73W	11	SW	SW	0	0	35	35	35	50	gray granite
188473	Nederland	1S	73W	11	SW	SW	1	0	6	6	7	42	gray schist
136186	Nederland	1S	73W	12	NE	SE	6	0	6	60+	6	60	mineralized granite
221691	Nederland	1S	73W	12	NE	SE	0	0	7	30+	7	30	red gneiss (medium)
24220	Nederland	1S	73W	12	SE	SE	0	0	0	10	0	20	ironstained, partially decomposed granite
9054	Nederland	1S	73W	12	SE	SE	0	0	0	30	30	30	gray granite
103811	Nederland	1S	73W	12	SW	SE	0	0	0	60	60	65	gray granite
51319	Nederland	1S	73W	17	NW	NW	2	0	31	31	33	60	gray granite (soft)
90504	Nederland	1S	73W	15	NE	NE	0	0	10	10+	10	60	brown granite
140546	Nederland	1S	73W	15	NE	NE	6	0	11	11	17	87	gray granite
88907	Nederland	1S	73W	15	NE	NE	0	0	28	28+	28	145	brown granite
232310	Nederland	1S	73W	15	NE	NE	0	0	12	12	12	65	gray granite
111730	Nederland	1S	73W	14	SW	NE	0	23	0	0	23	30	gray schist and white quartz
6916	Nederland	1S	73W	14	SE	NE	40	0	0	0	40	42	quartz sandstone
17462	Nederland	1S	73W	14	SE	SE	0	80	0	0	80+	80	sand and gravel
6658	Nederland	1S	73W	14	NE	NE	0	80	0	0	80+	80	sand, gravel, and clays
225915	Nederland	1S	73W	14	SE	NW	0	0	0	80+	0	80	red gneiss (medium)
22655	Nederland	1S	73W	14	NW	NW	0	0	20	20	20	30	ironstained, quartzite granite
163267	Nederland	1S	73W	14	NW	NW	0	0	12	12	12	15	gray granite
15976	Nederland	1S	73W	14	NE	NW	0	0	10	10+	10	70	brown and gray granite
132099	Nederland	1S	73W	14	SE	NE	0	32	0	0	32+	32	boulders and gravel
132570	Nederland	1S	73W	14	SE	NE	0	22	0	0	22	35	granite
149748	Nederland	1S	73W	14	SE	NE	4	29	0	0	33	59	gray granite
24910	Nederland	1S	73W	14	SE	NE	4	0	17	17+	21	23	brown granite
94301	Nederland	1S	73W	14	SW	NE	0	0	0	50+	0	50	brown granite
30582	Nederland	1S	73W	14	SW	NE	10	0	0	15	25	25	gray granite
61883	Nederland	1S	73W	14	SW	NE	18	0	0	0	18	60	gray granite
155620	Nederland	1S	73W	24	NE	NE	1	0	8	8+	9	645	brown and gray granite
135026	Nederland	1S	73W	24	NW	NE	1	0	0	24	25	110	gray granite
169478	Nederland	1S	73W	24	SE	NE	0	0	0	80	0	280	gray gneiss (medium)

204977	Nederland	1S	73W	24	SE	NE	3	0	0	27	30	360	gray and white gniess
72315	Nederland	1S	73W	24	SW	NE	0	0	18	34	34	101	gray granite (soft)
78256	Nederland	1S	73W	24	SW	NE	0	0	10	10	10	21	pink granite (soft)
177529	Nederland	1S	73W	24	NE	NW	0	0	26	26	26	230	gray gneiss (medium)
145642	Nederland	1S	73W	24	NE	NW	0	0	25	25	25	136	gray granite with quartz (medium)
17879	Nederland	1S	73W	24	NE	NW	18	0	3	56+	21	74	brown granite
209676	Nederland	1S	73W	24	NE	SE	2	0	0	36	38	230	gray gneiss
211507	Nederland	1S	73W	24	NE	SE	1	0	0	11	12	17	gray schist
180830	Nederland	1S	73W	24	NW	SE	0	0	17	17+	17	400	brown, gray, and pink granite (w/quartz)
150577	Nederland	1S	73W	24	SE	SE	8	0	0	26	34	400	gray granite with quartz
150576	Nederland	1S	73W	24	SE	SE	0	0	0	25	30	405	gray granite
139916	Nederland	1S	73W	24	NE	SW	0	0	12	12	12	138	gray granite
41369	Nederland	1S	73W	24	NE	SW	0	0	0	0	0	380	gray granite
193656	Nederland	1S	73W	23	NW	NW	12	0	0	0	12	141	shale
23331	Nederland	1S	73W	22	SW	SE	4	0	17	17	21	35	gray granite
34032	Nederland	1S	73W	22	SW	NE	37	0	0	0	37	190	gray granite
154092	Nederland	1S	73W	22	NW	SW	0	17	0	0	17	80	gray granite
157458	Nederland	1S	73W	22	NW	SW	0	30	0	0	30	80	granite, schist, and quartz
16846	Nederland	1S	73W	22	NW	SW	3	15	0	0	18+	18	rocks and gravel
23716	Nederland	1S	73W	22	SE	SW	0	20	0	0	20	80	light gray granite
22221	Nederland	1S	73W	22	SW	SW	8	0	29	29	37	128	gray granite
47210	Nederland	1S	73W	22	NE	SW	6	0	19	19+	25	42	brown and gray granite
196451	Nederland	1S	73W	30	NE	SE	1	0	0	0	1	80	gray schist
203756	Nederland	1S	73W	29	NE	NE	0	0	0	160	160	170	blue and black granite
28479	Nederland	1S	73W	29	SE	NE	0	91	0	39+	91	130	decomposed gray granite
18322	Nederland	1S	73W	28	SE	NE	0	0	10	10+	10	67	granite and quartz
23348	Nederland	1S	73W	28	NW	NW	23	0	0	0	0+	23	overburden
84424	Nederland	1S	73W	26	SW	SW	20	0	0	0	20	60	gray granite
71229	Nederland	2S	74W	1	SE	NE	20	26	0	0	46+	46	sand and gravel
39460	Nederland	1S	73W	31	NE	SE	0	0	34	70+	34	70	pink broken granite (medium)
58868	Nederland	1S	73W	31	SE	SE	0	0	0	0	9	11	granites
77905	Nederland	1S	73W	32	SW	SE	12	0	0	0	12	30	gray granite and quartz
184984	Nederland	1S	73W	34	SW	SE	4	0	0	0	4	12	gray granite
120899	Nederland	1S	73W	35	NE	SE	0	0	0	10	10	15	gray granite
149977	Nederland	1S	73W	35	NE	SE	5	0	18	80+	23	85	brown granite
153340	Nederland	1S	73W	35	NE	SE	0	18	0	0	18	40	gray granite and quartz
153339	Nederland	1S	73W	35	NW	SE	0	19	0	0	19	49	gray granite and quartz
52442	Nederland	1S	73W	35	SE	SE	2	0	28	28	30	53	schist
148963	Nederland	1S	73W	35	SE	SE	6	0	0	24	30	100	gray granite
197185	Nederland	1S	73W	35	SE	SE	2	0	0	37	39	75	tan granite
2437-F	Nederland	1S	73W	35	SW	SW	1	25	4	4+	26	30	brown decomposed granite
35364	Nederland	1S	73W	35	SW	SW	2	0	0	21	23	25	schist (medium)
93946-A	Nederland	1S	73W	35	SW	SW	0	28	0	0	28	35	brown schist
149768	Nederland	1S	73W	35	SW	SW	0	25	0	0	40	120	granite and quartz
217821	Nederland	1S	73W	20	NW	SE	0	28	0	0	28	295	granite
196689	Nederland	1S	73W	20	SE	NE	0	18	0	0	18	40	gray granite
202107	Nederland	1S	73W	20	NE	NW	40	0	0	40+	40+	40	top soil, fractured granite, mica
81753	Nederland	1S	73W	20	SW	NE	10	26	0	0	36+	36	sand, clay, and boulders
79827-A	Nederland	1S	73W	20	SW	NE	0	34	0	0	34	46	white quartz
56394-A	Nederland	1S	73W	20	SW	NE	0	34	0	0	34	45	gray granite
215293	Nederland	1S	73W	20	SE	NE	0	34	0	24+	34	58	gray schist (fractured)

310364	Nederland	1S	73W	20	SE	NE	26	0	0	0	26	40	granite
117739	Nederland	1S	73W	20	NW	NE	0	0	0	8+	0	30	brown granite
39979	Nederland	1S	73W	20	NE	NE	17	0	0	30+	35	47	decomposed granite
28157	Nederland	1S	73W	20	SE	NE	8	11	0	0	19	22	granite
90826-A	Nederland	1S	73W	21	SE	NE	0	35	0	0	35+	35	clay and boulders
17627	Nederland	1S	73W	21	SE	SE	2	33	0	0	35	40	gray granite with white quartz
5865	Nederland	1S	73W	21	NW	SE	1	9	0	0	10	25	solid granite
41684	Nederland	1S	73W	21	NE	SE	0	10	0	0	10	19	gray granite (medium)
181638	Nederland	1S	73W	21	NE	SE	0	28	0	0	28	60	gray schist
189582-A	Nederland	1S	73W	21	SW	NW	0	22	0	0	22	45	gray granite with white quartz
139295	Nederland	1S	73W	21	SW	NW	0	20	0	0	20+	100	white soapstone, granite, compressed glacial silt
101243	Nederland	1S	73W	21	SW	NW	10	19	0	0	29+	29	gravel
232075	Nederland	1S	73W	21	SE	NW	0	15	0	0	30	42	gray schist
204443	Nederland	1S	73W	21	SE	NW	0	20	0	0	20	67	gray schist
64238	Nederland	1S	73W	21	SW	NE	0	28	0	0	28+	28	gravel and boulders
92717	Nederland	1S	73W	21	SW	NE	0	33	0	0	33+	33	clay and boulders
33923	Nederland	1S	73W	13	SW	SW	8	0	11	11	19	45	gray granite
41651	Nederland	1S	73W	13	NW	SW	10	27	0	0	37+	37	boulders
41586	Nederland	1S	73W	13	NW	SW	0	45	0	0	45+	45	loose gravel and boulders
missing	Nederland	1S	73W	13	NE	SW	12	0	0	29	41	145	gray granite
23838	Nederland	1S	73W	13	SE	SE	0	0	0	30+	40+	40	tan, partially weathered Idaho Springs formation
233630	Nederland	1S	73W	13	NW	SE	0	23.5	0	0	23.5+	23.5	clayey gravel, cobbles
212175	Nederland	1S	73W	13	NE	SE	3	0	0	47	50	460	gray gneiss
189787	Nederland	1S	73W	13	SW	NW	0	19	0	0	36.5	36.5	quartz monzonite basement
233635	Nederland	1S	73W	13	SE	NW	0	15	0	0	15+	15	gravels
167591	Nederland	1S	73W	13	SE	NW	0	10.5	0	0	10.5+	10.5	sand, gravel, and clays
184195	Nederland	1S	73W	13	NW	NE	0	0	48	48	48	400	gray and pink granite
144821	Nederland	1S	73W	13	NW	NE	4	0	0	4+	4	160	brown and gray granite
7628	Nederland	1S	73W	13	NW	NE	0	0	2	15+	2	15	brown and gray granite (medium, hard)
204550	Nederland	2S	73W	5	SW	NW	0	12	0	0	12	320	gray granite
71227-A	Nederland	2S	73W	5	SE	NW	0	80	0	0	80+	80	boulders
63021	Nederland	2S	73W	5	NE	NW	0	51	0	0	51+	51	gravel and sand
219425	Nederland	2S	73W	5	SW	NE	0	38	0	0	38	140	gray granite
219424	Nederland	2S	73W	5	SW	NE	0	30	10	10	40	345	schist with scattered granite layers
154605	Nederland	2S	73W	3	SE	SW	12	0	0	3	15	180	gray granite
37752	Nederland	2S	73W	16	NW	NW	3	0	0	54+	20	57	brown granite
198651	Nederland	2S	73W	14	NE	NW	0	24	0	0	24	35	gray granite
51109	Nederland	2S	73W	11	NE	NE	0	0	0	78	78	126	schist, quartz (soft)
197116	Nederland	2S	73W	11	NW	SE	14	0	0	0	14	22	gray granite
131955	Nederland	2S	73W	11	SW	NE	0	16	0	0	16	55	gray granite
181819	Nederland	2S	73W	11	SW	NE	0	0	18	18	18	400	gray, pink granite with schist, talc, quartz
181567	Nederland	2S	73W	11	SW	NE	0	0	0	15	15	22	gray schist
228943	Nederland	2S	73W	11	SE	NE	0	0	0	3	3	22	gray schist
120034	Nederland	2S	73W	11	SE	NE	4	0	0	11	15	22	red quartz
227161	Nederland	2S	73W	13	NW	NW	3	0	21	21	24	57	gray granite
150193	Nederland	2S	73W	13	NW	NW	17	0	0	0	17	19	schist
166505	Nederland	2S	73W	13	NE	NW	1	0	0	0	1	165	gray granite
122086	Nederland	2S	73W	13	NE	NW	3	0	22	32+	25	35	brown granite
63983	Nederland	2S	73W	13	SE	NW	1	0	13	13	14	21	gray granite (hard)
178569	Nederland	2S	73W	13	NW	NE	0	0	0	0	0	37	gray granite
38959	Nederland	2S	73W	13	NW	NE	3	0	8	8+	8	35	brown granite

32908	Nederland	2S	73W	13	NW	NE	3	12	0	3+	15	18	brown granite
27143	Nederland	2S	73W	12	NE	NE	8	0	32	32	40	57	gray granite
41925	Nederland	2S	73W	12	SW	SW	0	0	0	65+	60	65	brown granite and quartz
219451	Nederland	2S	73W	12	SE	SW	4	0	11	11	15	100	gray schist
195837	Nederland	2S	73W	12	SE	SW	0	0	0	12	12	24	gray granite
37751	Nederland	2S	73W	12	SE	SW	0	0	0	30+	20	30	brown granite
162541	Nederland	2S	73W	12	SE	NW	3	0	3	3	6	45	gray granite
127677	Nederland	2S	73W	12	SE	NW	8	0	0	0	8	160	gray granite
16970	Nederland	2S	73W	12	SE	NW	3	0	0	0	3	40	gray granite
129296	Nederland	2S	73W	12	SE	NW	15	0	0	0	15	140	gray granite
11742-A	Nederland	2S	73W	12	SW	NE	0	0	15	38+	15	38	gray granite (fractured)
1437	Nederland	2S	73W	2	SW	NE	10	0	0	0	10	56	rose granite and mica
178686	Nederland	2S	73W	2	SW	NE	1	7	0	62+	8	70	brown granite
17383	Nederland	2S	73W	2	NW	SE	13	0	3	7+	16	20	brown granite
20760	Nederland	2S	73W	2	NW	SE	0	0	11	21+	11	21	brown granite
missing	Nederland	2S	73W	2	SW	SE	2	0	0	0	2	230	gray granite and talc
27543	Nederland	2S	73W	1	SW	SW	14	0	0	26	40	62	gray granite
212171	Nederland	2S	73W	1	SE	SW	0	0	15	29+	15	29	brown granite
104089	Nederland	2S	73W	1	SE	SW	3	0	0	37+	3	40	brown granite
47351	Nederland	2S	73W	1	NE	SW	0	0	62	62	62	127	schist and quartz (soft)
108904	Nederland	2S	73W	1	NW	SW	0	0	3	20+	3	20	brown granite
225221	Nederland	2S	73W	1	NW	SW	0	0	13	13+	13	42	brown and gray granite
224083	Nederland	2S	73W	1	SE	SE	0	0	6	10	16	260	pink and gray granite
234917	Nederland	2S	73W	1	NW	SE	0	0	12	27	27	400	schist
86747	Nederland	2S	73W	1	SW	NW	0	0	17	17	17	40	gray granite
37343	Nederland	2S	73W	1	SW	NW	2	0	0	18+	2	20	brown granite
70437	Nederland	2S	73W	1	NW	NW	10	0	0	0	10	50	pink granite
85328	Nederland	2S	73W	1	SE	NW	11	0	0	0	11	18	granite (medium, hard)
85328-A	Nederland	2S	73W	1	SE	NW	0	0	0	15	15	20	schist
37469	Nederland	2S	73W	1	NW	NW	0	4	0	21	25	60	gray granite
120123	Nederland	2S	73W	1	SW	NE	0	0	0	40	40	270	gray granite and talc
75486	Nederland	2S	73W	1	SW	NE	8	0	0	32+	8	40	brown granite
42561	Nederland	2S	73W	1	NW	NE	0	0	50	50	50	112	gray granite
38012	Nederland	2S	73W	1	NW	NE	0	0	12	28+	12	28	brown granite
230975	Nederland	2S	73W	1	NE	NE	2	0	0	15	17	24	gray granite
22218	Nederland	1S	73W	25	SE	SW	0	0	10	20	20	50	gray granite and quartz
22219	Nederland	1S	73W	25	NW	SW	0	0	12	21	21	35	gray granite
192240	Nederland	1S	73W	25	NE	SW	4	0	0	66+	4	70	brown schist
183657	Nederland	1S	73W	25	SE	SE	0	0	0	0+	0	247	brown and gray granite
183728	Nederland	1S	73W	25	NW	SE	0	0	17	33	33	300	gray-green granite
131768	Nederland	1S	73W	25	SW	NW	3	0	9	9	12	21	gray granite
130488	Nederland	1S	73W	25	SW	NW	0	0	0	10	10	55	gray granite
158056	Nederland	1S	73W	25	NW	NW	0	0	12	12+	12	72	brown and gray granite
59802	Nederland	1S	73W	25	SW	NE	3	0	0	0	3	140	schist and quartz (soft)
74685	Nederland	1S	73W	36	NE	NE	1	0	0	17+	1	18	brown granite (medium, hard)
74686	Nederland	1S	73W	36	NE	NE	1	0	17	26+	18	27	brown granite (medium, hard)
1963	Nederland	1S	73W	36	SE	NE	1	0	0	47	48	100	gray granite (hard)
6405	Nederland	1S	73W	36	SE	NE	0	0	24	24	24	27	gray granite
13940	Nederland	1S	73W	36	SE	NE	0	0	11	11	11	19	gray granite
85514	Nederland	1S	73W	36	SE	NE	1	0	0	19	20	80	gray granite
188253	Nederland	1S	73W	36	SW	NE	0	0	9	9+	9	281	brown, gray, and pink granite

210726	Nederland	1S	73W	36	SW	NE	0	0	0	32	32	254	gray granite with talc and quartz
214018	Nederland	1S	73W	36	SW	NE	1	0	0	26+	1	27	brown granite
36332	Nederland	1S	73W	36	NE	SW	0	9	0	0	9	13	gray granite (medium, soft)
221097	Nederland	1S	73W	36	NE	SE	0	0	8	54+	22	54	weathered granite (brown)
24513	Nederland	1S	73W	36	NE	SE	12	0	18	18+	12	30	brown decomposed granite
224210	Nederland	1S	73W	36	NE	SE	0	0	12	12	12	400	gray granite
86954	Nederland	1S	73W	36	NW	SE	30	0	0	5+	30	35	brown granite
96309-A	Nederland	1S	73W	36	NW	SE	3	5	0	15	30	60	quartz
202527	Nederland	1S	73W	36	NW	SE	0	0	16	38+	16	38	brown granite
140459	Nederland	1S	73W	36	SE	SE	0	0	0	30	30	160	gray granite and quartz
224044	Monarch Lak	1N	74W	34	NW	NW	0	17	0	2+	17	19	weathered shale
224045	Monarch Lak	1N	74W	34	NW	NW	0	15	0	0	15+	15	glacial sand
23580	Monarch Lak	1N	74W	35	SE	SW	3	52	0	0	55	65	shale
46028	East Portal	1S	74W	21	NE	SE	3	0	0	0	3	80	granites, schists
68888	Ward	1N	73W	13	NE	SW	0	0	5	5	5	23	granite
150105	Ward	1N	73W	24	NE	NE	0	0	6	34	34	41	gray granite
144819	Ward	1N	73W	24	SE	SW	3	0	0	37	40	180	gray granite
153889	Ward	1N	73W	25	NE	SE	0	0	0	35	35	65	gray granite
158494	Ward	1N	73W	25	NE	SE	0	0	0	45	45	94	gray granite and talc
82962	Ward	1N	73W	36	NE	SE	0	0	5	5	5	30	gray granite
100846	Ward	1N	73W	36	SE	NE	0	0	0	15	15	295	gray granite
59304	Ward	1N	73W	36	NW	NE	10	0	0	0	10	24	granite
29843	Ward	1N	73W	36	NE	NE	0	0	12	14	14	20+	gray granite
129031	Ward	1N	73W	36	NE	NE	5	0	0	15	20	120	gray granite
124887	Ward	1N	73W	36	NE	NE	0	0	0	30	30	38	gray granite
44631	Tungsten	1S	72W	6	NE	NE	0	0	0	38	38	69	gray granite (hard)
93422	Tungsten	1S	72W	6	NE	NE	0	0	0	4	4	25	gray granite
105119	Tungsten	1S	72W	6	NE	NE	0	0	0	18	18	100	gray granite (medium)
64051	Tungsten	1S	72W	6	NW	NE	3	28	18	18	49	50	granite (medium)
88395	Tungsten	1S	72W	6	NW	NE	1	0	0	14	15	40	gray granite
139821	Tungsten	1S	72W	6	SW	NE	2	0	0	0	2	60	gray granite
193744	Tungsten	1S	72W	6	SW	NE	0	0	10	10+	10	164	brown and gray granite
229226	Tungsten	1S	72W	6	NW	NW	0	0	3	10	10	245	pink and gray granite, talc
48041	Tungsten	1S	72W	6	SE	NW	3	0	0	62	65	105	pink granite (medium)
39128	Tungsten	1S	72W	6	SW	NW	10	0	0	0	10	28	gray granite (medium)
176705	Tungsten	1S	72W	2	NW	NW	4	0	0	0+	4	500	brown and gray granite with quartz
54491	Tungsten	1S	72W	2	NW	NW	2	0	4	4	6	30	granite and schist (medium)
242458	Tungsten	1S	72W	17	SW	NW	0	1	0	0	1	152	biotite w/thin intruded layers granite pegmatite
240244	Tungsten	1S	72W	17	NW	NW	0	0	8	8+	8	53	brown granite
104360	Tungsten	1S	72W	17	NW	NW	0	0	0	65	65	405	gray granite
21417	Tungsten	1S	72W	19	SW	NW	24	0	0	42	66	92	gray granite and quartz
239214	Tungsten	1S	72W	19	NE	SW	0	0	5	17	17	460	gray granite and talc
180800	Tungsten	1S	72W	19	NW	SW	0	0	0	0	45	110	gray granite
103074	Tungsten	1S	72W	19	SE	SW	1	0	0	19	20	140	gray schist
234189	Tungsten	1S	72W	19	SW	SW	4	0	0	0	4	22	gray granite
13550	Tungsten	1S	72W	20	SE	SE	0	0	0	13+	13	230	brown granite, partially decomposed and fractured
66194	Tungsten	1S	72W	20	SW	SW	2	0	0	15	17	83	medium/hard brown and gray granite (mixed)
82976	Tungsten	1S	72W	20	SE	SW	1	0	0	6	7	61	medium/hard granite
82966	Tungsten	1S	72W	20	SE	SW	1	0	0	0	1	118	medium/hard brown granite, granite
79403	Tungsten	1S	72W	20	SE	SW	0	0	0	150+	0	150	brown granite (soft)
77856	Tungsten	1S	71W	18	NW	NW	0	0	50	50	50	95	gray granite, schist (medium)

42042	Tungsten	1S	71W	18	NW	NW	4	11	4	4+	19	80	harder brown granite
73874	Tungsten	1S	71W	18	NW	NW	0	0	10	10	10	17	pink granite (soft, medium)
50867	Tungsten	1S	71W	18	SE	NW	8	0	0	0	8	106	broken gray granite (medium)
43257	Tungsten	1S	71W	18	SW	NW	3	0	0	4	7	12	gray granite (hard)
155761	Tungsten	1S	72W	26	SE	NE	6	0	0	13	19	54	gray granite with white quartz
66823	Tungsten	1S	72W	26	NE	SW	2	0	0	0+	2	125	brown granite and quartz
170300	Tungsten	1S	72W	26	NW	SW	0	0	0	12	12	45	gray granite
169547	Tungsten	1S	72W	26	SW	SW	0	0	0	2	2	79	gray granite and quartz
16052	Tungsten	1S	72W	23	NW	NW	0	0	0	37	37	73	brown granite (hard)
27161	Tungsten	1S	72W	23	SW	NW	0	0	0	40	40	55	white quartz
46678	Tungsten	1S	72W	23	SE	NW	2	0	0	25	27	73	broken gray granite (medium)
113485	Tungsten	1S	72W	23	SW	NW	0	0	2	2+	20	35	brown granite
113199	Tungsten	1S	72W	23	SW	NW	8	0	0	72	80	121	gray granite
30714	Tungsten	1S	72W	23	SW	NW	0	0	20	20+	20	20	brown granite (decomposed)
35526	Tungsten	1S	72W	23	SW	NW	2	0	0	0+	2	43	brown granite (hard)
88781	Tungsten	1S	72W	23	SW	SE	0	0	0	18	18	205	gray granite
172264	Tungsten	1S	72W	23	NE	SW	4	0	11	11+	15	300	brown, gray, pink, green granite w/quartz, talc
152688	Tungsten	1S	72W	23	NW	SW	4	0	0	0	4	54	gray granite
106120	Tungsten	1S	72W	23	NW	SW	4	0	0	0	26	352	gray granite
154973	Tungsten	1S	72W	23	NW	SW	2	0	0	4+	6	66	brown and gray granite
21033	Tungsten	1S	72W	23	NW	SW	0	0	10	10+	10	24	brown granite
88757	Tungsten	1S	72W	21	NE	NE	0	0	0	10	10	550	gray granite
151793	Tungsten	1S	72W	21	NE	NE	0	0	0	11	11	53	gray granite (soft)
158863	Tungsten	1S	72W	21	SW	NE	0	0	0	0+	25	29	brown granite and quartz
152953	Tungsten	1S	72W	21	SE	NW	1	0	0	23+	24	234	brown granite
157534	Tungsten	1S	72W	21	NE	SE	0	0	0	8	8	410	gray granite (hard)
167415	Tungsten	1S	72W	21	NW	SE	0	0	0	32	32	97	gray granite and talc
107087	Tungsten	1S	72W	21	SE	SW	0	0	0	30	30	35	gray granite
58481	Tungsten	1S	72W	21	SW	SW	2	0	158	158+	160	235	decomposed brown, gray granite w/copper traces
64471	Tungsten	1S	72W	21	SW	SW	0	0	23	123	123	154	red and gray granite
22594	Tungsten	1S	72W	21	SW	SW	0	0	14	14+	14	500	brown and gray granite (mixed)
228580	Tungsten	1S	72W	21	SW	SW	0	0	13	13+	13	400	brown and gray granite (mixed)
231169	Tungsten	1S	72W	21	SW	SW	0	0	0	17+	17	65	brown and gray granite
177926	Tungsten	1S	72W	10	NW	NW	1	0	5	10	11	36	white quartz
62590	Tungsten	1S	72W	10	NW	NW	1	0	5	5	6	18	quartz, feldspar, black mica (hard)
32210	Tungsten	1S	72W	10	SE	SE	2	0	13	41	43	56	pink and white quartz (hard)
94886	Tungsten	1S	72W	10	SW	SE	0	0	0	1	6	35	gray granite
54917	Tungsten	1S	72W	10	SW	SE	2	0	0	2	4	200	gray granite (medium)
39409	Tungsten	1S	72W	10	SW	SE	0	0	8	8	8	11	gray, pink granite (medium)
76338	Tungsten	1S	72W	10	SE	SE	0	0	0	12	12	30	tan granite (medium)
34461	Tungsten	1S	72W	10	SE	SE	0	0	5	5	5	110	gray granite (soft)
29406	Tungsten	1S	72W	10	SE	SE	1	0	0	13	14	75	fractured granite (soft) and talc
87481	Tungsten	1S	72W	10	NW	SE	0	0	0	8	8	22	gray granite
58613	Tungsten	1S	72W	10	NW	SE	2	0	0	0	2	125	gray granite
38023	Tungsten	1S	72W	10	NW	SE	0	0	6	20	20	26	gray granite (medium)
210417	Tungsten	1S	72W	10	NE	SE	0	0	16	16+	16	35	brown granite
100059	Tungsten	1S	72W	10	NE	SE	0	0	5	5	5	235	gray granite
186009	Tungsten	1S	72W	10	NE	SE	1	0	9	9+	10	38	brown and gray granite
66948	Tungsten	1S	72W	5	NE	NW	1	0	8	8	9	30	gray granite (hard)
71993	Tungsten	1S	72W	5	NE	NW	2	0	4	4	6	18	gray granite (hard, medium)
74198	Tungsten	1S	72W	5	NE	NE	2	0	18	18	20	51	gray granite w/pink granite (streaks)

missing	Tungsten	1S	72W	5	SE	NW	1	0	0	0+	1	80	brown granite with quartz schist and talc
missing	Tungsten	1S	72W	5	SE	NW	1	0	0	0	5	23	gray granite (hard)
131767	Tungsten	1S	72W	5	SW	NW	0	0	0	2	2	97	gray granite
156892	Tungsten	1S	72W	5	SW	NW	13	0	0	0	13	40	gray granite
64250	Tungsten	1S	72W	5	SE	SE	10	0	0	58	60	112	gray granite (hard)
168570	Tungsten	1S	72W	5	SW	SE	3	0	0	17	20	215	white quartz
178252	Tungsten	1S	72W	5	SW	SE	0	0	50	50	50	220	gray granite (hard)
115175	Tungsten	1S	72W	5	SW	SE	5	0	0	9	14	200	granite
206388	Tungsten	1S	72W	5	NE	SW	0	0	0	3+	3	60	red gneiss
196087	Tungsten	1S	72W	5	NE	SW	6	0	16	16+	22	195	brown and gray granite
226575	Tungsten	1S	72W	5	NE	SW	0	27	0	0	27	200	gray granite (medium)
151788	Tungsten	1S	72W	5	NW	SW	0	39	0	0+	39	50	red granite and talc
16845	Tungsten	1S	72W	5	NW	SW	3	0	11	11+	14	22	solid brown granite
69198	Tungsten	1S	72W	5	NW	SW	4	0	13	13	17	57	gray granite (medium)
168950	Tungsten	1S	72W	5	SE	SW	0	0	4	4	4	80	gray granite (hard)
184137	Tungsten	1S	72W	5	SE	SW	0	0	10	17	17	284	gray and pink granite
112494	Tungsten	1S	72W	5	SW	SW	1	0	0	14	15	95	schist
115355	Tungsten	1S	72W	5	SE	SW	0	0	0	22	22	60	gray granite
146031	Tungsten	1S	72W	5	SE	SW	0	0	0	12	12	20	gray granite
230531	Tungsten	1S	72W	5	SW	SW	0	0	0	33	33	49	granite
215916	Tungsten	1S	72W	5	SW	SW	0	0	0	16+	16	346	gray and brown granite, talc
212327	Tungsten	1S	72W	5	SW	SW	0	0	0	0	18	24	gray schist
113368	Tungsten	1S	72W	4	SE	NE	1	0	0	29	30	35	schist
203193	Tungsten	1S	72W	4	SW	NE	0	0	6	6+	6	400	gray, pink, brown, and green granite
195940	Tungsten	1S	72W	4	SW	NW	0	0	0	10	10	210	gray gneiss (medium)
169780	Tungsten	1S	72W	4	NE	SE	0	0	4	4	4	11	gray schist
170054	Tungsten	1S	72W	4	NE	SE	0	0	7	7	7	400	gray, gray-green granite w/talc, quartz
170495	Tungsten	1S	72W	4	NE	SE	0	0	5	5+	5	72	brown and gray granite
199396	Tungsten	1S	72W	4	NE	SE	3	0	0	0	3	78	gray granite
212183	Tungsten	1S	72W	4	SE	SE	0	0	6	6	6	250	gray granite
212172	Tungsten	1S	72W	4	SE	SE	0	0	0	0+	0	89	brown and gray granite and talc
226578	Tungsten	1S	72W	4	SE	SE	0	0	0	20	20	143	gray granite
62603	Tungsten	1S	72W	4	SE	SE	0	0	0	4	4	80	gray granite
167333	Tungsten	1S	72W	4	SW	SE	0	0	10	10+	10	500	brown, gray, pink, granite w/some quartz, talc
139510	Tungsten	1S	72W	4	SW	SE	0	0	17	17	17	74	gray granite
151678	Tungsten	1S	72W	4	SW	SE	0	0	0	6	6	267	gray granite
163150	Tungsten	1S	72W	4	SW	SE	4	0	0	0	4	118	gray and pink granite
168951	Tungsten	1S	72W	4	SE	SW	0	0	8	8	8	362	gray granite (hard)
96123	Tungsten	1S	72W	4	SE	SW	0	0	0	14	14	31	gray granite
114564	Tungsten	1S	72W	4	SE	SW	1	0	0	18	19	135	gray granite
199212	Tungsten	1S	72W	4	SE	SW	0	0	4	4	4	180	dark gray gniess
119809	Tungsten	1S	72W	4	SW	SW	2	0	0	3	5	290	gray granite
70096	Tungsten	1S	72W	4	SW	SW	14	0	0	0	14	148	hard gray granite, schist
152988	Tungsten	1S	72W	7	NE	NE	0	0	12	12	12	100	gray granite and talc
149193	Tungsten	1S	72W	7	SE	NE	2	0	14	14+	16	34	brown granite
65257	Tungsten	1S	72W	7	SE	NE	18	0	0	0	18	95	gray granite (medium)
219975	Tungsten	1S	72W	7	SW	NE	4	0	0	4	8	360	gray granite with quartz
157470	Tungsten	1S	72W	7	NE	NW	0	11	0	24	35	40	pink granite
169550	Tungsten	1S	72W	7	NE	SE	0	0	15	15+	15	434	brown, gray, pink, gray-green granite w/talc, qz
133671	Tungsten	1S	72W	7	NE	SE	0	0	0	50	50	305	gray granite and talc
38022	Tungsten	1S	72W	7	NE	SE	0	0	45	45+	45	110	gray granite (soft)

175152	Tungsten	1S	72W	7	NW	SE	1	0	2	2	3	43	gray granite
126680	Tungsten	1S	72W	7	NW	SE	13	0	0	15	28	360	gray granite
135411	Tungsten	1S	72W	7	NW	SE	1	0	0	34	35	55	gray granite
148368	Tungsten	1S	72W	7	SE	SE	3	0	0	27	30	40	gray granite
missing	Tungsten	1S	72W	7	SE	SE	2	0	28	28	30	43	gray granite
17227	Tungsten	1S	72W	7	SE	SE	0	0	17	35	35	80	gray granite
24970	Tungsten	1S	72W	7	SE	SE	0	0	0	15	15	30	gray granite (medium)
148472	Tungsten	1S	72W	7	SW	SE	0	0	17	17+	17	46	brown granite
212868	Tungsten	1S	72W	7	SW	SE	0	0	0	16+	16	118	brown and gray granite
87448	Tungsten	1S	72W	7	NE	SW	0	0	0	35	35	305	gray granite
130753	Tungsten	1S	72W	7	NW	SW	0	0	0	0+	0	125	brown granite and schist
14008	Tungsten	1S	72W	7	SE	SW	0	0	0	15	15	50	gray granite
28013	Tungsten	1S	72W	7	SW	SW	1	0	0	14	15	20	solid granite
127103	Tungsten	1S	72W	8	NE	NE	3	0	0	5	8	60	gray granite
55932	Tungsten	1S	72W	8	NE	NE	4	0	16	16	20	80	gray granite
161527	Tungsten	1S	72W	8	NW	NE	0	0	12	12	12	136	gray granite with quartz (medium)
161326	Tungsten	1S	72W	8	NW	NE	0	0	17	17+	17	118	brown and gray granite
100330	Tungsten	1S	72W	8	SE	NE	0	0	2	15	15	25	gray granite
178249	Tungsten	1S	72W	8	NE	NW	0	0	24	24+	24	53	brown granite
115668	Tungsten	1S	72W	8	NE	NW	0	0	0	15	15	25	gray granite
114152	Tungsten	1S	72W	8	NW	NW	0	0	0	7	7	15	gray granite
79948	Tungsten	1S	72W	8	NW	NW	0	0	17	35	35	40	quartz and schist (medium)
180317	Tungsten	1S	72W	8	SW	NW	0	0	0	85	85	112	gray granite
24464	Tungsten	1S	72W	8	SW	NW	0	0	65	65	65	150	gray granite (soft)
50224	Tungsten	1S	72W	8	NE	SE	4	0	33	62+	62	81	brown broken granite (medium)
133670	Tungsten	1S	72W	8	SW	SE	0	21	9	9	30	50	gray granite
167385	Tungsten	1S	72W	8	NE	SW	2	0	0	0	2	35	gray granite
168269	Tungsten	1S	72W	8	NE	SW	0	0	14	14	14	124	gray granite with quartz (hard)
174943	Tungsten	1S	72W	8	NE	SW	0	0	8	8+	8	440	brown, gray, pink, green granite w/some qz, talc
106653	Tungsten	1S	72W	8	NE	SW	3	0	0	29	32	300	gray granite
181267	Tungsten	1S	72W	8	NW	SW	6	0	0	0+	6	289	brown, gray, pink granite
186423	Tungsten	1S	72W	8	NW	SW	0	0	4	10	10	167	gray granite and talc
107306	Tungsten	1S	72W	8	NW	SW	2	0	0	18	18	45	gray granite
116893	Tungsten	1S	72W	8	NW	SW	2	0	0	4	6	55	schist
201211	Tungsten	1S	72W	8	SE	SW	0	0	17	17	17	27	gray granite
91361	Tungsten	1S	72W	9	NW	NE	0	0	0	10	10	90	gray granite
41176	Tungsten	1S	72W	9	NW	NE	3	0	0	3+	3	40	broken gray granite (medium)
112403	Tungsten	1S	72W	9	NE	NW	3	0	0	22	25	60	gray schist
157749	Tungsten	1S	72W	9	NE	NW	0	0	0	6	6	249	gray granite
86110	Tungsten	1S	72W	9	NE	NW	0	0	0	10	10	345	gray granite
110950	Tungsten	1S	72W	9	NW	NW	0	0	0	3	3	60	gray granite
114941	Tungsten	1S	72W	9	NW	NW	3	0	0	0	3	500	gray granite
129409	Tungsten	1S	72W	9	NW	NW	3	0	27	30	30	305	gray granite and schist
143190	Tungsten	1S	72W	9	NW	NW	0	0	4	4+	4	10	tan granite
105023	Tungsten	1S	72W	9	NW	SW	0	0	0	10	10	240	gray granite
131341	Tungsten	1S	72W	9	NW	SW	3	0	77	77+	80	130	brown granite and quartz
139512	Tungsten	1S	72W	9	SW	NW	2	0	13	15	15	200	blue granite
163468	Tungsten	1S	72W	9	SW	NW	0	0	11	11+	11	150	brown and gray granite
23880	Tungsten	1S	72W	18	NE	NE	1	0	0	9	10	20	gray granite
29128	Tungsten	1S	72W	18	NE	NE	2	0	0	0+	2	50	brown granite (medium)
34260	Tungsten	1S	72W	18	NE	NE	1	0	0	9	10	20	gray granite

61205	Tungsten	1S	72W	18	NW	NE	0	0	0	70+	70	185	talc, pegmatite (soft)
61418	Tungsten	1S	72W	18	NW	NE	0	0	63	63	63	171	schist, quartz, talc (soft)
27341	Tungsten	1S	72W	18	NE	NW	8	0	0	37	45	100	gray granite and quartz
31248	Tungsten	1S	72W	18	NE	NW	1	0	17	17+	18	43	brown granite (hard)
17006	Tungsten	1S	72W	18	NE	NW	3	0	70	70+	70	320	broken gray granite (soft)
199536	Tungsten	1S	72W	18	NW	NW	0	0	5	5+	5	360	brown, gray, pink granite and talc
175715	Tungsten	1S	72W	18	NW	NW	0	0	32	32	32	250	gray granite (medium)
46117	Tungsten	1S	72W	18	NW	NW	5	0	70	75	75	152	gray broken granite (soft)
15024	Tungsten	1S	72W	18	NW	NW	0	0	17	17	17	24	gray granite (medium)
22012	Tungsten	1S	72W	18	SE	SW	3	0	0	17	20	25	gray granite
79817	Tungsten	1S	72W	13	NE	NE	6	0	0	0	6	12	tan, fractured rock
84376	Tungsten	1S	72W	13	NE	NE	4	0	12	12	16	45	gray granite (hard)
65485	Tungsten	1S	72W	13	NW	NE	2	0	4	4	6	21	gray granite (hard)
175048	Tungsten	1S	72W	13	SW	NE	0	0	0	12	12	465	gray granite (hard)
46196	Tungsten	1S	72W	13	SW	NE	2	0	2	2	4	24	gray granite (hard)
missing	Tungsten	1S	72W	13	NW	NW	0	0	0	15	15	155	gray granite
156820	Tungsten	1S	72W	13	SE	NW	0	0	4	4+	4	143	brown and gray granite
86111	Tungsten	1S	72W	13	SE	NW	12	0	8	8	21	57	hard pink granite
147797	Tungsten	1S	72W	13	SW	NW	0	0	0	18	18	80	gray granite
66689	Tungsten	1S	72W	13	SW	NW	0	0	0	0	0	120	gray granite
55935	Tungsten	1S	72W	13	NE	SW	6	10	0	0	16+	16	sandy clay
90816	Tungsten	1S	72W	13	NE	SW	5	0	0	75	80	140	gray granite
202965	Tungsten	1S	72W	13	NE	SW	2	0	16	16+	18	470	layered red and gray gneiss
71312	Tungsten	1S	72W	13	NW	SW	3	0	0	0	3	11	hard gray granite (medium)
72984	Tungsten	1S	72W	13	NW	SW	8	0	0	0	8	202	pink and gray granite
92236	Tungsten	1S	72W	14	NW	NE	0	0	3	3+	3	15	brown granite
126918	Tungsten	1S	72W	14	SW	NE	2	0	0	16	18	155	gray granite
152541	Tungsten	1S	72W	14	SW	NE	3	0	15	15+	18	180	brown granite
65188	Tungsten	1S	72W	14	SW	NE	1	0	20	20+	21	70	hard brown granite (medium)
72473	Tungsten	1S	72W	14	SW	NE	0	0	15	15	15	70	gray granite
152550	Tungsten	1S	72W	14	NE	NW	0	0	11	11	11	187	gray granite
165042	Tungsten	1S	72W	14	NE	NW	0	0	8	8	8	357	gray granite with quartz (soft)
107438	Tungsten	1S	72W	14	NW	NW	0	0	0	40	40	320	gray granite
139511	Tungsten	1S	72W	14	NW	NW	5	0	8	18	18	305	gray granite
163162	Tungsten	1S	72W	14	NW	NW	0	0	12	12	12	107	gray granite with quartz (medium)
146216	Tungsten	1S	72W	14	SE	NW	0	0	0	23	23	256	gray granite
41594	Tungsten	1S	72W	14	SE	NW	5	0	13	13	18	90	gray granite
41596	Tungsten	1S	72W	14	SE	NW	0	0	0	30	30	95	gray granite
54021	Tungsten	1S	72W	14	SE	NW	2	0	0	0	2	25	gray and pink granite (medium)
137025	Tungsten	1S	72W	14	SW	NW	1	0	16	16	17	24	gray granite
137889	Tungsten	1S	72W	14	SW	NW	1	0	29	29	35	110	gray granite
159298	Tungsten	1S	72W	14	SW	NW	0	0	15	15+	15	109	brown and gray granite
169330	Tungsten	1S	72W	14	NE	SE	5	0	5	5	5	40	gray granite
187949	Tungsten	1S	72W	14	NE	SE	0	0	0	20	20	40	gray granite
40886	Tungsten	1S	72W	14	NE	SE	1	0	19	20+	20	42	brown and gray granite (medium/hard)
139823	Tungsten	1S	72W	14	NW	SE	0	0	10	10	10	280	granite/quartz mix
232392	Tungsten	1S	72W	14	NW	SE	0	0	18	18	18	144	gray and pink granite
21766-A	Tungsten	1S	72W	14	SW	SE	0	0	6	6	6	68	tan granite with tan quartz
108543	Tungsten	1S	72W	14	NE	SW	2	0	0	13	15	27	gray granite
109501	Tungsten	1S	72W	14	NE	SW	0	0	4	80	80	225	gray granite
48207	Tungsten	1S	72W	14	NE	SW	1	0	2	3	3	10	granite (hard)

49635	Tungsten	1S	72W	14	NE	SW	0	0	30	30	30	200	gray granite
153302	Tungsten	1S	72W	12	NW	NE	0	0	3	3	3	21	gray granite
107084	Tungsten	1S	72W	12	NW	NW	0	0	3	3	3	5	gray granite
133973	Tungsten	1S	72W	12	NW	NW	1	0	0	9	10	15	gray granite
134421	Tungsten	1S	72W	12	NW	NW	0	0	0	60	60	68	gray granite with quartz
12785	Tungsten	1S	72W	12	SE	NW	2	0	0	0	2	15	granite (hard)
40119	Tungsten	1S	72W	12	SE	NW	0	0	15	15	15	150	gray granite
40120	Tungsten	1S	72W	12	SW	NW	0	0	20	20	20	105	gray granite
123648	Tungsten	1S	72W	12	NW	SE	1	0	0	49	50	425	gray granite
153642	Tungsten	1S	72W	12	NW	SE	1	0	14	14+	15	46	brown granite
41354	Tungsten	1S	72W	12	NW	SE	6	0	55	55	61	69	brown granite
44286	Tungsten	1S	72W	12	SE	SE	1	0	3	3	4	20	gray granite (hard)
50261	Tungsten	1S	72W	12	SE	SE	16	0	0	22+	16	38	gray granite, broken (medium)
48949	Tungsten	1S	72W	12	SW	SE	7	0	0	0	7	48	gray granite (medium)
41595	Tungsten	1S	72W	12	NE	SW	3	0	0	67	74	125	pink feldspar and quartz
44847	Tungsten	1S	72W	12	NE	SW	2	0	0	0	2	45	feldspar
72254	Tungsten	1S	72W	12	SE	SW	0	0	4	4	4	245	gray granite
47209	Tungsten	1S	72W	1	NE	NW	10	0	0	50+	10	60	brown granite
144021	Tungsten	1S	72W	1	NE	SW	2	0	36	36	38	45	gray granite
missing	Tungsten	1S	72W	1	NE	SW	1	0	28	28	29	30	granite (hard)
61107	Tungsten	1S	72W	1	NE	SW	2	0	0	106+	108	142	gray granite (soft)
72470	Tungsten	1S	72W	1	NE	SW	1	0	0	14+	15	20	brown, gray granite (medium)
147864	Tungsten	1S	72W	1	NW	SW	0	0	0	15	15	25	gray granite
49218	Tungsten	1S	72W	1	NW	SW	1	0	23	23	24	34	granite (hard)
86107	Tungsten	1S	72W	1	NW	SW	4	0	10	10	14	100	gray granite
141122	Tungsten	1S	72W	1	SE	SW	2	0	18	18	20	50	granite (orange to pink)
160318	Tungsten	1S	72W	1	SE	SW	0	0	0	115	115	240	gray granite
84920	Tungsten	1S	72W	1	SE	SW	4	0	14	14+	18	25	hard brown and gray granite
188942	Tungsten	1S	72W	1	SE	SW	0	0	12	12+	12	63	brown and gray granite
157390	Tungsten	1S	72W	1	SW	SW	0	0	18	18	18	74	tan granite with white quartz
45736	Tungsten	1S	72W	1	SW	SW	2	0	12	12+	14	36	hard brown and gray granite
48685	Tungsten	1S	72W	1	SW	SW	1	0	29	29	30	72	gray granite (hard)
75094	Tungsten	1S	72W	1	SW	SW	10	0	12	12	22	100	blue granite
204045	Tungsten	1S	72W	3	NE	NE	0	0	0	74	74	500	gray granite with quartz layers
233905	Tungsten	1S	72W	3	NE	NE	0	0	10	10	10	35	gray granite
156196	Tungsten	1S	72W	3	SE	NW	0	0	10	10	10	120	gray granite
133668	Tungsten	1S	72W	3	SW	NW	0	0	0	10	15	130	gray granite
116528	Tungsten	1S	72W	3	NW	SE	0	0	0	40	40	42	gray granite
168989	Tungsten	1S	72W	3	NE	SW	0	0	5	5	5	24	gray granite
207093	Tungsten	1S	72W	3	NW	SW	0	0	0	7	7	45	gray granite
172265	Tungsten	1S	72W	3	NW	SW	3	0	5	5	8	36	gray granite
129788	Tungsten	1S	72W	3	NW	SW	2	0	0	16	18	610	gray granite and schist
131234	Tungsten	1S	72W	3	NW	SW	8	0	0	0	8	480	gray granite
158698	Tungsten	1S	72W	3	NW	SW	0	0	30	30+	30	48	brown and gray granite
72305	Tungsten	1S	72W	3	SE	SW	1	0	0	0	1	19	hard granite with soft streaks
194657	Tungsten	1S	72W	3	SW	SW	0	0	5	5	5	124	gray granite
173553	Tungsten	1S	72W	3	SW	SW	1	0	7	18	27	40	white quartz
161096	Tungsten	1S	72W	3	SW	SW	0	0	5	11	11	360	gray and pink granite
163537	Tungsten	1S	72W	3	SW	SW	0	0	12	12+	12	201	brown and gray granite
38297	Tungsten	1S	72W	11	NE	NE	0	0	10	10+	10	40	pegmatite (soft, broken)
29973	Tungsten	1S	72W	11	SW	NE	0	0	12	12+	12	33	hard brown granite with quartz (mixed)

31430	Tungsten	1S	72W	11	SW	NE	1	0	2	2	3	17	gray granite (hard)
34980	Tungsten	1S	72W	11	SW	NE	0	0	13	13	13	15	gray granite (medium)
35676	Tungsten	1S	72W	11	SW	NE	1	0	4	4	5	14	granite (hard)
116157	Tungsten	1S	72W	11	NE	SE	0	0	0	15	15	35	pink granite
96367	Tungsten	1S	72W	11	NW	SE	0	0	0	10	10	15	gray granite
135409	Tungsten	1S	72W	11	NW	SE	0	0	0	10	10	30	gray granite
144546	Tungsten	1S	72W	11	NW	SE	0	0	18	18	18	30	gray granite
40118	Tungsten	1S	72W	11	NW	SE	0	0	20	20	20	125	gray granite
100867	Tungsten	1S	72W	11	SE	SE	0	0	0	200+	0	200	red granite
54070	Tungsten	1S	72W	11	SE	SW	1	0	2	2	3	200	gray granite (hard)
150958	Tungsten	1S	72W	11	SW	SE	0	0	16	16	16	146	gray granite
167703	Tungsten	1S	72W	11	SW	SE	6	0	0	0	6	342	gray granite (hard)
105481	Tungsten	1S	72W	11	NE	SW	2	0	0	73+	2	75	brown and pink granite
140555	Tungsten	1S	72W	11	NE	SW	4	0	14	14	18	380	gray granite
63985	Tungsten	1S	72W	11	NE	SW	4	0	14	14	18	123	gray granite (medium)
64242	Tungsten	1S	72W	11	NE	SW	3	0	59	59	62	74	gray granite (medium)
407419	Tungsten	1S	72W	11	NW	SW	1	2	7	7	10	27	gray granite (hard)
39283	Tungsten	1S	72W	11	SW	SW	0	0	0	0	0	14	gray granite (medium)
44575	Tungsten	1S	72W	15	NE	NE	1	0	0	0	1	6	hard granite (medium)
179666	Tungsten	1S	72W	15	NW	NE	0	0	7	7	7	405	gray granite with quartz
97506	Tungsten	1S	72W	15	NW	NE	0	0	0	26	26	62	gray granite
32351	Tungsten	1S	72W	15	NW	NE	0	0	3	15	15	37	gray granite
38296	Tungsten	1S	72W	15	NW	NE	0	0	3	3	3	13	pink granite (medium), granite (hard)
111744	Tungsten	1S	72W	15	SE	NE	4	0	8	8	12	150	gray granite
145904	Tungsten	1S	72W	15	SE	NE	5	0	15	15+	20	34	brown granite
164901	Tungsten	1S	72W	15	SE	NE	0	0	6	6+	6	81	brown and gray granite
36806	Tungsten	1S	72W	15	SE	NE	0	0	18	18+	18	28	brown granite, some quartz
202906	Tungsten	1S	72W	15	SW	NE	0	0	26	26+	26	130	brown and gray granite and talc
145033	Tungsten	1S	72W	15	SW	NE	0	0	15	15	15	28	gray granite
163161	Tungsten	1S	72W	15	SW	NE	0	0	14	14	14	279	gray granite (medium)
28232	Tungsten	1S	72W	15	SW	NE	0	0	60	60	60	245	gray granite, streaks of quartz
28085	Tungsten	1S	72W	15	NE	NW	2	0	8	8+	10	37	brown granite
48947	Tungsten	1S	72W	15	NE	NW	0	0	17	17+	17	20	brown granite
73800	Tungsten	1S	72W	15	NE	NW	1	0	6	6+	7	53	medium-hard brown and gray granite
84731	Tungsten	1S	72W	15	NE	NW	1	0	4	4+	5	18	medium-hard brown granite
133826	Tungsten	1S	72W	15	SE	NW	0	0	0	4	4	20	gray granite
63000	Tungsten	1S	72W	15	SE	NW	24	0	0	21+	24	45	brown granite (soft)
635144	Tungsten	1S	72W	15	SE	NW	0	0	10	10+	10	42	brown granite (soft)
158700	Tungsten	1S	72W	15	SW	NW	0	0	8	8+	8	450	brown and gray granite
172618	Tungsten	1S	72W	15	NE	SE	0	0	15	15+	15	355	brown, gray, pink granite
177422	Tungsten	1S	72W	15	NE	SE	0	0	14	14+	14	140	brown and gray granite
149461	Tungsten	1S	72W	15	NE	SE	0	0	16	16+	16	26	red granite
159970	Tungsten	1S	72W	15	NE	SE	2	0	0	0	2	400	pink and gray granite
63986	Tungsten	1S	72W	15	NW	SE	0	0	28	75+	28	75	brown granite
168577	Tungsten	1S	72W	15	SE	SE	1	0	0	59	60	135	gray schist and white quartz
26785	Tungsten	1S	72W	15	NW	SW	2	0	0	0	2	95	gray granite (hard)
96732	Tungsten	1S	72W	15	NW	SW	2	0	0	0	2	200	gray granite
192346	Tungsten	1S	72W	15	NW	SW	0	0	5	5	5	90	layered red and gray granite
169175	Tungsten	1S	72W	15	SE	SW	0	0	12	12	12	187	gray granite with quartz seams (medium)
34461	Tungsten	1S	72W	22	NE	NW	2	0	0	0	2	25	gray granite (hard)
31437	Tungsten	1S	72W	22	NW	NW	1	0	1	1	2	24	gray granite (hard)

37488	Tungsten	1S	72W	22	NW	NW	1	0	12	12	13	21	gray granite (hard)
62360	Tungsten	1S	72W	22	SW	NW	4	0	4	150+	4	154	brown granite (soft)
104449	Tungsten	1S	72W	22	NE	SE	4	0	0	0	4	61	gray granite
107944	Tungsten	1S	72W	22	NE	SE	8	0	22	22+	30	50	brown granite
120240	Tungsten	1S	72W	22	NE	SE	1	0	0	79+	1	80	brown granite and quartz
54376	Tungsten	1S	72W	22	NE	SE	2	0	0	0	2	30	schist (medium)
169896	Tungsten	1S	72W	22	NW	SE	0	0	18	18+	18	253	brown and gray granite
90221	Tungsten	1S	72W	22	NW	SE	0	0	2	2+	2	107	brown granite
100335	Tungsten	1S	72W	22	NW	SE	0	0	0	33	33	150	gray granite (medium)
109707	Tungsten	1S	72W	22	NW	SE	5	0	0	145+	5	150	brown granite
110531	Tungsten	1S	72W	22	SE	SE	1	0	0	6	7	180	gray granite
118019	Tungsten	1S	72W	22	SE	SE	0	0	0	0	0	60	schist
20343	Tungsten	1S	72W	22	SE	SE	11	0	7	7	18	50	blue granite (hard)
187329	Tungsten	1S	72W	22	SE	SE	2	0	12	12+	14	20	brown granite and white quartz
171269	Tungsten	1S	72W	22	SW	SE	0	0	4	4	4	35	gray schist
185890	Tungsten	1S	72W	22	SW	SE	2	0	0	7	9	14	gray schist
108870	Tungsten	1S	72W	22	SW	SE	0	0	0	15	15	155	gray granite
30310	Tungsten	1S	72W	22	SW	SE	8	0	0	8+	8	20	brown granite
170855	Tungsten	1S	72W	22	NE	SW	0	0	10	10+	10	47	brown granite
154648	Tungsten	1S	72W	22	NE	SW	4	4	0	52+	8	60	brown and gray granite
61703	Tungsten	1S	72W	22	NE	SW	2	0	16	16	18	27	gray granite (hard)
71140	Tungsten	1S	72W	22	NE	SW	1	0	0	16+	1	17	brown granite (medium)
177386	Tungsten	1S	72W	22	NW	SW	0	14	132	132	146	209	gray schist (soft)
115793	Tungsten	1S	72W	22	NW	SW	10	0	0	170+	10	180	broken brown granite (soft)
136327	Tungsten	1S	72W	22	NW	SW	10	0	0	340	10	350	brown granite and schist
154314	Tungsten	1S	72W	22	NW	SW	0	0	13	445	13	445	brown, gray granite and talc (alternating layers)
154415	Tungsten	1S	72W	22	NW	SW	4	0	61	61+	65	300	brown and gray granite
186453	Tungsten	1S	72W	22	SE	SW	0	0	9	81+	9	81	red granite
165380	Tungsten	1S	72W	22	SE	SW	0	0	19	19+	0	19	brown, gray, pink, gray-green granite w/qz, talc
86739	Tungsten	1S	72W	22	SE	SW	0	165	0	0	165	245	gray granite
93084	Tungsten	1S	72W	22	SE	SW	0	0	3	255+	3	255	brown and gray granite (alternating layers)
170411	Tungsten	1S	72W	22	SW	SW	0	0	2	12+	2	12	brown granite and quartz
140340	Tungsten	1S	72W	22	SW	SW	0	0	7	95+	7	95	brown granite
53222	Tungsten	1S	72W	22	SW	SW	21	119	0	0	140	305	schist with quartz (soft)
65484	Tungsten	1S	72W	22	SW	SW	2	0	7	7	9	18	gray granite (hard)
99479	Tungsten	1S	72W	22	SW	SW	0	0	10	310+	10	310	brown granite
23880	Tungsten	1S	72W	18	NE	NE	1	0	9	9	10	20	gray granite

Appendix D. Geochemical data for MJ-PRFL-1, MJ-PRFL-2, and MJ-PRFL-3

	depth (m)	thickness (m)	density (g/mL)										
ELEMENT				SiO2	Al2O3	Fe2O3	MgO	CaO	Na2O	K2O	TiO2	P2O5	MnO
SAMPLES				%	%	%	%	%	%	%	%	%	%
MJ-PRFL-1df	surface	0.15	1.04	67.68	12.68	4.33	1	2.17	2.14	2.71	0.54	0.05	0.04
MJ-PRFL-1dc	surface	0.15	1.04	66.9	14.42	3.56	0.74	2.17	2.55	3.36	0.36	0.1	0.04
MJ-PRFL-1a	1	2	2.24	57.87	17.02	8.51	2.48	3.79	2.33	2.73	1.19	0.36	0.06
MJ-PRFL-1b	5	2	2.61	70.43	14.32	4.66	0.87	3.58	3.47	1.27	0.46	0.08	0.04
MJ-PRFL-1c	7	2	2.51	63.57	15.63	6.88	1.74	4.6	3.09	1.92	0.86	0.57	0.06
MJ-PRFL-2df	surface	0.1	0.98	60.52	13.17	7.16	1.16	3.2	2.18	2.85	1.32	0.46	0.06
MJ-PRFL-2dc	surface	0.1	0.98	60.56	13.52	5.21	0.81	3.07	2.38	3.26	0.82	0.46	0.05
MJ-PRFL-2a	1.5	3.3	2.44	53.87	14.69	9.34	1.38	8.42	2.68	2.34	2.44	2.82	0.09
MJ-PRFL-2b	8	3.3	2.48	69.43	11.87	6.65	0.49	1.19	1.65	6.23	0.74	0.37	0.04
MJ-PRFL-2c	10	3.3	2.56	52.61	13.52	14.33	1.42	7.61	2.52	2.4	2.43	2.15	0.09
MJ-PRFL-3df	surface	0.15	0.96	65.67	14.7	3.67	1.08	2.84	2.75	2.39	0.36	0.09	0.04
MJ-PRFL-3dc	surface	0.15	0.96	69.66	14.52	2.58	0.54	2.55	2.83	2.59	0.19	0.14	0.03
MJ-PRFL-3a	1	1	1.31	65.35	16.61	4.52	1.24	2.65	3.21	1.87	0.46	0.18	0.05
MJ-PRFL-3e	3	1	2.35	59.6	17.48	6.55	2.52	5.92	3.48	1.84	0.63	0.63	0.09
MJ-PRFL-3b	4	1	2.49	60.82	17.48	5.61	2.08	6.08	3.6	1.65	0.48	0.66	0.07
MJ-PRFL-3f	5	1	2.31	57.84	17.57	8.06	2.04	4.05	3.19	2.62	0.86	0.91	0.07
MJ-PRFL-3c	6	1	2.64	60.64	16.68	7.54	2.28	5.89	3.32	1.78	0.54	0.69	0.07
MJ-PRFL-3g	7	1	2.26	66.3	15.74	4.42	0.23	0.31	1.47	9.46	0.24	0.08	0.03
RE MJ-PRFL-3g	7	1	2.26	66.57	15.78	4.41	0.23	0.3	1.47	9.5	0.24	0.08	0.03
STANDARD SO-17/CSB				61.47	13.78	5.96	2.34	4.66	4.15	1.41	0.6	0.99	0.53

From ACME ANALYTICAL LABORATORIES LTD. 852 E. HASTINGS ST. VANCOUVER BC V6A 1R6 PHONE(604)253-3158 FAX(604)253-1716 @ CSV TEXT FORMAT
To Williams College PROJECT Boulder Proterozoic
Acme file # A205415 Received: DEC 11 2002 * 11 samples in this disk file.
Analysis: GROUP 4A - 0.200 GM

STANDARD SO-17/CSB

Acme file # A205415 Received: DEC 11 2002 * 11 samples in this disk file.
Analysis: GROUP 1DX - 0.50 GM

Trace metals

STANDARD DS4

Acme file # A205415 Received: DEC 11 2002 * 11 samples in this disk file.

Minor elements

STANDARD SO-17

Cr2O3	Ba	Ni	Sc	LOI	TOT/C	TOT/S	SUM		ELEMENT	Mo	Cu	Pb	Zn	Ni	As	Cd	Sb
%	ppm	ppm	ppm	%	%	%	%		SAMPLES	ppm	ppm	ppm	ppm	ppm	ppm	ppm	ppm
0.004	834	< 20	8	6.2	2.54	0.04	99.64		MJ-PRFL-1df	0.2	13	20.9	49	12.3	0.8	0.2	0.1
0.005	983	31	7	5.2	2.14	0.02	99.53		MJ-PRFL-1dc	1	16.4	9	37	15.1	1.1	0.7	0.2
0.008	790	35	22	3.1	0.14	0.01	99.55		MJ-PRFL-1a	0.2	43.6	7.6	103	25.7	0.5	0.7	< .1
0.006	155	< 20	10	0.4	0.06	0.01	99.61		MJ-PRFL-1b	1.6	32	10.7	47	17.7	< .5	0.2	0.3
0.008	552	25	17	0.8	< .01	0.01	99.79		MJ-PRFL-1c	1.4	54.1	5.8	82	20.9	< .5	0.1	0.2
0.006	1404	< 20	12	7.3	3.09	0.03	99.55		MJ-PRFL-2df	0.6	16.4	20.2	88	8.6	1.9	0.3	0.1
0.003	1649	24	10	9.1	4.34	0.05	99.44		MJ-PRFL-2dc	1	17.6	13.1	63	10.1	1.4	0.2	0.2
0.003	1421	26	32	1.1	0.05	0.05	99.33		MJ-PRFL-2a	1.3	35.2	4.4	85	10.1	0.8	0.2	0.2
0.003	2665	< 20	9	0.6	0.06	0.02	99.56		MJ-PRFL-2b	1.9	32.2	8.1	52	10.9	< .5	0.3	0.3
0.005	1315	< 20	24	0.5	0.05	0.35	99.73		MJ-PRFL-2c	2.4	48.7	6.3	94	15.6	< .5	0.3	0.4
0.008	888	20	6	6.3	2.21	0.02	100		MJ-PRFL-3df	0.2	15.8	13.2	45	16.6	1.4	0.3	0.1
0.005	902	< 20	3	4	1.44	0.03	99.74		MJ-PRFL-3dc	0.7	15.9	7.6	23	11.6	1.1	0.2	0.2
0.006	736	30	8	3.6	0.1	< .01	99.83		MJ-PRFL-3a	0.3	42.9	17.9	84	24.9	< .5	0.3	0.1
0.007	998	31	24	1.1	0.03	0.02	99.96		MJ-PRFL-3e	1.7	18.1	2.2	63	35	0.9	0.2	0.3
0.009	1127	36	21	1.1	0.02	< .01	99.77		MJ-PRFL-3b	1.6	21.4	2.7	56	30.4	< .5	0.2	0.3
0.014	572	51	15	2.5	0.05	0.01	99.8		MJ-PRFL-3f	1.8	65.1	6.3	83	38	0.5	0.2	1.1
0.014	1097	44	17	0.5	0.09	0.04	100.07		MJ-PRFL-3c	5	146.1	5.9	60	48.9	1.3	0.2	0.8
0.004	1851	26	3	1.1	0.04	< .01	99.59		MJ-PRFL-3g	2.8	44.2	9.6	28	18.3	0.8	0.3	0.8
0.005	1861	< 20	3	1.1	0.06	< .01	99.93		RE MJ-PRFL-3g	2.7	46.3	9.9	30	18.8	0.7	0.6	0.9
0.437	398	42	23	3.4	2.45	5.41	99.77		STANDARD DS4	6.5	126.2	31.8	159	33.3	22.6	5.3	4.3

Bi	Ag	Au	Hg	Tl		ELEMENT	Co	Cs	Ga	Hf	Nb	Rb	Sn	Sr	Ta	Th	U	V	W
ppm	ppm	ppb	ppm	ppm		SAMPLES	ppm	ppm	ppm	ppm	ppm	ppm	ppm	ppm	ppm	ppm	ppm	ppm	ppm
0.1	< .1	0.9	0.01	0.2		MJ-PRFL-1df	9.3	1.4	17.1	5.5	9.3	97.8	< 1	276.6	0.5	14.6	0.8	66	0.9
< .1	< .1	< .5	0.01	0.2		MJ-PRFL-1dc	7.4	1.1	18.4	6.3	6.6	118.5	< 1	333.8	0.4	17.9	1.1	42	0.6
< .1	< .1	1.6	0.02	0.8		MJ-PRFL-1a	21.6	3.9	28	10.2	16.8	167.4	4	269.3	1	11.2	2.4	151	< .1
< .1	0.1	1	< .01	0.3		MJ-PRFL-1b	8	2.4	20.2	11.5	12.1	73.9	4	241.5	1	19.6	2.3	55	0.2
< .1	< .1	2.1	0.01	0.6		MJ-PRFL-1c	14.9	2.7	23.6	14.8	12.6	112.9	4	311.8	0.8	27.4	3	105	< .1
0.1	< .1	0.8	0.02	0.2		MJ-PRFL-2df	11.7	2.2	23.1	9.7	22.1	114	2	439.1	1.3	25.4	2.6	122	1.7
< .1	< .1	< .5	0.01	0.2		MJ-PRFL-2dc	26.9	1.3	21.3	11	13.7	115	2	475.2	0.8	15.4	1.6	80	1.1
< .1	< .1	< .5	0.01	0.3		MJ-PRFL-2a	24.3	1.4	28	41.7	30	80.8	4	589.6	1.3	23.5	5.3	170	0.4
< .1	< .1	2	< .01	0.1		MJ-PRFL-2b	7.2	1.2	18.5	19.9	13.6	159.8	3	411.9	0.9	12.2	2.7	70	0.5
0.1	0.1	0.8	0.01	0.3		MJ-PRFL-2c	29.7	1.5	28.2	38.1	37	89.3	7	543.8	1.6	26.9	4.7	239	0.7
0.1	< .1	< .5	0.02	0.2		MJ-PRFL-3df	9.4	2.4	18.6	2.9	4.4	87.9	< 1	650.2	0.3	6.6	0.8	57	1
< .1	< .1	< .5	0.01	0.1		MJ-PRFL-3dc	5.9	1.6	17.6	2.5	3.1	82.6	< 1	672.9	0.2	6	0.8	27	0.9
< .1	< .1	1.8	0.01	0.3		MJ-PRFL-3a	13.7	4.7	24.1	2.9	5.3	93.8	2	654.6	0.4	2.1	0.6	88	0.3
0.1	< .1	< .5	0.01	0.3		MJ-PRFL-3e	18.6	3.1	25.3	10.6	5.9	72.2	3	1020.5	0.3	3.7	1.7	107	0.6
0.1	< .1	0.9	< .01	0.2		MJ-PRFL-3b	15	2.6	23.6	11.7	5.8	60	3	1071.3	0.3	3.5	1.9	97	0.3
< .1	0.1	< .5	< .01	0.6		MJ-PRFL-3f	20.4	12	28.6	9.3	13.1	143.5	5	553	0.7	4.1	1.6	134	0.9
< .1	0.1	1.2	< .01	0.4		MJ-PRFL-3c	17.7	3.2	23.2	11.6	6	72.8	5	997.8	0.4	3	1.9	104	0.9
< .1	< .1	1.7	0.51	0.2		MJ-PRFL-3g	7.2	4.4	17	0.7	3.9	222.4	3	485	0.2	15.8	0.5	33	3.1
< .1	< .1	0.9	0.54	0.2		RE MJ-PRFL-3g	6.8	4.5	16.5	0.6	3.8	216.5	3	503.1	0.2	16.4	0.4	31	3.2
4.9	0.3	27.5	0.28	1.1		STANDARD SO-17	18.2	3.7	19.6	12.2	25.4	23	10	301.3	4.6	12.6	10.9	128	10.8

Zr	Y	La	Ce	Pr	Nd	Sm	Eu	Gd	Tb	Dy	Ho	Er	Tm	Yb	Lu
ppm	ppm	ppm	ppm	ppm	ppm	ppm	ppm	ppm	ppm	ppm	ppm	ppm	ppm	ppm	ppm
186	18.6	47.2	87.7	10.14	42	6.3	1.39	4.83	0.62	3.31	0.62	1.84	0.28	1.49	0.22
214.1	21.6	68.8	128.8	15.09	56.6	10	1.61	6.67	0.88	3.97	0.66	2.04	0.27	1.77	0.28
389.2	34.6	56.9	111.6	12.59	49.7	9.8	1.99	7.6	1.15	6.64	1.27	3.36	0.47	2.69	0.48
392.5	17.5	47.8	95.4	9.76	37.5	6.2	1.12	4.48	0.61	3.23	0.58	1.78	0.27	1.8	0.35
518.9	41.2	97.9	167.2	21.07	82.9	14.3	2.21	10.9	1.55	8.08	1.48	3.7	0.5	2.94	0.5
375.6	34.7	116.1	207.1	23.7	89.7	14.1	2.57	9.26	1.12	6.29	1.11	3.02	0.44	2.72	0.36
427.7	23.2	68.7	131.9	15.16	56.3	9.2	1.9	5.91	0.82	4.07	0.72	2.3	0.3	1.91	0.25
1645.8	63.6	180.3	359	44.35	173.9	28.4	5.75	17.59	2.31	11.95	2.11	5.83	0.84	5.45	0.74
732.3	26.7	62.4	127	15.97	63.6	10.1	2.9	6.72	0.89	4.96	0.95	2.52	0.42	2.77	0.42
1577.1	67	187.3	325.4	49.66	196.1	30.8	5.73	19.64	2.52	12.36	2.16	6.29	0.95	5.45	0.86
117.5	12.4	33.5	61	7.51	30.5	4.9	0.99	3	0.42	2.27	0.38	1.02	0.16	0.98	0.14
83.6	8.8	24.9	44.3	5.44	22.1	3.3	0.94	2.44	0.34	1.62	0.3	0.74	0.11	0.57	0.07
105.4	14.1	38.5	76.1	8.97	34.9	6	1.4	4.43	0.57	2.87	0.46	1.28	0.17	1.07	0.13
388.8	35.7	53.7	118.1	14.55	62.2	11.9	2.63	8.93	1.35	6.65	1.23	3.18	0.46	2.74	0.37
439.4	33.3	61.3	127.8	15.89	67.9	12.9	2.68	9.28	1.22	6.32	1.06	3.04	0.41	2.83	0.41
336.7	49.2	59.9	120.9	15.3	65.9	14.9	2.08	12.84	1.9	9.56	1.76	4.2	0.59	2.86	0.37
424.5	31.2	53.6	110.5	14.01	58.8	10.8	2.38	8.84	1.16	5.4	1.06	2.79	0.43	2.54	0.38
23.9	12	52.7	104.9	11.19	37.4	7	1.81	4.23	0.6	2.48	0.39	1	0.12	0.67	0.11
22.5	12.2	53.6	107.2	11.36	41.1	7.4	1.57	4.58	0.53	2.56	0.39	1.08	0.12	0.71	0.07
348.4	27.1	11.3	23.7	3.04	14	3.4	1.08	3.72	0.63	4.35	0.94	2.82	0.43	2.85	0.44